7819614

JASWA, VIJAY CHINUBHAI
AN EXPERIMENTAL STUDY OF REAL-TIME COMPUTER CONTROL OF A HEXAPOD VEHICLE.

THE OHIO STATE UNIVERSITY, PH.D., 1978

AN EXPERIMENTAL STUDY OF REAL-TIME COMPUTER CONTROL OF A HEXAPOD VEHICLE

DISSERTATION

Presented in Partial Fulfillment of the Requirements for the Degree Doctor of Philosophy in the Graduate School of The Ohio State University

by

Vijay C. Jaswa, B.Tech, M.S.

* * * * *

The Ohio State University

1978

Reading Committee:

Prof. K. J. Breeding

Prof. R. B. McGhee

Prof. F. C. Weimer

Approved by

R. B. McGhee

Advisor
Department of Electrical Engineering

To my parents

ACKNOWLEDGEMENTS

I am indebted to my advisor Prof. Robert B. McGhee for his constant guidance and encouragement throughout my graduate work. I wish to acknowledge not only his personal involvement in the work of this dissertation, but also his contributions to the entire field of legged locomotion research. I am grateful to Prof. K. J. Breeding and Prof. F. C. Weimer for their contribution to my education and for their review of this work.

I would like to thank Ms. Joanne Alt for her excellent typing, for painstakingly putting this dissertation together, and for her cheerful cooperation. Thanks are also due to Mr. Henry Pagean for the fine photographic services he provided, and to Dr. David Shultheis and the Biomedical Engineering Center for the use of the PDP-11 computing facilities.

I would especially like to thank my friend Mr. Randal Briggs for his assistance in the recording of angle and rate measurements, and Mr. James Buckett, Dr. David Orin, and Dr. Peter Camana for providing stimulating discussions and a very pleasant working atmosphere. I also wish to acknowledge the help of Dr. A. A. Frank for some initial consultations with regard to the mechanical design and Mssrs. Jesse Wolfe, Ernest Beery, Harry Ellis, and Robert Bielic for their part in the mechanical construction of the hexapod vehicle. I wish to thank Mr. Robert Bockemuehl, Dr. George Kimm, and Dr. James

Rillings of the Instrumentation Department of the General Motors Research Laboratory for providing me with an opportunity to complete my dissertation.

Finally, I would like to thank my parents for their constant faith in me and my wife Sandhya, for her patience and encouragement during the long time that it took to complete this dissertation.

This research was supported by the National Science Foundation under Grant Nc. ENG74-21664.

VITA

June 14, 1951	Born - Bombay, India
1973	M. Tech., Electrical Engineering, Indian Institute of Technology, Bombay, India
1974 - 1976	Graduate Research Associate, Communication and Control Systems Laboratory, Ohio State University, Columbus, Ohio
1975	M.Sc., Department of Electrical Engineering, Ohio State University, Columbus, Ohio
1976 - 1978	Research Engineer, General Motors Research Laboratory, Warren, Michigan

PUBLICATIONS

Dynamic Stability and Control of a Three-Link Model of a Human Being, M.Sc. thesis, The Ohio State University, Columbus, Ohio, June 1975.

"Some Alternative Formulations of Manipulator Dynamics for Computer Simulation Studies," Proc. of 13th Allerton Conference on Circuit and System Theory, University of Illinois, October 1975, (with H. Hemami, and R. B. McGhee).

"Design of a Manipulator Arm for an Interactive Computer-Controlled Legged Locomotion System," Proc. of Milwaukee Symposium on Automatic Computation and Control, April 1976, (with A. A. Frank, D. E. Orin, and J. R. Buckett).

"Interactive Computer-Control of a Six-Legged Robot Vehicle with Optimization of Stability, Terrain Adaptability, and Energy," Proc. of 1976 IEEE Conf. on Decision and Control, Clearwater Beach, Florida, December 1976, (with D. E. Orin and R. B. McGhee).

"On a Three-Link Model of the Dynamics of Standing Up and Sitting Down," IEEE Trans. on Systems, Man and Cybernetics, Vol. SMC-8, No. 2, pp. 115-120, February 1978, (with H. Hemami).

FIELDS OF STUDY

Major Field: Electrical Engineering

Studies in Computer Engineering. Professors Kenneth J. Breeding, Robert B. McGhee, Karl W. Olson and Robert B. Lackey

Studies in Control Engineering. Professors Robert E. Fenton, Robert B. McGhee, H. Hemami and F. C. Weimer

Studies in Computer and Information Science. Professors M. T. Liu and Richard I. Hang

Studies in Statistics. Professors Edward J. Dudewicz and Paul I. Feder

TABLE OF CONTENTS

TABLE OF CONTENTS (Contd)

TABLE OF CONTENTS (Contd)

LIST OF FIGURES

LIST OF FIGURES (Contd)

LIST OF FIGURES (Contd)

CHAPTER 1

INTRODUCTION

1.1 General Background

Artificial legged locomotion is a new field that is only now coming into its own. The reason for the delay has been a combination of lack of technological support and also a lack of understanding. Technical support in the field of locomotion means a host of items--powerful lightweight actuators, low cost electronics, and the availability of powerful computing machines for dedicated functions. Lack of understanding of the theory of locomotion means that we still do not fully understand how animals walk. McGhee [1-5], Hildebrand,[6,7] and Muybridge [8,9] were the pioneers in this field, trying to explain the process of locomotion in terms of formulas, matrices and combinatorics. Yet the control process is only incompletely understood.

One of the best ways to gain a further understanding of the problems involved in legged locomotion is to build an actual machine. The present level of technology makes this feasible. Hence it is the purpose of this dissertation to present the design and construction of such a legged vehicle. A considerable amount of work and research done over the past ten years has culminated in the building of this vehicle.

Apart from building a legged vehicle, the other work that concerns this dissertation is to show that real-time control of a legged vehicle is possible with current computer technology. This dissertation demonstrates the feasibility of walking machines by actually achieving locomotion with an experimental vehicle. The vehicle has been demonstrated to walk on level terrain in a straight-line with real-time computer control of the joints. An important contribution of this dissertation is the development of guidelines for future work both on the design of the electro-mechanical components of such machines and the design of their associated control software.

1.2 Organization

Chapter 1 introduces the basic problems of building a legged vehicle. Much of the previous work done in this and related fields is outlined in Chapter 2 with an emphasis on some of the theory that is used in this dissertation, but which was developed earlier.

Chapter 3 deals with the specific problem of straight-line legged locomotion. The vehicular system and control system are defined. Chapter 4 is concerned with the mechanical details of the hexapod vehicle design and also covers a few areas of possible improvement. The design of the real-time software is covered in Chapter 5 and a detailed description of the algorithms and routines are presented.

Chapters 6 and 7 are concerned with performance evaluation, a description of the limits imposed by hardware and software, and a discussion of further research that might be done with the help of this vehicle.

CHAPTER 2

SURVEY OF PREVIOUS WORK

2.1 Introduction

This chapter attempts to cover briefly most of the work that has been done in the field of legged locomotion until now. Both the mathematical theory of legged locomotion, on which this dissertation is based, and previous attempts to realize legged vehicles will be discussed.

The first section of this chapter deals with gait selection and implementation while the second and third are concerned with various leg geometries and with techniques for achieving stable locomotion. The fourth section is concerned with techniques for obtaining limb motion coordination; i.e., with the <u>control</u> problem. These four sections encompass the entire theory of legged locomotion employed in this work. The next section of this chapter provides a historical background concerning the development of legged vehicles. A hierarchy of machines built to date is perceived in terms of their complexity and their ability to perform functions. This chapter concludes with a section dealing with leg joint actuators following by a short summary.

2.2 Gait Description and Classification

In common usage, the term "gait" refers to the sequence in which an animal lifts and places its feet with respect to the supporting surface [1]. Much can be learned about possible gaits for legged vehicles by studying animals, whose gaits have been perfected through years of evolution. Quite a few researchers have undertaken such investigations and their findings are outlined below.

The early work of Muybridge on the kinematics of locomotion made many fundamental contributions to the detailed understanding of animal [8] and human gait [9]. Muybridge succeeded in producing the first revealing photographs of animals in natural and successive phases of motion. Later, Hildebrand [6,7] carried out an extensive study of quadruped locomotion with modern photographic equipment and obtained results to enlarge the work of Muybridge. McGhee [1] in turn extended this work by imbedding it in a more quantitative and general mathematical theory of locomotion. He gave mathematical descriptions to the notions of stride length, duty factor and phase and incorporated these ideas into a gait formula [1] as follows:

1) The stride length, λ, is the distance by which the body of a legged locomotion system is translated during any complete leg cycle.

2) The duty factor, β_i, for leg i, is the fraction of a leg locomotion cycle during which each leg i is in contact with the ground.

3) The phase, ϕ_i, is the fraction of a cycle by which the contact of leg i with the ground lags the contact of leg 1 with the ground.

4) A symmetric gait is defined as a gait in which the

duty factor of each right-left pair is identical and the phase shift of each right leg with respect to the corresponding left leg is exactly one-half of a cycle.

5) A gait formula for a particular mode of K-legged locomotion is a point in a unit (2K-1) cube defined by

$$k = (\beta_1, \beta_2, \beta_3, \ldots \beta_K, \phi_2, \phi_3, \ldots \phi_K).$$

A gait formula is said to implement a particular gait.

It can be noted from Definitions 4 and 5 that for a K-legged machine with a symmetric gait there are only K/2-1 independent phase variables. This is true because once the phase of one leg of a right-left pair is defined, then the phase of the other leg of the pair is restricted to be different by exactly one half of the locomotion cycle. Most of Hildebrand's work is restricted to symmetric gaits and since he dealt primarily with quadruped locomotion, most of his work concerns only a single phase variable.

Tomovic and Karplus [10] applied finite state theory to legged locomotion. In particular, the notion of binary output-state (1 or 0) for each leg was introduced by recognizing that at any given instant in time a leg could only be in one of two possible states--either in the transfer phase in the air or on the ground in the support phase. McGhee further formalized this notion by a representation of gaits called a gait matrix. A gait matrix is defined as a K-column matrix whose successive rows are binary K-triples corresponding to the successive states of a particular gait of a K-legged machine and whose total number of rows is equal to the length of one cycle of the gait sequence. A gait matrix for a periodic gait can therefore have at most 2K rows. Each row corresponds to a particular event such as the setting down or lifting up of one or more legs [1].

Another mathematical description, the "event sequence", has been defined by McGhee and Jain [3]. To obtain such sequences, the legs of a K-legged machine are numbered from 1,2, ..., K. The event of placing leg i is denoted by event i whereas its lifting is denoted by event i + K. When none of the 2K events occurs simultaneously, the sequence is said to be totally ordered. Gaits associated with totally ordered sequences are called connected gaits while partially ordered sequences correspond to singular gaits.

McGhee and Jain [3] next presented a condition called regular realizability which is advanced as an explanation of gait preferences exhibited by animals. A gait is regularly realizable if it is possible to assign a time duration to each row of the gait matrix G so that β_i is the same for all legs. A necessary condition for regular realizability of a gait matrix is that no column of the matrix may be such that its one entries overlap the one entries of any other column. Gaits described by such a gait matrix are said to be column compatible gaits. With few exceptions, animals tend to use only such gaits. McGhee and Jain [3] also noted that column compatibility is a temporal property of gaits that is not affected by permutation of gait matrix columns. Regularly realizable gaits are the only gaits attempted by the hexapod built in connection with this research. Out of the

5040 theoretically possible connected quadruped gaits, McGhee and Jain [3] showed that only 492 are column compatible and Sun [11] further reduced this to a set of only 14 equivalence classes. Obviously, gait selection is greatly simplified by consideration of only 14 equivalence classes in comparison to the 5040 original gaits. Sun [11] obtained an even more remarkable simplification of the gait selection problem for six-legged machines. He showed that out of the 39,916,800 possible connected hexapod gaits, only 145 equivalent classes of compatible gaits exist. These equivalence classes are listed in [11].

Sun's work was based upon his observation that there are four different kinds of transformation groups that can be used to reduce the number of equivalence classes of connected gaits; namely,

1) The <u>row rotation</u> group first introduced by McGhee [1]. This group contains 2K elements when applied to a K-column (2K-rows) gait matrix. Each element merely rotates the rows of a gait matrix by n steps where $0 \leq n < 2K$. This group may be thought of as rotating event sequences.

2) The <u>row and column canonical form</u> group contains all of the transformations of the previous group plus arbitrary permutations of columns 2, 3, ... K together with all combinations of these two types and was first used by McGhee and Jain [3].

3) The <u>complementation</u> group obtained by changing all the 0's to 1's and vice versa [3].

4) The <u>relabelling</u> group includes complementation together

with all column permutations as well as all row rotations.

Event sequence permutations under these four groups preserve the connectivity, compatibility, regular realizability and symmetric realizability properties of a gait. Consideration of gait equivalence classes obtained by such transformations can greatly simplify the selection of a particular gait for a vehicle [4,11].

2.3 Leg Geometry

Several researchers have investigated the problem of choosing a leg geometry for legged locomotion and their results as presented here are especially pertinent to the choice of the leg geometry for the hexapod vehicle built in connection with this dissertation.

McGhee [12] notes that most natural bipeds and quadrupeds possess a quite highly developed nervous system which allows the animal to cope with unstable gait phases. Normal human locomotion consists of a sequence of fall and recovery cycles involving a very tightly managed exchange of kinematic and potential energy to produce a rather efficient system. The same is also true for high speed quadruped gaits. However, implicit in the notion of an efficient energy management scheme is the idea of a complex neural control system that can successfully achieve such locomotion. No walking machine has ever employed such principles, at least to date. Rather, as discussed further in subsequent sections of this chapter, all experimental legged systems have relied on the much simpler concept of achieving stable motion by maintaining static stability at all times.

There are at least two familiar leg geometries employing revolute joints. The anthropomorphic leg (Figure 2.1) is driven about a rotational axis oriented like an axle on a wheeled vehicle. Lateral motion is accomplished by connecting the leg to the body through a universal joint while leg length is varied through knee flexure. This type of leg is common among bipeds and quadrupeds, but never occurs in insects. Such a leg amounts to a sort of tuned double pendulum and is capable of developing a quite efficient exchange of kinetic and potential energy. Moreover, the human leg also includes an ankle and a foot and is attached to a strong muscular pelvic structure, both of which interact in a complicated way. This is also true of the more efficient cursorial quadrupeds. Thus, as noted before, the leg geometry, the idea of minimal energy consumption, and complexity of control are all interdependent and interrelated [2].

Morawski and Wojcieszak [13] come to similar conclusions regarding biped locomotion upon observing the performance of a small model called the "Miniwalker". This model makes use of certain resonant conditions within the leg-body system to minimize the energy cost of walking. The model consists of a pair of legs with feet and a body, with the legs suspended, like pendula, on a horizontal axis mounted in the body perpendicular to the direction of the model's motion. The propulsive power for progressive motion is obtained as a component of the gravitational force when the model walks down a sloped surface. The swinging leg, when in the transfer phase, behaves like a pendulum and motion is sustained through

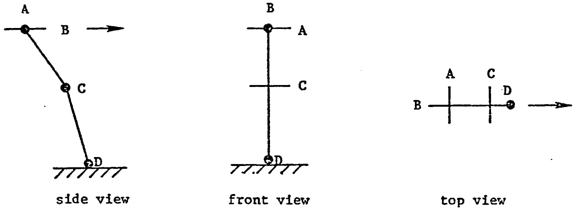

A = hip forward drive axis
B = hip lateral axis
C = knee axis
D = foot

a) Anthropormorphic Leg (extended forward)

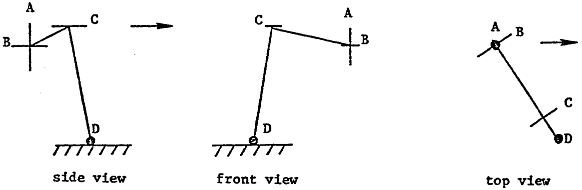

A = hip azimuth axis
B = hip elevation axis
C = knee axis
D = foot

b) Arthropod Leg (extended forward)

Note: Arrows indicate direction of forward motion.

Figure 2.1. Alternative Leg Geometries Employing Revolute Joints.

oscillations in the frontal plane due to the leg geometry. As the model changes legs it gains some energy due to the fact that it passes from a "longer" leg to a "shorter" leg on the sloped surface. This energy is sufficient to maintain motion within the next step. The authors extrapolated the results of the miniwalker to a human being by considering scale factors and figure that a power of 10 watts may be expected for man. They also find that resonant gait appears at very low speed, much slower than the speed of walking. However, if one takes into account the muscle action at the hips and knees, then the resonant frequency increases due to the additional stiffness that is imposed, which leads the authors Morawski and Wojcieszak to conclude that human beings must make use of the resonant or tuned nature of the pendula that form the legs.

In contrast to the resonant locomotion observed in more complex systems, the efficiency of the non-resonant "arthropod" [12] type of legs is derived from an entirely different principle. In the leg geometry suggested by Okhotsimsky et al. [14], (Figure 2.1), the leg drive axis is vertical rather than horizontal and the leg cycle resembles a rowing action when viewed from above. Leg length and body elevation are both controlled by rotation about a second hip axis and a knee axis nominally parallel to the vehicle velocity vector. Hence one sees that the major rotation required for locomotion is about a vertical forward drive axis requiring a rather small moment, while the major moment is about the body elevation axis, which rotates negligibly in level forward motion. Thus, such legs achieve efficiency due to a principle of orthogonality of force and motion [12]. This discussion will later be recalled in Chapter 3 when the leg geometry for the hexapod vehicle is chosen.

2.4 Gait Stability

No matter what kind of leg geometry is utilized, certain aspects of locomotion such as gait stability are common to all locomotion systems. Gait stability is of fundamental importance in choosing a control technique for legged locomotion. Animals often solve the problem of stability by maintaining leg-body configurations that are statically stable at all times. This is generally true of the low speed gaits, but not of the higher speed gaits [4].

Static stability has been defined by McGhee as follows [2]: A vehicle is statically stable if the vertical projection of the vehicle center of gravity onto the supporting surface lies within the "support polygon" defined by the feet in contact with the ground. Gaits that are statically stable at all times should be dynamically stable if inertial forces are negligable. A measure of the degree of static stability can be obtained for a periodic gait as follows [2,4]: At any time t, let s(t) be the shortest distance to the front or rear boundary of the support polygon from the vertical projection of the center of gravity onto the supporting plane as measured in the direction of travel. The longitudinal stability margin, S, associated with a given gait pattern is then

$$S = \min_{0 < t < T} s(t) \qquad (2\text{-}1)$$

where T is the gait period.

For a given gait characterized by a specific sequence of foot placings and liftings, some kinematic degrees of freedom remain (the relative timing between the foot liftings and placings). These can be described by a kinematic gait formula, k, and k can be varied to find the optimum kinematic relationships to yield the minimax longitudinal stability margin, S*. Specifically, S* defined as [2,4,11]

$$S^* = \max_{k \in K} \min_{0 \leq t \leq T} s(t) \qquad (2\text{-}2)$$

where K is the set of all gait formulas implying the given gait. Bessonov and Umnov [15] showed that for a six-legged gait, S* is maximized by a regular symmetric gait in which,

$$\phi_3 = \beta \quad \phi_5 = 2\beta - 1, \quad \beta \geq 0.5 \qquad (2\text{-}3)$$

where ϕ_3 is the time delay for the left middle leg and ϕ_5 is the delay of the left rear leg, both measured as a fraction of a total leg cycle and relative to the placing of the left front leg. Eq. (2-3) describes a "wave" gait in which a wave of placing events runs from the rear to the front along either side of the vehicle with a constant time interval between the action of adjacent legs on the same side [11].

As pointed out in later work by Bessonov and Umnov, caution must be exercised in attempting to extrapolate results obtained in gait studies of six-legged vehicles to machines with more than six legs. For example, in their study of stability in eight-legged machines [16], they showed that for a duty factor $\beta = 3/8$, only four gaits proved to be stable, of which two were non-symmetric gaits! One of the gaits also happens to be a wave gait, but it is the two non-symmetrical gaits that display the utmost stability. Yet it should be noted that the non-optimality of the wave gait in an eight-legged machine is observed only for duty factors close to the minimum value, $\beta = 3/8$. The picture changes with an increase in the duty factor. For all values of duty factor greater than one half, symmetric gaits are optimally stable for eight-legged locomotion. Even so, the most stable symmetric gaits are not the wave gaits but a wider variety of symmetric gaits which do not share equality of phase shift in all legs on one side.

Apart from the notion of strict static stability, there exist two variations to this approach which may be viewed as extensions of the static stability concept and are thus interrelated. Frank [17] and Vukobratovic [18] define a point called the <u>zero moment point</u> in their study of bipedal locomotion. If all elementary reaction forces are reduced to the center of the support surface, then a force N and a moment M are obtained. Since the ground cannot hold the foot, but only support it, the ground reaction can be reduced to a resultant R. This resultant passes through a point on the ground surface called the zero moment point and denoted ZMP. Vukobratovic then prescribes the motion of other links in a bipedal model by constraining the

ZMP to move in a particular fashion. That is, by defining the motion of the ZMP, he obtains constraints by his method of dynamic connections on the links of the biped. However, in the case of static stability alone, since there are no moments due to the frictional forces, the resultant of the ground reaction forces must pass through the center of gravity on the ground surface. Therefore, for static stability only, the ZMP coincides with the projection of the center of gravity on the ground surface.

When considering dynamic stability, one must take into account the moments due to the frictional forces and hence it is not sufficient in general for the projection of the center of gravity on the ground surface to lie within the support polygon. Rather, it is necessary for the ZMP to lie within the support polygon.

McGhee and Orin [19] use a different approach which yields the same results. In their linear programming formulation of the control of joint positions and torques, they find a unique solution to a statically indeterminate system by imposing certain inequality constraints and by optimizing a criterion function. The inequality constraints have to do with a limit on the maximum torque available at each joint and also with preventing the feet from slipping on the supporting surface. The ground reaction force on each individual supporting leg is constrained to act on the supporting surface and must be contained within the <u>friction cone</u> defined by the coefficient of friction, μ. Again, in the static case, the ground reaction must be vertical, but in the quasistatic case it must be directed within a certain cone angle.

Apart from using the notion of static or dynamic stability for locomotion on level terrain, recently Kugushev and Jaroshevskij [20] and Iswandhi and McGhee [21] have studied the problem of "free gait" generation for locomotion over irregular terrain. Algorithms for selecting the gait, footholds, and leg motion schedules depend on the availability or lack of adequate information about the terrain at the moment when the motion is being performed. The problem is solved by organizing interaction, a kind of dialogue, between the information system that views the terrain and the motion design system or the gait generator. The Kugushev and Jaroshevskij algorithm is a heuristic procedure which compromises between the two conflicting criteria of maximizing the stability margin and minimizing the possibility of deadlock, which is a situation where the vehicle cannot move forward without remaining stable. Iswandhi and McGhee provide a more elaborate algorithm which is similar to the one proposed by Kugushev and Jaroshevskij.

2.5 Control of Locomotion

2.5.1 Kinematic Control

Kinematic control of a machine is control that uses a knowledge of only the desired positions and velocities of every link in the body, completely neglecting the forces on those links. Since forces are neglected, the control algorithms used by the control computer are mostly some form of kinematic command generation that produces a fixed course of action when there is an error in the actual velocities and coordinates of body links [2,19].

Okhotsimsky, Platonov et al. [22,23] have investigated the movement of a legged vehicle over uneven terrain. In their work, the control computer determines the timing of foot liftings and placings from a knowledge of the "standpoints" or foot placement points. Algorithms for calculating the timing or tracking schedule depend on the gait employed while the setpoints are generated from another algorithm that uses a knowledge of the terrain.

McGhee and Orin [24] have produced a digital computer simulation of an interactive computer control system for a quadruped robot and also for a six-legged robot [19,25]. Automatic gait selection, turning, sidestepping,and accelerating were all incorporated in this simulation. Much as been learned from these simulations and the work in this dissertation is based in part upon these simulation results.

Chao [26] reduced the computing time required to calculate joint torques by using a more efficient linear programming approach than the one used by McGhee and Orin. He separated Orin's software into several functional blocks. The <u>motion planning</u> block, which is an interface between the environment and the control system, and the <u>simulation block</u>, which consists of a kinematic command generator and a simulated terrain model, are similar to the ones written by McGhee and Orin. The <u>force distribution</u> block utilizes his improved linear programming algorithm. He also added a servo-microprocessor block to act as an interface between the vehicle hardware and the control system. This block could conceivably be realized by an array of microprocessors.

Petternella and Salinari [27] built a legged locomotion system originally intended for use with operator interactive computer control. Interactive control was to allow the operator control of vehicle speed, elevation, and other parameters with the computer solving leg stability and coordination problems. As of the present time, however, only constant speed locomotion without computer control has been exhibited by this machine and this project is not currently active.

2.5.2 Dynamic Control

Dynamic control is an approach to limb joint motion coordination which permits the inclusion of statically unstable phases [28,29]. It is the hardest type of control to implement, not only because of control complexity, but because of computational difficulties -- too many simplifying assumptions about the structure of the machine must be made before an analyzable linkage system is obtained.

In non-redundant linkage systems, where the number of unknowns (joint torques) is equal to the number of constraint equations for motion of the system, joint torques have been generated by use of an inverse plant [28]. However in legged locomotion systems, due to the formation of closed kinematic chains, or due to static instability in certain phases, the dynamic equations of motion give either an underspecified or an overspecified problem. In Park's simulation for a quadruped [29], the dynamic equations of motion gave fewer unknown torques than constraint equations. Certain phases of the locomotion cycle were statically unstable and the combined action of the joint torques could not produce the exact values of body forces and moments necessary to achieve the desired system trajectory. Joint torques are generated therefore by a linear programming approach, to minimize the difference between actual and desired body accelerations. On the other hand, in Orin's simulation of a six-legged robot [25], he was faced with an under-specified problem. That is, he had fewer equality conditions than joint torques and so he had a subspace of solutions to choose from. The underspecification of the problem arose due to the guaranteed static stability of the machine at all times in contrast to Park's overspecified problem due to the statically unstable phases. Orin adopted an approach involving optimization of a weighted combination of power consumption and load balancing in contrast to Park's optimization of acceleration errors.

2.6 Existing Legged Vehicles

This section of this dissertation attempts to provide a historical perspective on the development of legged vehicles. In the following discussion, each of the major approaches to legged vehicle design is represented by what is believed to be its most advanced implementation.

2.6.1 Linkage Controlled Machines

A very large number of truly ingenious mechanisms have been used to obtain joint coordination in legged vehicles. An almost infinite variety of toys that walk have been made where stability is usually achieved by large feet with legs rigidly interconnected so that only one degree of freedom exists. Shigley [30] at the University of Michigan made an extensive study of linkage systems for legged locomotion and designed and constructed a quadruped vehicle based on his findings. While his machine did function, it required the use of non-circular gears and this was found to be impractical.

A group at Space General Corporation in Azusa, California, became interested in linkage-controlled machines for lunar locomotion. This group first built a six-legged machine and then an eight-legged machine capable of carrying a small child. The eight-legged machine was especially interesting since it could climb ordinary stairs, and also demonstrated exceptional off-road mobility due to its unusually high drawbar-pull to weight ratio [31]. Its most serious shortcoming was its limited adaptability to terrain because it possessed so few independent degrees of freedom.

2.6.2 Manually Controlled Machines

The largest walking machine ever built is also the world's largest off-road vehicle. "Big Muskie", constructed by Bucyrus-Erie Company weights 27 million pounds and is powered by four hydraulically powered legs at the corners. Normally, Big Muskie rests on a 105 foot cylindrical base. During walking this machine utilizes twenty-four electric motors of 600 horsepower each to provide hydraulic power for raising the base off the ground while transferring the weight to the four feet. A second set of actuators then moves the machine forward for a stride of up to fourteen feet at which time it settles again on its base. The walking action is accomplished with the aid of an electronic sequencer which cycles the legs [32].

The General Electric quadruped [33] is another large walking machine, weighing about 3000 pounds. Each of the four anthropormorphic legs of this vehicle possesses three degrees of freedom - two at the hip and one at the knee, and is controlled manually. The driver or operator wears an exoskeleton incorporated into a position-following, force-reflecting servomechanism system to provide him with feedback regarding the interaction of the feet and the terrain. The force reflecting servomechanisms produce an exoskeletal joint torque that is equal to about 1% of the vehicle joint torques. This machine first walked in 1968 and later exhibited a significant ability to climb over obstacles and to traverse difficult terrain. Unfortunately, the task of coordinating twelve independent joints was so demanding of the operator that operation of the vehicle was restricted to a few minutes. Thus, the primary contribution of this machine was to illustrate the need for computer control of walking machines with so many degrees of freedom. Another very serious shortcoming of this machine was that it used very large amounts of power. The reason for this should be clear from the discussion on resonant and non-resonant legs in the preceding section on leg geometry. While the GE quadruped employed an anthropomorphic leg geometry, the control scheme employed was so primitive that it could not make use of any energy management scheme to reduce power requirements. Until the state of the art in locomotion control systems reaches a point where it can make use of the resonant properties of an anthropomorphic leg, it would appear to be better to utilize the arthropod leg geometry, based upon consideration of energy requirements alone.

The first machine to walk autonomously under computer control was the "Phoney Pony" constructed by Frank and McGhee [2,34] at the University of Southern California in 1966. This vehicle was a four-legged machine, each leg having a single degree of freedom hip joint and an independent single degree of freedom knee joint. A passive suspension system was also included to permit vertical excursion of each leg relative to the body. The machine weighed about one hundred pounds and was roughly the size of a small pony.

The eight independent joints of the USC machine were controlled by an electronic sequencer. The machine demonstrated one important capability: that the joint coordination problem could be solved with an "electronic linkage" rather than a mechanical linkage.

In parallel with the work at the University of Southern California, an affiliated group at the Institute Mihailo Pupin in Belgrade, Yugoslavia, developed a powered biped exoskeleton intended for application to the locomotion of paraplegics. Successful operation of this brace, both with and without the inclusion of a patient, was reported in 1972 [18].

Both the above machines were true robots with autonomous control. More recently, however, a system has been developed employing interactive control. A research program directed by Prof. I. Kato [35] at Waseda University in Tokyo, Japan has produced a series of computer controlled biped robots with stairclimbing capability. Although these machines are very slow, they do represent the furthest advance in interactive computer control systems for legged machines prior to the present research.

A hexapod vehicle has recently been built at the Institute of Mechanics in Moscow. The legs of this machine have an arthropod type of leg geometry and are instrumented to provide contact sensing and joint angle and joint rate feedback. The control system is implemented on an analog computer and the robot develops a rather smooth motion over even terrain. Coordinate transformations from the leg tip coordinates into joint angles are done in the analog computer hardware. Only a few details concerning this machine are presently available.

In conclusion, it may be said that current work on legged vehicles is generally progressing in the direction of more sophisticated control systems and better and more powerful actuators.

2.7 Leg Joint Actuators

In the design of legged locomotion systems, it is always the joint actuator which sets the eventual limits on the performance capability of the machine, since it is the only active element of the leg. In this section of this chapter, past actuator designs are presented in a somewhat detailed fashion because of the bearing they had on the actuator designed for the hexapod built in connection with this dissertation.

Tomovic and McGhee [36] first introduced the concept of a cybernetic actuator and defined it as an actuator with four possible states - a free state,a forward rotation state, a rearward rotation state and a locked state. Such an actuator represents the ideal upon which the design of an actual joint actuator may be based.

The GE Quadruped used hydraulic actuators for moving the joints due to their large torque and power capabilities as well as the speed of response of a hydraulic actuator. By employing servo flow-control valves, both force and speed can be controlled. While the GE machine used a constant pressure hydraulic supply, valve-controlled hydraulic actuators can be made more efficient by using a variable pressure, variable flow-rate pump, so that speed requirements can be reduced while climbing uphill with a corresponding increase in the pressure or available torque [12].

The photograph of the Phoney Pony leg in Figure 2.2 shows an electrical type of actuator. The block diagram in Figure 2.3 shows the actual power conversion process in the knee joint actuator. A planetary gear train in the DC electric motor first reduces the speed. An external worm gear reductor offers a further speed reduction and directly drives the joint. The use of a worm gear drive allows forward and rearward rotation as well as a locked state. With no motor input, the gear is capable

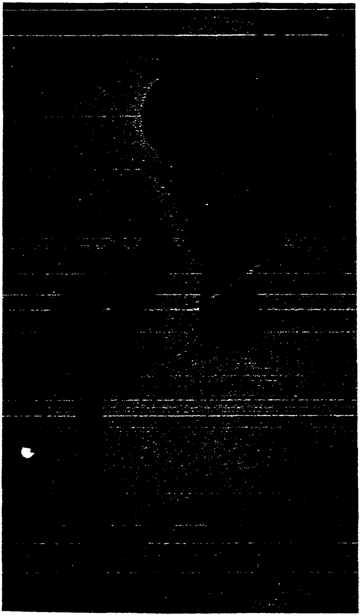

Figure 2.2. Details of the Phoney Pony Leg.

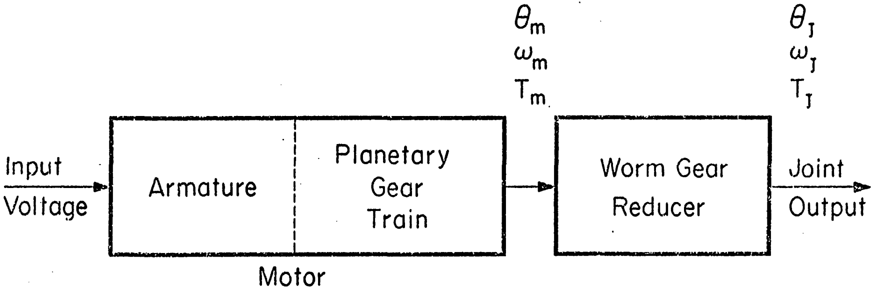

Figure 2.3. Phoney Pony Knee Joint Actuator Block Diagram

of withstanding large torques at the output without slipping. Also, the use of a worm gear permits a large reduction ratio to be obtained in a small space with very little weight.

If worm gears must be avoided due to the backlash or hysteresis problems generally associated with them, then planetary or epicyclic gear trains offer the most volume efficiency for gear reduction. The Soviet machine discussed earlier uses this kind of a gear train to provide speed reduction from the DC motor to the joint.

In conclusion, it is noted that the lack of really efficient light-weight actuators seem to be one of the major limitations in the design of legged machines. Worm gear reduction units are strong and small, but quite inefficient with regard to energy transmission, with operating efficiences of about 60% or less. Spur gears are much more efficient, but tend to be bulky and lack other desirable properties of a cybernetic actuator such as the availability of a locked state.

2.8 Summary

This chapter has first dealt with the theory of legged locomotion in general, then tried to define some of the theory relating to control of limb segment motion, and finally attempted to give an overall summary of the development of legged machines to date including the problem of finding suitable joint actuators. It has been shown that while a better understanding of the control problem is being gained, the development of mechanical hardware has proceeded at a slower pace.

The next chapter defines the problems posed by straight line locomotion - both the definition of a locomotion system which is comprised of a vehicle itself, and the control system which is in turn comprised of the algorithms, control hierarchy and control equipment available. The rest of this dissertation will show how a six-legged vehicle was built and programmed to walk in a straight line over level terrain under computer control.

CHAPTER 3

OVERALL SYSTEM CONFIGURATION AND PROBLEM FORMULATION

3.1 Introduction

The problem to be solved concerning computer control of locomotion has two distinct aspects; interlimb coordination and intralimb coordination. For a six-legged machine with three joints in each leg, both problems taken together constitute an overwhelmingly difficult problem for a human operator and make computer control the only reasonable solution. Realization of computer control therefore requires the accomplishment of two fairly well-defined tasks: first of all maintaining interlimb coordination by choosing an appropriate gait [4] and secondly maintaining intralimb coordination by means of tight feedback control of each joint. The rest of this chapter is devoted to defining the various subsystems involved in a legged vehicle and to specifying the problems to be solved by the research of this dissertation.

3.2 Hexapod Electro-Mechanical System Definition

The mechanical and electrical design of a legged vehicle is a rather unusual engineering problem because there is very little precedent to go by. As seen from the previous chapter, few of the existing walking machines resemble one another except perhaps in cases where several models have been built by the same group. Several questions need to be answered in deciding the very structure of the legged vehicle. How many legs should the machine have? Does the machine need a suspension system and if so, of what kind? What kind of joints and actuators should be used? How should the legs be connected to each other? These questions are treated in order in the following paragraphs.

3.2.1 Choosing the Number of Legs

The more advanced animals seem to prefer to make use of an even number of legs symmetrically arranged along or around a central body [4]. Such a left-right symmetry is certainly desirable in a vehicle that does not possess a preferred direction of turning. Hence, most certainly an even number of legs is appropriate in the vehicle to be constructed. Falling back upon nature again, one observes that in terrestrial animals the number of legs is more or less inversely related to the complexity of the central nervous system. Specifically, millipedes and centipedes use a very large number of legs in conjunction with a simple forward-moving wave of stepping actions, spiders and other arachnids use eight legs and display a more complex stepping pattern than does a millipede [37], and insects with six legs exhibit a still greater variability in limb motions [38]. Quadrupeds sometimes use gaits with no statically stable phases and bipeds, as typified by man, make use of elaborate optical, inertial, and tactile sensing to achieve essentially arbitrary behavior. Thus, in nature, the number of legs possessed by an animal seems to be intimately related to a neural control complexity which is traded off against the "hardware" expense of additional legs. A machine with four or fewer legs would have difficulty maintaining stability without a correspondingly complex control system to maintain balance. A machine with six legs gains stability at the expense of the increased hardware cost of two legs. In view of the present primitive state of legged locomotion machines, a machine with six legs seems to present a reasonable compromise between hardware cost and software or computational complexity. This conclusion has been reached on the basis of similar considerations by all currently active legged vehicle research groups [39].

3.2.2 Choice of Leg Geometry

As discussed in Chapter 2 in the section on leg geometry, two basically different leg structures are observed in nature - the anthropomorphic leg and the arthropod (insect) leg. It was also observed that the anthropomorphic leg is more appropriate to systems with advanced sensing and control capabilities which permit it to achieve efficient locomotion by developing an effective exchange of kinetic and potential energies. For the same reason that leads one to use six legs in a walking machine rather than four, an arthropod type of leg geometry is preferred at present for such vehicles. There are other advantages to the arthropod leg geometry which are important to this work. Each leg has three degrees of freedom so that it can be placed at any point within a specified working volume. The working volume afforded by this type of geometry is very large so as to permit the maximum degree of vehicle adaptation to terrain. For all of the above stated reasons, the vehicle configuration chosen for this research is a six-legged machine with arthropod legs.

3.2.3 Suspension System Alternatives

While a vehicle may be dynamically stable with respect to gross body motions by virtue of the static stability of all its locomotion phases, there still exists the possibility of instabilities or undue vibrations resulting from the mutual coupling between legs through the body structure [40]. This can be avoided by providing a sufficiently compliant suspension system which serves to isolate the legs from such interactions. A suspension system might also be required to dampen the shock to the on-board electronics. Finally, the choice of the suspension system directly affects the type of force feedback available to the central control system. A suspension system between each leg and body alters the dynamic forces felt by the body and hence given foot reaction forces could imply different body forces depending on the type of suspension system used.

<u>Compliance</u> is the reciprocal of the property called <u>stiffness</u>, which is the ratio of force to the corresponding deflection. By employing an element which yields to a deflecting force, it is possible to achieve what is known as <u>passive</u> compliance; e.g., the legs of a vehicle might flex due to the weight of the machine as each step is taken. On the other hand, one may imagine an "active" suspension system that dynamically adjusts the actuator torques in order to achieve an effective spring constant. This could be done by actually measuring the joint rotations and torques and then forming a weighted linear combination of position

errors and torque errors for use in a feedback control system to determine actuator commands. Such a system is said to employ active compliance. Analogous to active and passive compliance is the "inherent" and "controlled" compliance observed in the muscles of living creatures. Nichols and Houk [41] suggest that length regulation of natural muscle occurs through two contributing phenomena - the muscular stiffness due to the mechanical properties of the muscle (inherent compliance) and the stretch reflex which results from a balanced interplay between length-related excitation and force related inhibition (controlled compliance). While this type of control would also be ideal for a vehicle, the attainment of active compliance in artificial system is itself a major topic for research and is beyond the scope of this dissertation. Instead only passive compliance will be considered in what follows.

While it is difficult to decide what type of compliance is necessary for a vehicle and how it should be implemented, it is still harder to determine the amount of compliance that is needed. If a very stiff leg and suspension system are used, then since such a system effectively does not yield to forces, it is possible to know the foot position very accurately. However, if significant compliance is introduced between the foot and the leg, or between the leg and the body, then, since the compliance of the terrain is unknown, it follows that the foot position is not very accurately known.

The contrary argument to the above considerations is that by introducing appropriate compliant elements, it is possible to obtain force control. There are at least three ways of getting compliance in the leg of a vehicle, each way differing in the point at which the compliance is introduced. Compliance can be introduced at the foot, in the joints, or at the point of attachment of the leg to the body. If compliance is introduced at the foot, then the exact foot position is not very accurately known. A further disadvantage of putting the compliance in the foot is that this is not easy to do. On the other hand, an advantage of this approach is that if the compliance is instrumented to read force, then the forces at the foot are direcly obtained. If compliance is put in the joints, then the foot position as well as the joint positions are fairly accurately known since each joint is instrumented for position. While this is perhaps the most desirable way of obtaining compliance, there are as yet no good means for combining actuation with passive compliance in artificial systems. Finally, if compliance is introduced at the point of attachment of the leg to the body as is typical of automotive vehicles, the entire leg "floats" with respect to the body and hence the leg position is not very accurately known, and it is therefore difficult to control. The only evident advantage of introducing compliance at the point of leg attachment is that it seems to be the easiest to achieve of the three alternatives which have been discussed.

It should be noted that, regardless of the means by which compliance is obtained, the ability of an articulated leg to move its foot in three dimensional space means that the null force position of the compliance can be correspondingly moved under computer control. This is in striking contrast to the fixed location of the null force position in conventional wheeled or tracked vehicles.

3.2.4 Joint Design and Actuator Design

While it is clear that, in the arthropod leg geometry, the knee joint must rotate about a horizontal axis so as to permit leg length variation, there are two distinct alternatives to the placing of the degrees of freedom at the hip. One degree of freedom must provide for elevation of the leg and is called the <u>elevation axis</u>. The other must provide for a fore-aft motion and is called the <u>azimuth axis</u>. The two alternatives relate to the relative placing of these two degrees of freedom at the hip. In Figure 3.1, the hip joint is constructed so that the elevation axis of the hip is always parallel to the knee joint axis, and the hip azimuth joint is fixed to the body. In Figure 3.2, it is the hip elevation axis that is fixed to the body and the azimuth axis moves with the hip elevation angle. There are several advantages to the first arrangement in which the azimuth axis is fixed to the body. Since the hip elevation axis and the knee axis are always parallel to each other in this configuration, the inverse Jacobian transformation from the foot Cartesian coordinates to the joint angles is much simplified [42]. Another reason for fixing the azimuth axis to the body is that in this case the torque due to the body weight is supported by bearing reaction moments of the azimuth joint as can be seen from the Figure 3.3. On the other hand, if the elevation axis is fixed to the body, then whenever both the elevation and azimuth angles change from the

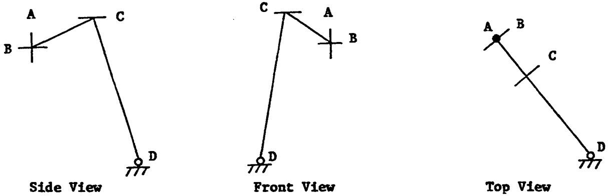

Figure 3.1. Hip Azimuth Axis Fixed to Body (Leg Extended Forward).

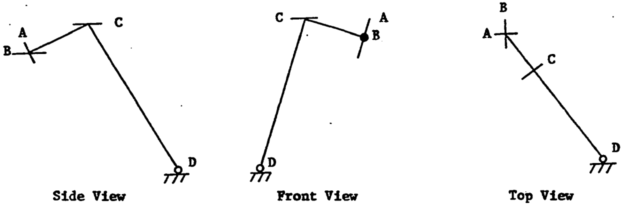

Figure 3.2. Hip Elevation Axis Fixed to Body (Leg Extended Forward).

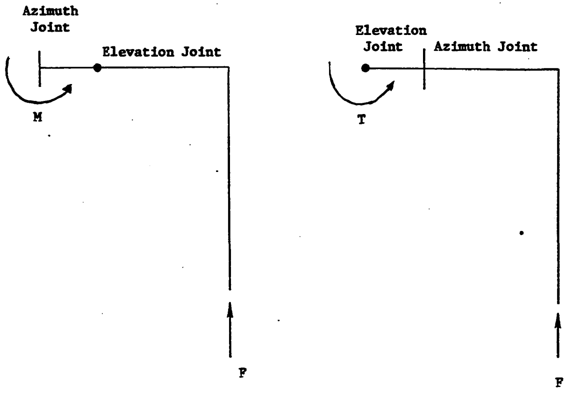

Figure 3.3. Foot Reaction Force Countered by Bearing Reaction Moment M, and by Hip Elevation Torque, T.

rest position shown in Figure 3.3, a component of the foot reaction moment due to the weight must be countered by the azimuth torque and must therefore be generated by the hip azimuth joint motor.

It is known that the relations linking foot position to joint angles assume their simplest form when the two hip axes intersect [42]. However, such a relationship may be difficult to achieve within the space and weight limitations associated with an effective vehicle design. Therefore, a small displacement between these axes will be allowed in the final design for the leg to be developed later in this dissertation.

Sliding joints offer another interesting possibility in the design of legs for vehicles, but they are not very practical due to the fact that the joint is exposed to the dust and dirt of the environment. In a revolute joint, the only parts that rub against each other are the gears and they can be enclosed in a housing, but the members that form a sliding joint in a leg are parts of the limb and are therefore exposed.

Another major problem relating to joint design is the design of the actuator itself. The aim is to design a strong and lightweight actuator that is self-protecting in case the joint stalls. This feature amounts to an adjustable torque limit after which the drive train separates from the motor, in short, a mechanical clutch. It is also desirable to design an actuator with a self-locking feature upon power-off so that, in case of power failure, the machine does not simply collapse to the floor. Finally, the actuator should also be so designed that it is possible to instrument it so as to read joint position and joint rate. Of course it remains to be determined if either or both of these need to be known to achieve a desired control characteristic. For example, it is possible to integrate joint rate information to obtain joint position information so long as the drift in the integrators can be corrected periodically by limit switches, although this might not be a good idea from the standpoint of the sampling rate required for the rate information. Conversely, it is also possible to differentiate the position information to obtain rate information. However, this introduces a large amount of noise in the rate information, although it has been done [43]. While analog differentiators are known to be noisy, even digital differentiation can introduce a large amount of noise. For example, as shown in [43], in a simple second order system with no damping or springs, but with only a torque T acting upon an inertia J to produce a joint rotation θ, the equivalent noise torque due to quantization is

$$T_n = K \times J \times e \tag{3-1}$$

where $K = Kp + Kv$ and Kp, Kv are the position and velocity feedback gains, and e is the quantization noise due to the number of bits used in the analog to digital converter that measures position. In any case, if velocity is to be obtained by differentiation of position, the joint position monitoring potentiometer cannot be mounted at the joint output because the joint output changes too slowly with respect to time. On the other hand, if the potentiometer were mounted before the final speed reduction unit or gear train output, then a multi-turn potentiometer would have to be used.

So far as the type of power to be used for joint actuation is concerned, there are three alternatives which have been used in the past for articulated mechanisms; namely, hydraulic, pneumatic, and electric power. Hydraulic actuators have the advantage of producing both large forces and rapid response in a relatively small volume. In fact, the largest walking machines that have been built to date, such as the General Electric Quadruped and Big Muskie as described in Chapter 2, have used hydraulic actuators. However, valve-controlled hydraulic actuators are quite inefficient because they use a constant pressure supply. By making use of a variable pressure hydraulic power supply capable of delivering low flow at high pressure or high flow at low pressure it is possible to improve the efficiency of a hydraulic actuator. Pneumatic actuators are plagued with more problems than are hydraulic actuators. Since pneumatic actuators use a compressible fluid such as air, they are extremely inefficient, noisy, and even dangerous due to the high pressure supply. They also require either an air compressor or large volume accumulator as an air supply source. The primary advantage of pneumatic actuators also stems from the compressibility of the air that is used for actuation. With such actuators an adjustable compliance could conceivably be introduced in the actuator joints making them more akin to natural joints, as mentioned in the previous section. The Mihailo Pupin exoskeleton uses pneumatic actuators and thereby to some extent achieves this desirable characteristic [44].

Electric actuators are the most efficient of all three of the possibilities which have been mentioned and are invariably used where efficiency is an important consideration such as in practical vehicles; e.g., in locomotives. Electric actuators are also safer, and besides being more efficient in terms of power transfer, they are also reasonably efficient in terms of space requirements for a given power output. Their major disadvantage is that they have a low torque output which must generally be boosted by speed reduction gear trains. Electric actuators are also more reliable than either hydraulic actuators or pneumatic actuators because there is no moving fluid involved so there is no need to provide for sealed ducts, pumps, pressure chambers, etc. For all of the above reasons, only electric actuators will be considered further in this dissertation.

Actuator design also includes the selection of a specific motor, a gear reduction unit, the instrumentation on the actuator to derive feedback information, plus safety features to prevent damage to the actuator unit on overload. A worm gear reduction unit offers a large reduction in a small volume and has a very desirable self-locking property which prevents the joint from going limp when power is removed. The disadvantages are the backlash in the gear and the low efficiency (about 65% or less). Spur gear trains have higher efficiency and less backlash, but lack the important self-locking feature. The matter of choosing a particular type of gear reduction and designing a specific reduction unit for the hexpod vehicle is treated in detail in Chapter 4.

3.2.5 Overall Electro-Mechanical System Characteristics

The vehicle structural characteristics are determined by the design objectives or applications intended for it. Since the purpose of the research done in connection with this dissertation is to build a vehicle for laboratory testing of walking machines, to prove their maneuverability and superiority in negotiating obstacles, speed has never been a design objective. In what follows, it will be assumed that a vehicle speed of the order of 1 ft/sec will be more than adequate. However, flexibility is an important criterion; that is, the machine must be able to adapt to a wide variety of terrain conditions. The vehicle should be built to be able to negotiate slopes, staircases found in buildings, and it should be able to climb over large obstacles. The vehicle must also be computer-controlled so that operator interaction is restricted to higher level commands such as speed and direction of motion whereas the computer performs all coordinate transformations and all individual joint coordination functions to yield the desired speed. Since the vehicle is a laboratory vehicle, power is assumed to be available from a 60Hz AC electrical outlet.

3.3 Control Computer Characteristics

The mechanical system dictates the kind of parameters that are available to the control system to a large extent. From the hexapod system definition it has been seen that it is possible to make joint angles and rates available to the controller and in turn the controller can directly command the torques to be applied to the joints. Due to the complexity of the system, it is obvious that manual control is not feasible, and therefore computer control must be the solution. The requirements of the control computer can then be outlined as follows.

3.3.1 Computational Speed

The computer must be able to do coordinate transformations from the foot rectangular coordinates to the joint angles and rates and vice-versa. Since these involve a large number of trignometric calculations, and since they must be done in real-time, speed is important. Precision is important too, and at least a 16 bit computer should be used for obtaining the required precision. It would also be desirable to have a floating point hardware unit within the computer to save time. At the very least, the computer should have software floating point arithmetic so that the functions do not have to be written down in assembly language since that could be a project in itself. The other reason for computation speed is that the stability of the servo loops dictate a minimum sampling rate. If sampling is done at a slower rate than the minimum, the loop could become unstable.

3.3.2 Real Time I/O Capability

Due to the large number of inputs and outputs (at least 36 inputs consisting of measured angles and rates and 18 motor commands), the computer must be able to quickly scan all inputs periodically and update the outputs. In future work, the number of inputs could further be increased by force feedback which is essential for walking over uneven terrain. Hence, the computer must be equipped with a real-time data acquisition facility that is capable of reading a large number of analog inputs and that can provide a large number of analog outputs.

Another aspect of the input-output capability is expandability of the computer into a multiprocessor structure. A bus-oriented architecture favors multiprocessing since all processors can share either the input/output bus or the data bus. The multiprocessing feature would allow individual processors to control each leg and these could be centrally controlled by a master processor. Hence, in view of possible future expansion, a bus-oriented computer architecture seems to be a desirable feature.

3.3.3 Other Desirable Features of the Central Computer

Apart from computational speed, analog input/output capability and a bus-oriented architecture, it is also desirable to have a real-time clock, a timed interrupt capability, utility routines for reading the clock, for doing either direct access or at least sequential access input/output such as on magnetic tape, and some file management capability. The real-time clock is essential for keeping track of the time since time-dependent variables such as speed and acceleration are to be governed by the control computer. Some form of fast input/output medium such as disk or tape is required for reading source and data files, and for logging data. The need for a timed interrupt capability will be explained further in Chapter 5.

Taking into account all of the above considerations, a PDP-11/45 was chosen as the control computer for the task of controlling the vehicle.

Since the vehicle is to be operated only in a laboratory environment, communication with the computer can be accomplished by a trailing umbilical cord which carries vehicle state information from each joint back to the computer and motor controller commands for each individual joint from the computer to the vehicle. For purposes of this dissertation, state information consists only of the angular position and angular velocity of each joint. It may later include vertical gyros for maintaining a fixed body attitude. It could in the future also include foot load sensors that would accurately measure the vector force at each foot from the terrain. The interrelationships between the human operator, the electromechanical vehicle, and the control computer as described in this section of this dissertation are illustrated diagramatically by Figure 3.4.

3.4 Straight-Line Locomotion Control Problem

Only straight-line level locomotion is considered in this dissertation. Of the two problems mentioned in the introduction, namely, interlimb coordination and intralimb coordination, the first becomes primarily a matter of defining a proper gait to achieve straight-line locomotion. By straight-line locomotion it is meant that the course of the vehicle is set in a straight line; by level body locomotion it is meant that the body maintains itself parallel to the terrain. It is further assumed that the terrain is flat. When dealing with a flat terrain or a regularly defined terrain, it is not necessary to have force feedback from each individual foot unless

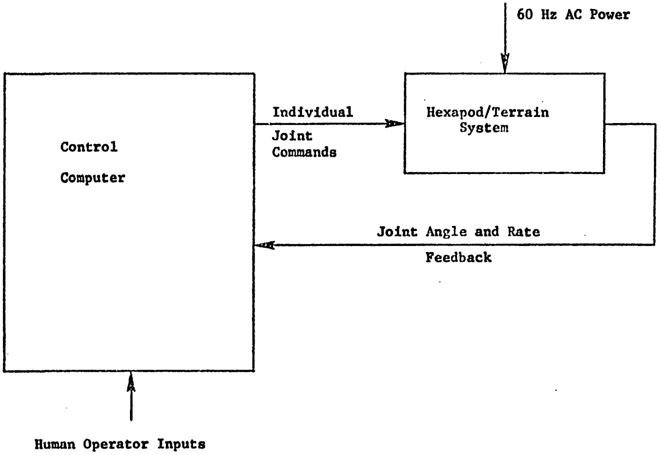

Figure 3.4. Overall Block Diagram of Hexapod Vehicle System Hardware.

the machine is mechanically constructed so that there exist significant differences in leg lengths, etc. Also, the need for gyros to provide feedback about body orientation is eliminated because the vehicle is constrained to move in a straight line and on flat ground only.

Despite the above simplifications, the control problem still remains fairly complex. A gait must be chosen and the control system must be able to implement this gait in real-time. The feet of the opposing legs on each side must be so placed as to not develop any lateral forces that would distort the body in the absence of a mechanical suspension system, or force feedback. The legs must also be coordinated so as to eliminate leg "binding" in which one foot is dragged by the body. When McGhee and Frank built the first digitally controlled machine, the "Phoney Pony", they observed this phenomenon, and also came up with the cure for the problem by incorporating additional "wait" states [2,45]. Finally, while the various aspects of computational speed of the control processor are not a locomotion problem, nonetheless these do make the actual practical implementation of the control system a problem. The PDP-11/45 with only software routines available to perform mathematical functions become intolerably slow for real-time control of the vehicle, even when the vehicle is only walking in a straight line on level ground. To calculate the gait and translate speed and stride commands from the human operator into individual joint commands requires a coordinate transformation with mathematical functions that take too long to calculate. If all this must be done in real time, then, even with a mechanical system such as a vehicle with time constants of the order of 100 to 200 milliseconds, the sampling time must be of the order of 1/30 second to prevent instability and sustain smooth motion.

For the above stated reasons, off-line computation will be allowed in this dissertation for the <u>motion planning</u> phase of control in which joint trajectories are determined from a knowledge of the desired speed, stride length, and other higher level commands from the operator. In contrast to motion planning, <u>motion execution</u> is the actual implementation of the planned motion. While motion planning is an open-loop type of calculation and involves a large number of computations because of coordinate transformations from foot positions to joint angles, motion execution is a closed loop control operation. That is, during motion execution, the controller tries to implement the planned joint trajectories by comparing the actual joint motion with the planned motion and adjusts joint commands to compensate for any errors in the joint trajectories.

3.5 Summary

The problem of legged locomotion system design has been divided in this dissertation into two distinct parts: the hexapod vehicular system and the control system. The problems posed by the vehicular system were shown to be related to hardware and several major conclusions were reached based upon the constraints and other considerations discussed in this chapter. The constraints imposed on the vehicular system are as follows: The vehicle is to be operated in a laboratory only and there will be no self-contained power unit aboard the machine; all power will be obtained from a 60Hz AC source. Control of the vehicle is to be accomplished by an off-board computer with communication between the control computer and the vehicle taking place through a trailing umbilical cord. There will be no joystick control of the vehicle which will only travel on level ground for the purpose of this dissertation, but which should have kinematic and structural capabilities adequate to permit eventual travelling on irregular terrain, negotiating staircases, slope-climbing, and climbing of obstacles. Based upon these constraints, the vehicle will be a six-legged machine with an arthropod leg geometry. The joints will be driven by electric joint actuators. Feedback information will consist of separate channels of joint position and joint rate information. Force feedback is related to future work to be done on the hexapod.

Certain constraints are also laid down upon the control computer architecture. The control computer must be able to do floating point arithmetic. The real-time input/output capability must extend to a minimum of 36 A/D channels and 18 D/A channels. A real-time clock, interrupt capability, and utility routines for reading the clock and for doing input/output to a sequential access medium such as magnetic tape are other important features.

Finally, the straight-line locomotion problem was shown to have several aspects - choice of gait, maintaining a level body, preventing leg binding, and so on.

In the next chapter, a specific design for the hexapod vehicle hardware will be presented in detail, together with suggestions for improvements in the mechanical design. Chapter 5 describes the hexapod real-time software, while Chapter 6 presents experimental results and discusses the limits imposed by the hardware and those imposed by the software. Chapter 7 lists the contributions of this research and suggests areas for further research.

CHAPTER 4

HEXAPOD SYSTEM HARDWARE DESIGN

4.1 Introduction

In this chapter the hexapod mechanical system is described in detail covering the design of the joints, the interconnection of joints to form the limb, and the interconnection of limbs to form the body. Only a brief description of the vehicle electronic system [46] is presented since the design of the electronics was not directly part of this dissertation research. In the design of the mechanical system, derivations for critical dimensions of parts are presented where required so as to provide an indication of the limitations of the mechanical design. Finally, the overall electromechanical system specifications are presented to show the capabilities of the machine in terms of power, output torque capability, and structural strength.

4.2 Joint Design

Although the knee, hip elevation, and hip rotation joints are all subjected to quite different types of loads, it was decided that a common design for all three joints would be adopted There are two advantages to having a common joint design - first, replaceability of common parts becomes possible and secondly, it is feasible to set up almost an assembly-line for machining the different parts of the joint. Replaceability of common parts means that by making a few spares for every part needed in the joint, it becomes possible to quickly repair any part in any joint that fails, thus minimizing the number of spare parts to be made. By setting up an assembly-line for machining, it is meant that it is possible to use common jigs and fixtures for machining a part for all eighteen joints so that considerable time can be saved in the machining. Having decided to use a common design for all three leg joints, the joint must obviously be designed around the maximum load that any one of the three joints is likely to encounter. This of course is the penalty that is paid for a common design; viz., the knee joint strength requirements are considerably lower than those for the other two joints so that it is overdesigned. For the hip elevation and hip rotation joints, the hip elevation joint is subjected to the heaviest loads during locomotion on level terrain but the hip rotation joint might also be subjected to the same kind of heavy loads while walking up slopes.

If the hexapod is walking with the fastest optimal wave gait, the tripod gait, then at any instant of time there are only three legs on the ground. Two of these are on one side of the vehicle and one is on the other. Thus, assuming that the weight of the vehicle is not to exceed 200 pounds, each leg must be capable of exerting a reaction of 100 pounds on the ground. Thus the required elevation torque is

$$T = F \times \ell = 100\ell \tag{4-1}$$

where F is the ground reaction force and ℓ is the corresponding lever arm.

Assuming once more that ℓ is about one foot (since the machine must be able to negotiate commercial staircases, the width is restricted) then the maximum torque is 100 foot-pounds. For a safety factor of 2, the design torque is therefore 200 foot-pounds. The entire power train is thus designed around this value. All elements of the power train are described in the following section.

4.2.1 The Power Transfer Train

The power transfer train consists of the following members: the drive motor and its internal gear reduction unit, an external spur gear train, and a worm gear train which provides the final speed reduction. The last two gear trains and an associated housing were designed by A. A. Frank [34] and first used in the "Phoney Pony". A similar housing and worm gear train have been retained in the joint for the hexapod vehicle. The worm gear specifications are listed on the next page [47].

From the input horsepower, the worm rpm, and the output torque, it is possible to compute the output hp and the worm gear efficiency at the maximum rpm that it is likely to operate.

$$\text{Output rpm} = \frac{600}{\text{velocity ratio}} = \frac{600}{N} = \frac{600}{50} = 12 \text{ rpm} \tag{4-2}$$

$$\text{Output hp} = \frac{12 \text{ rpm} \times 998 \text{ in-lb}}{63{,}025} = 0.19 \tag{4-3}$$

$$\text{Efficiency} = \frac{\text{Output hp}}{\text{Input hp}} = \frac{0.19}{0.30} = 63\% \tag{4-4}$$

Boston Worm Gear Specifications

Boston Catalog No. GB1053

Part - 1/2" face bronze worm gear
Number of teeth - 50
Pressure Angle - 14½°
Pitch - 12 single thread right-hand
Pitch Diameter - 4.167 inches

Boston Worm (steel) Specifications

Boston Catalog Part No. H1056R

Pitch Diameter - 1 inch
Keyway - 1/8 inch
Lead Angle - 4°46'
Lead - 0.2618 inch

For a GB1053 and H1056R worm gear combination
Input hp at worm RPM = 600 - 0.3
Output torque at above rpm and input hp - 998 in-lb.

The output torque rating of 998 in-lb (90 ft-lb) at 600 rpm worm speed is for continuous duty. The torque rating is much higher for intermittent operation. From [48], the lead angle should be less than 5° for the worm to be self-locking or irreversible. This condition is satisfied by the worm used. The price that must be paid for this self-locking feature is that the efficiency is quite poor. Specifically, efficiency is related to the lead angle by the following formula [49],

$$\mu = \frac{\cos\phi_n - \tan\lambda}{\cos\phi_n - \mu\cos\lambda} \qquad (4\text{-}5)$$

where ϕ_n is the normal pressure angle, μ is the coefficient of friction, and λ is the lead angle. Hence it follows that the smaller the lead angle, the lower must be the resulting efficiency.

The theoretically predicted efficiency for the worm gear train is, with $\phi_n = 14\frac{1}{2}°$, $\lambda = 4.46°$, and $\mu = 0.062$ [50], $\eta_{predicted} = 56\%$. This efficiency is lower than that given by Eq. (4-4) because the value used for μ in Eq. (4-5) corresponds to the average joint speed anticipated rather than the maximum speed associated with the 63% efficiency figure.

4.2.2 The Spur Gear Train and Overload Clutch

The worm is driven by a spur gear through an overload clutch plate assembly. A clutch is necessary so that if the leg is trapped or otherwise unable to move such that the joints are unable to rotate, then the drive motor should not burn out. The clutch plate assembly is mounted on the larger of the spur gears because of the large surface area available.

The spur gear train consists of Boston Gear parts number GA21 and GA61. These gears use the involute system of gearing. In this system the gears are developed to operate with a rack having straight sided teeth oriented at a standard pressure angle. This makes the gears interchangeable because they are made to operate with the rack. These gears incorporate a standard $14\frac{1}{2}°$ pressure angle. A $14\frac{1}{2}°$ pressure angle is used in cases where backlash is to be minimized. The factory specifications for this gear train are given on the next page [47].

Figures 4.1 and 4.2 show the clutch plate assembly and the manner in which it is mounted on the larger spur gear. The spur

Boston Gear Spur Gear Ratings

Boston Catalog No. GA21 Spur Gear

Part - Steel change gear, 3/8" face
Diametrical Pitch - 20
Pressure Angle - 14½°
Number of teeth - 21
Approximate hp rating - 0.35 @ 1000 RPM

Boston Catalog No. GA61 Spur Gear

Part - Cast iron change gear - 3/8" face
Diametrical Pitch - 20
Pressure Angle - 14½°
Number of teeth - 61
Approximate hp rating - 0.35 @ 300 RPM

gear is initially faced off to a depth of 1/16" to provide a seat for the clutch plates. The actual clutch plates are made of cork and are 2½" in diameter. The clamping force required to obtain a torque at which the clutch disc just begins to slip can be derived as follows (See Figure 4.3):

Assuming that the pressure P on the plate is constant, the normal force on the circular element of arc $2\pi rdr$ is given by

$$dF_n = P \times 2\pi rdr \tag{4-6}$$

The frictional force is therefore

$$dF = \mu P \times 2\pi rdr \tag{4-7}$$

and the incremental torque due to the frictional force is

$$dT = dF \times r \tag{4-8}$$

Figure 4.1. Gear and Clutch Plate.

Figure 4.2. Clutch Plate Assembly.

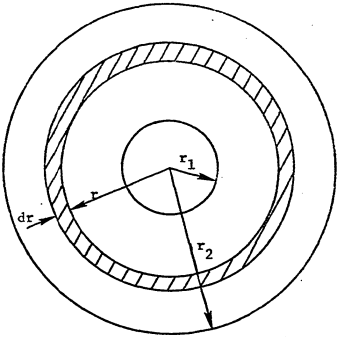

Figure 4.3. Calculation of Friction Torque on Clutch Plate.

Therefore, the net torque at which the plate just begins to slip when subjected to a torque is given by,

$$T = 2\int_{r_1}^{r_2} dT = 2\int_{r_1}^{r_2} \mu P \times 2\pi r dr \times r \tag{4-9}$$

where the factor of 2 enters since there are two clutch plate surfaces. Thus

$$T = \mu P \int_{r_1}^{r_2} 4\pi r^2 dr \tag{4-10}$$

$$= \frac{4}{3}\pi\mu P(r_2{}^3 - r_1{}^3) \tag{4-11}$$

Now since it is assumed that the pressure P due to the clamping force is constant over the entire surface area, then,

$$P = \frac{F_c}{\pi(r_2^{\,2}-r_1^{\,2})} \tag{4-12}$$

where F_c is the required clamping force. Thus

$$T = \frac{4}{3}\ F_c \times \mu \times \frac{(r_2^{\,3}-r_1^{\,3})}{(r_2^{\,2}-r_1^{\,2})} \tag{4-13}$$

$$= \ \frac{4}{3}\mu F_c \times \frac{r_2^{\,2}+r_1r_2+r_1^{\,2}}{r_1+r_2} \tag{4-14}$$

With $r_1 = 5/16$ and $r_2 = 1\ 1/4$, $\mu = 0.4$, and a slip torque $T = 2$ ft-lbs, the clamping force is given by $F_c = 150$ lbs. Obviously, an extremely stiff spring must be selected.

A 1/4" wire diameter, 2-turn, 1 5/8" coil diameter spring is chosen with a spring constant of about 1000 lbs/inch. This clamping force is applied by the circular internally threaded nut which applies the clamping force and also serves to seat the spring properly on the plate (Figure 4.1).

The hollow screw which is fixed to the lower clutch plate slips over the worm and is keyed to the ½" shaft on which the worm is mounted (Figures 4.4 and 4.5). The shearing stress due to torque on the hollow screw is probably the most severe load that any member of clutch plate assembly is subjected to. This shearing stress can be calculated as follows [49]:

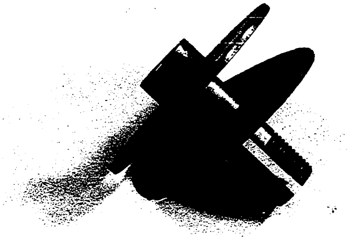

Figure 4.4. Lower Clutch Plate Assembly.

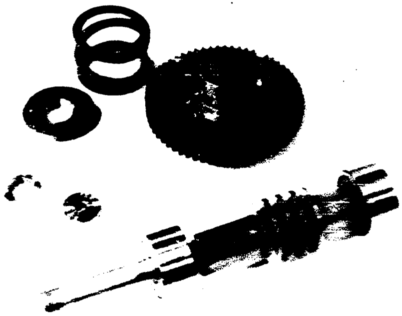

Figure 4.5. Parts for the Clutch Plate and for Coupling to the Worm Shaft.

$$S_s = \frac{T}{2AC} \tag{4-15}$$

where S_s is the shearing stress, T is the torque to which the screw is subjected, A is the area enclosed by a line running through the center of the wall section, and C is the smallest width of the wall. For T = 24 in-lb = 2 ft-lb.

$$A = \frac{\pi}{4} \times \frac{5}{8}^2 \tag{4-16}$$

and c = 0.030 inch (after subtracting the depth of the thread), so S_s = 1600 psi. The maximum shear stress for mild steel 21,500 psi [49] so this design yields a large margin of safety.

The ½" shaft on which the worm is mounted is supported in the gear housing by a pair of New Departure No. 5501 bearings. The specifications for these bearings are listed below. The 5501 bearings are double row ball bearings for increased axial and radial rigidity, with a single shield.

New Departure Catalog Part No. 5501
Double Row Ball Bearings

Width - 5/8"
Weight - 0.15 lb
Outer Diameter - 1 7/16"
*Radial Load Rating @ 33 1/3 RPM - 1390 lbs
@ 500 RPM - 565 lbs

*Radial load rating based upon 1500 hours minimum life.

4.2.3 Drive Motor

The power source for driving the gear trains described above consists of an industrial quality Black and Decker drill motor. The power source or drive motor must be inexpensive, easily available (preferably off-the-shelf) and must be extremely rugged and reliable. The motor must be inexpensive since 18 motors have to be used and therefore cost savings on an individual motor are multiplied by a factor of 18. It must be easily available and extremely rugged, reliable and replaceable since the motors are likely to get burnt out when experimenting with new modes of locomotion. The motor should further have a stall torque capability greater than 2.6 ft-lbs. This number is arrived at by dividing the maximum design torque of 200 ft-lbs by the gear ratio of the spur gear train (1: 2·9) and again by the gear ratio of the worm gear train (1:50) and by the efficiencies of the spur and worm gear trains. The drive motor must also be capable of providing at least 100 ft-lbs at the normal walking speeds that the vehicle is likely to encounter. Again, for a net gear reduction of 1:145, this speed corresponds to a motor speed of about 300 RPM. The drive motor must also be compact and lightweight. Drill motors have this advantage, as well as several of the other above mentioned desirable characteristics. Commercial drill motors are readily available, and if an industrial motor is chosen, the the motor is also extremely rugged and reliable. A Black and Decker drill type #1174 has been selected as the drive motor (Figure 4.6). It is an industrial drill motor, available at a moderate cost and is readily available on an

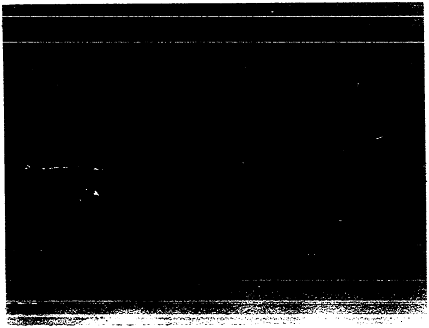

Figure 4.6. Modified Black and Decker Drill Motor No. 1174.

"off-the-shelf" basis from local suppliers. The factory specifications for this drill are given below.

Black and Decker Drill # 1174 Type 3

Part - 3/8" heavy duty holegun drill
Voltage - 120 volt ac/dc
No load rpm - 1000 rpm
Rated current - 3A
Rated output - 1.7 ft-lb at 650 rpm
H.P. - 0.21 hp
Stall torque - 13.6 ft-lb

The selected motor has an internal gear reduction as illustrated in Figure 4.7. The total reduction ratio from the armature to the drill output is 29.4:1. The motor also drives a fan which is required for cooling. All of the rotating parts use ball type or needle type bearings. This makes the unit highly reliable with a long life expectancy.

Electrically, the motor is a universal series wound type. Series wound motors are extensively used for drives in power tools, appliances and other such applications. They offer high starting torques and large power capabilities within a compact unit. As shipped from the factory, the motor comes with the armature connected in series with a split field, but the motor was modified so as to allow separate excitation of the armature and field. A series of experiments were carried out [46] to find the motor electrical characteristics. These are listed on the next page [46].

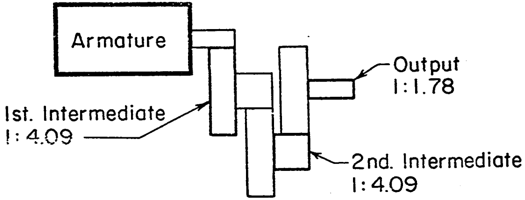

Figure 4.7. Drill Motor Internal Gear Reduction.

Experimental Motor Parameters for
Black and Decker Drill #1174

1) Resistance - $R = 11$ ohms from V-I curve
$R = 10.4$ ohms from bridge measurement
($R_F = 3.9$ ohms, $R_A = 6.5$ ohms)

2) Inductance - $L = 25$ mH from bridge measurements
($L_F = 18.8$ mH, $L_A - 6.2$ mH)

3) Starting Current - $I_s = 0.7$ amps

4) No-Load Current - $I_{NL} = 1.8$ amps (at 1000 rpm) from a plot of $\Delta I_{NL}/\Delta\omega$, no-load current as a function of a motor rate can be written as

$$I_{NL}(\omega) = 1.1 \times 10^{-3}\,\omega + 0.7$$

5) Electrical Time Constant - $t_e = 2.27$ ms (from L/R)

$= 2.3$ ms (from oscilloscope)

6) Mechanical Time Constant - $t_m = 175$ ms

7) Speed Torque Curves - See Figure 16 in [46]

8) Static Friction Torque - $T_F = 0.25$ ft-lbs

9) Internal Torque Loss - $T_L = 1.17$ ft-lbs (at 1000 rpm) From a plot of $\Delta T_L/\Delta\omega$, internal torque loss as a function of motor rate can be written as

$$T_L(\omega) = 0.92 \times 10^{-3}\,\omega + 0.25$$

10) Torque Constant - $K_T = 0.9$ ft-lbs/amp

The bronze worm gear that meshes with the worm is only a segment of an entire gear. Each No. GB1053 bronze worm is cut into two halves and each half is mounted on an aluminum mount the other end of which also forms the stub onto which the limb segment is attached (Figure 4.8). The aluminum mount is keyed to a 5/8" diameter "floating" steel shaft, which is called a "floating fulcrum" since it does not carry any torque, but merely serves as a fulcrum about which the gear can rotate. The floating shaft also serves another purpose, namely, to provide a convenient point for monitoring the joint angle. This is discussed further in the next section.

4.2.4 Joint Instrumentation

As discussed in Chapter 3 both joint angle and joint rate feedback are required for the control concept implemented in this research. Instrumentation for measuring each of these quantities is discussed in turn in the following paragraphs.

4.2.4.1 Joint Angle Measurement

The joint angle can be measured quite simply by coupling a potentiometer to the joint output shaft (Figure 4.9). The "floating" shaft turns with the bronze worm gear since a flat surface has been machined on the 5/8" shaft for a set-screw that is screwed through the aluminum mount for the gear and rests on the flat. Since no torque is to be transmitted by the floating shaft, this arrangement is adequate and no keying is necessary. The shaft turns within two Fafnir No. S7KDD bearings. These are extra-small light bearings with two shields and are not

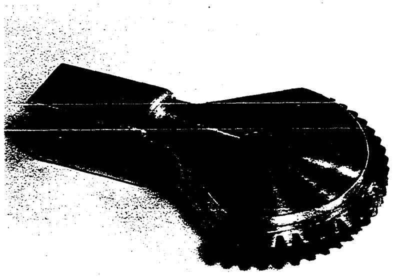

Figure 4.8. Bronze Worm Gear and Aluminum Mounting.

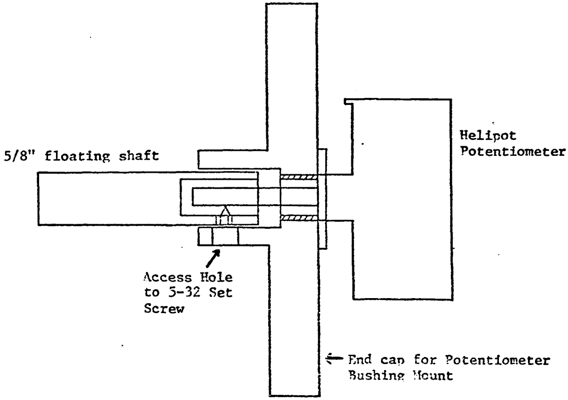

Figure 4.9. Side View Drawing Showing Coupling of the Potentiometer Shaft to the Joint Output Shaft.

really designed to carry radial, axial thrust, or combined loads. The relevant information about these bearings is given below [51].

Fafner S7KDD Extra-Small Single Row Ball Bearings

Bore - 5/8"
Outer Diameter - 1 3/8"
Width - 0.2812
Shield Width - 11/32"
Fillet Radius - .031"
*Radial Load Rating - 1180 lbs at 33 1/3 rpm
1030 lbs at 50 rpm
815 lbs at 100 rpm
476 lbs at 400 rpm

*Load rating is based on 1500 hours minimum life.

Since the leg joint can only move through about half of a circle, a one-turn potentiometer may be used. The particular potentiometer chosen must be easy to couple to the shaft. A Helipot Precision Potentiometer was chosen for this purpose. The electrical and mechanical characteristics of this device are listed below [52].

Helipot Model G Precision Potentiometer

Resistance - 1KOhm (C.T.)
Linearity - 0.5%
Shaft Diameter - 1/4"
Bushing Mount Diameter - 1 5/16"

By choosing a 1 KOhm potentiometer, the current drain on the power supply is very much larger than if a larger resistance were used, but better linearity in the amplification circuit for the potentiometer is obtained. The helipot shaft is coupled to the floating shaft as shown in Figure 4.9. The No. 5-32 set screw couples the motion of the 5/8" shaft to the potentiometer shaft which moves the wiper arm of the potentiometer. The bushing mount is screwed onto the end-cap which is in turn fixed to the aluminum housing for the joint. The potentiometer can be zeroed by loosening the lock-nut that locks the bushing mount to the threaded end-cap, turning the potentiometer in either direction till a zero is read, and then tightening the locknut to once again fix the potentiometer bushing mount to the end-cap.

4.2.4.2 Joint Rate Measurement

Joint rate measurement is accomplished by a tachometer It is not feasible to differentiate the joint position information from the potentiometer since this information is too slowly varying to be usable in this way. Furthermore, for the same reason it is best to place the tachometer at the fastest moving output since a larger output voltage can be obtained thereby for a tachometer with a small volts/rpm gain constant. Considering that the motor no-load RPM is 1000 RPM, a SERVO-TEK SA769A-2 7V/1000 RPM tachometer was chosen to provide rate information. The SERVO-TEK SA769A-2 is a permanent magnet type DC tachometer. The specifications for the tachometer are listed on the next page [52].

Characteristics of SERVO-TEK
SA769A-2 PM DC Tachometer

Output - 7V/1000 RPM
Linearity - 0.1%
Max. Speed - 12000 RPM
Body Diameter - 1.130 inches
Shaft Diameter - 0.120 inches
Shaft Length - 1/2"
Face Mount, 3 tapped holes on
3/4" centers
Pilot Diameter - 1/2"

The tachometer is mounted in an aluminum mount (Figure 4.10) for coupling to the motor output shaft. The mount has a 1 7/16" hole with a 1/8" shoulder for aligning the motor and smaller spur gear or pinion to the larger spur gear. It also has three holes drilled at 3/4" centers for face-mounting the tachometer. The aluminum mount also serves to center the spur gear train and hence this is a critical part since loose tolerances would be reflected in excessive backlash in the spur gear train and also excessive tooth wear.

The hip rotation joint is slightly different in design compared to the other two joints because of the manner in which it is attached to the hip elevation joint. Instead of attaching it at the stub of the aluminum mount for the worm gear, the elevation joint is attached at the hip rotation joint output shaft so that, unlike the floating shaft in the other two joints, this shaft transmits joint-torque and hence is much heavier in

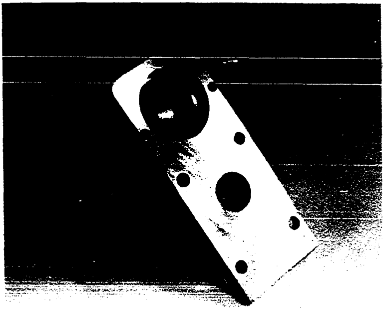

Figure 4.10. Tachometer Mounting Bracket.

design. This aspect of the hip rotation joint design is discussed in Section 4.3 on the attachment of the hip elevation joint to the hip rotation joint.

4.3 Overall Mechanical Design

The overal mechanical design concerns the manner in which the three joints, the hip azimuth joint, the hip elevation joint and the knee joint are connected together to form a leg and also the manner in which the legs are put together to form the entire hexapod vehicle.

The aluminum mount for the bronze worm gear presents a natural stub on the other end which is an eminently suitable place for mounting the limb segment. The stub on which the limb is mounted (Figure 4.11), also serves another useful purpose. It serves to act as a mechanical stop or end of travel for the worm gear when it hits the aluminum gear housing so that the worm gear never runs off the worm and disengages. Hence limbs are attached to the joints at the elevation joint and to the knee joint by this rather simple technique. Four 1/4-20 socket head cap-screws are used to attach the limbs to the stubs.

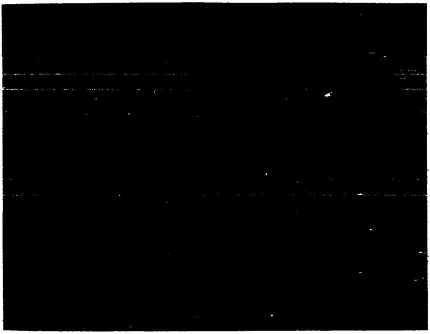

Figure 4.11. Attachment of Limb Segment to Joint.

4.3.1 Attachment of Knee to the Upper Limb

This joint is very simple to make. The limbs are made of 1 1/2 inch square aluminum extrusions, 1/8 inch thick. This makes them quite rigid so that very small deflections may be expected. This statement is justified below.

The effect of a foot reaction force perpendicular to the limb is shown in Figure 4.12. The joint on the other hand is perhaps somewhat inaccurately modelled as remaining fixed under the application of a load at the foot. Nevertheless, under this assumption it can be shown [49], that the maximum perpendicular deflection that can be expected due to the foot reaction force is given by

$$y_{max} = \frac{Pl^3}{3EI} \tag{4-17}$$

where P is the load in pounds, l is the limb length in inches, E is the Young's modulus of elasticity, and I is the moment of inertia.

When climbing a hill or a slope, the maximum tangential force that a leg might expect to see would be approximately 1/3 of the body weight (assuming a very steep slope and a tripod gait). Hence the maximum force P is about 80 pounds.

The required moment of inertia I is,

$$I = \frac{1}{12} (1\tfrac{1}{2})^4 - (1\tfrac{1}{4})^4 = 0.128 \text{ in}^3$$

and $E = 10 \times 10^6$ psi for aluminum so that y_{max} is .033 in. for $\ell = 14$ inches which is the longest limb segment.

The knee joint is attached to the hip elevation limb as shown in Figure 4.13. A spacer of the dimensions shown in the figure has been made to attach the upper segment to the aluminum housing for the knee joint. Four 1/4-20 socket-head cap-screws are used to make the attachment to both.

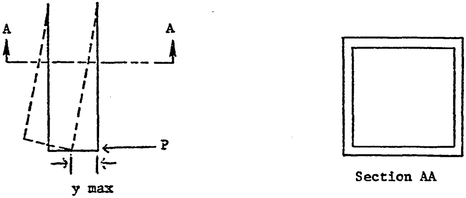

Figure 4.12. Effect of a Foot Reaction Force P on the Lower Limb.

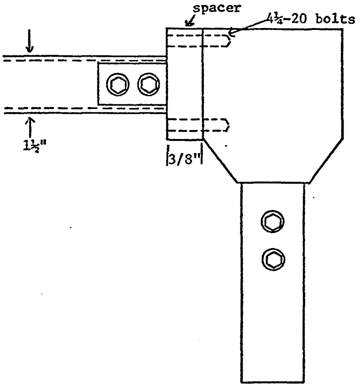

Figure 4.13. Attachment of Knee Joint to Hip Elevation Joint.

4.3.2 Attachment of the Hip Elevation Joint to the Hip Azimuth Joint

Although there are advantages to designing all joints identically, the very nature of the hip rotation joint requires a slight difference in the design. This is so because the intention was to build a hip joint as alike as possible to a two-degree of freedom joint by utilizing two one-degree of freedom joints. Since the two degrees of freedom were to be placed as close as possible within certain space and mechanical design constraints, it was not possible to use the stub of the worm gear mounting on the rotation joint to mount the hip elevation joint. Instead, another design was sought that could give closer proximity of the two axes of rotation. As discussed in Chapter 3, the decision had already been made to fix the azimuth joint to the body and to attach the elevation joint to the azimuth joint. Two different ways of coupling the azimuth shaft to the elevation joint are shown in Figures 4.14 and 4.15. The manner of coupling shown in Figure 4.14, requires the construction of a special yoke whereas in Figure 4.15, the shaft has a flat surface that is milled onto it so that the required attachment can be made by drilling and tapping holes for three bolts. By using the yoke arrangement, it would be possible to avoid any offset between the axes of rotation of the two joints thereby providing intersecting azimuth and elevation axes. The advantage that this presents has been discussed in Chapter 3. While the design in Figure 4.15, does not offer this advantage, it is very simple to construct. No special yoke has to be made. Hence the design in

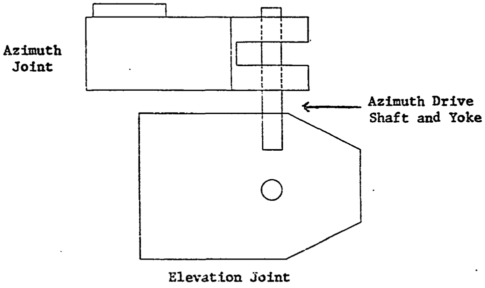

a) Front view

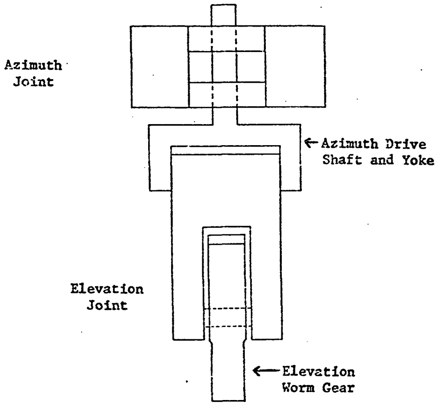

b) Side view

Figure 4.14. Attachment of Leg to Hip Azimuth Shaft by Means of a Yoke in Order to Obtain Intersecting Axes.

Figure 4.15 was utilized for making the connection between the two joints.

Since the shaft of the azimuth joint is unlike the"floating" shafts of the elevation and hip joints discussed earlier it has to be redesigned and must be much more sturdy. The azimuth axis shaft truly transmits the azimuth torque and therefore it was designed as follows.

As in the design of all other components, a design torque value of 200 ft-lbs is assumed.

Figure 4.15. Simplified Method of Attaching Leg to Hip Azimuth Shaft.

Then [49],

$$S_s = \frac{16T}{\pi d^3} \tag{4-18}$$

where S_s is the maximum shear stress and T is the torque and d is the shaft diameter.

This formula assumes that there is no transverse loading or bending. By the maximum shear theory of failure [49],

$$S_{max} = \frac{0.5S_{yp}}{FS} \tag{4-19}$$

where S_{yp} is the yield point and FS is the factor of safety.

For steel $S_{yp} = 40000$ and for FS = 2,

$$S_{s_{max}} = 10{,}000 \text{ psi} \tag{4-20}$$

Thus,

$$10{,}000 = \frac{16 \times 200 \times 12}{\pi d^3} \tag{4-21}$$

Solving for d, the result is:

$$d = 1.07 \text{ inches} \tag{4-22}$$

Hence, a 1" diameter steel shaft is used for the azimuth joint. New Departure No. R-16 shielded bearings are used to support this shaft. The specifications for the bearings are listed on the next page [51].

Because of the different shaft that is used in the azimuth joint, a slightly different approach has been taken to coupling a potentiometer to the 1" shaft. A 1/8" x 1/8" slot has been milled

New Departure No. R-16 Extra Small Single
Row Radial Type Ball Bearings

Bore - 1"
Outer Diameter - 2"
Width - 3/8"
Weight - 0.18 lbs
*Radial Load Rating at 33 1/3 rpm - 1730 lbs
at 100 rpm - 1200 lbs
at 500 rpm - 700 lbs

*Radial Load Rating based on 1500 hours minimum life.

to couple the potentiometer shaft to the 1" steel shaft with a set screw. This is shown in Figures 4.16 and 4.17.

The azimuth joint is attached to the elevation joint as shown in Figure 4.15 with three 1/4-20 bolts. The maximum shear stress on the bolts occurs when the machine has only three legs on the ground so that each leg must support almost 100 pounds.

Then the shear stress in each bolt is given by

$$S_s = 1/3 \times \frac{100}{\pi d^2/4} \qquad (4\text{-}23)$$

where $d = 1/4$. Thus $S_s = 679$ psi which is far less than the S_{yp} of 40,000 psi. However considerably greater momentary stresses could occur on impact of the leg with a rock or an unexpected obstacle and hence it is wise to provide a good safety margin.

4.3.3 Interconnection of the Legs

The body of the vehicle serves mainly to interconnect the legs of the machine and to provide a convenient place for

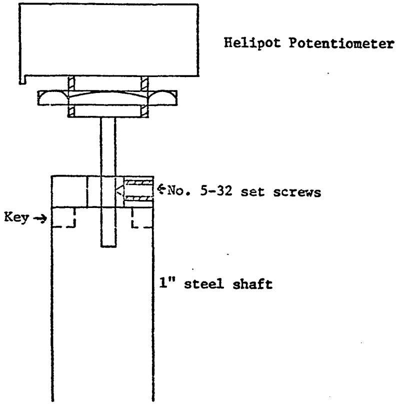

Figure 4.16. Coupling of Potentiometer to Hip Rotation Joint Shaft.

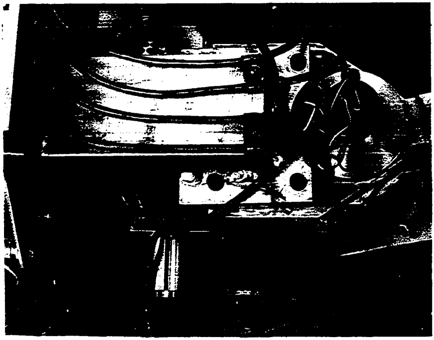

Figure 4.17. Photograph Showing Means of Attachment of Leg Assembly to Body and Mounting of Azimuth Potentiometer.

mounting electronics that drive the motors and perform signal conditioning for the potentiometers and the tachometers. Since it was decided that no explicit suspension system would actually be designed, but that the flexibility of the joints, the limbs, and the frame would be adequate, the design of the body of the machine consists of a long central square 1/8" thick aluminum extrusion, 2" x 2" across which cross-bars are laid out as shown in Figure 4.18 The legs are attached to the cross-bars at the hip rotation joint as shown in Figure 4.17.

4.4 Electronic System Description

The electronic system for the vehicle may be divided into two parts: the motor controller or the power section, and the joint instrumentation or the signal section. Both of these are briefly discussed below. Full details regarding vehicle electronics can be found in [46].

4.4.1 The Motor Controller

Figure 4.19 shows a block diagram of the motor controller. The armature winding is placed inside a full rectifier bridge so that current always flows through the motor in the same direction. However, depending on whether the triac is fired during the positive half-cycles or negative half-cycles only, the current through the field can flow in either direction. This gives the motor the capability to turn in either direction. Further, by controlling the firing angle of the triac, the amount of power that is transferred to the motor from the 120V, 60Hz ac source, can be controlled. The trigger electronics accepts a voltage ranging

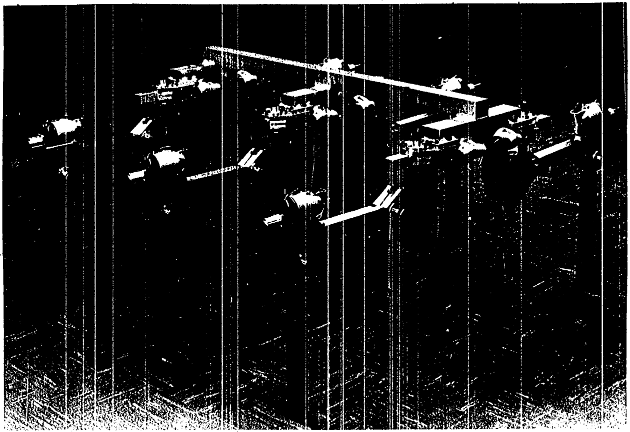

Figure 4.18. Completed Hexapod Leg and Body Assembly Prior to Mounting of Electronic Components.

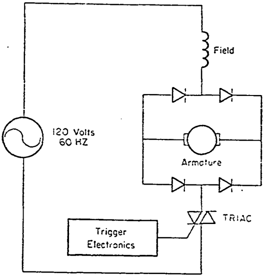

Figure 4.19. Half-Wave Motor Controller.

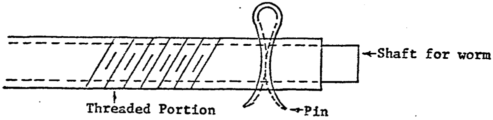

Figure 4.20. Use of a Tapered Pin to Couple the Clutch Plate to the Worm Shaft.

from -10V to +10V called the motor controller input, and fires the triac so that the average output voltage across the motor terminals varies approximately linearly with the motor controller input. The control voltage is provided under computer control through the 18 digital to analog converter channels.

4.4.2 The Joint Instrumentation Electronics

This system consists of the amplification and signal conditioning for the potentiometric and tachometric output signals. The tachometer output is a large signal (in volts), therefore it primarily needs to be filtered to eliminate 60Hz noise. The potentiometric output is also large signal. Both outputs are normalized with adjustable gain amplifiers so that 10 volts represents full scale. The conditioned outputs from the 18 potentiometer and 18 tachometer channels go to the analog to digital converter channels in the computer.

4.5 Improvements and Additions in Design

Based upon the performance of the vehicle, the difficulties encountered in machining and manufacturing the machine, and sheer hindsight, it is possible to suggest several modifications or improvements to the mechanical design of the hexapod vehicle. Some of these suggested designs involve more labor, but are perhaps desirable due to improved performance, while others offer the excellent combination of more performance for less work. These suggestions for improvements and for additions are presented next.

4.5.1 An Improved Clutch

The present clutch has a few problems associated with it. The threaded hollow bolt which is part of the lower clutch plate assembly (Figure 4.4), has slots cut into the threaded portion for keying to the shaft for the worm. Since the slots are cut into the threaded portion where the minimum thickness of the hollow bolt is only 30 thousandths of an inch, there is a possibility of the threads shearing off. This can happen because after tolerances for gear cutting and boring of the 1/2" diameter hole and the tolerance of the 5/8" diameter bolt, the net minimum thickness of the thread may be considerably less than 30 thousandths of an inch. Finally, if the two keys are not cut exactly so they fit just right in the two 1/8" slots, then all the force might be exerted by one key on only one key slot. Hence it is suggested that instead of keying to the shaft with two keys, a single taper pin made of spring steel should be used. This is illustrated in Figure 4.20. A great deal of machining time can be saved and also a stronger coupling can be obtained. This pin should be used to couple to the shaft at an unthreaded portion of the shaft for additional strength.

4.5.2 An Integrated Housing for the Worm Gears, Motor and Tachometer

As mentioned in Section 4.2.1 the housing used in the hexapod vehicle was designed for another vehicle [34] and has been only slightly modified. However it is possible to manufacture a housing for the worm gears that would also include the motor and tachometer. This would cut down on the number of parts to be made and simplify the tachometer mounting and motor mount which in the present vehicle takes a large amount of machining time to manufacture.

The advantages of using an integrated housing are many. First, all elements within the housing are protected, the motor, and the tachometer in particular. Since the tachometer is particularly vulnerable in the present arrangement, this is an important advantage. Secondly, all parts can be more efficienly arranged so as to reduce the amount of space that is required. Thirdly, since the tachometer housing is no longer in the way of the clutch, the clutch can be more easily removed. This is also true for removal of the tachometer. Finally, since all parts except the clutch and spur gear train are enclosed in a housing, such a design should be aesthetically appealing. It is also believed that there would be a net reduction in the amount of machining that has to be done. However, care would have to be taken to see that the motor runs cool. This could be done by ventilating the housing in the proximity of the motor.

4.5.3 Other Suggestions

Apart from the two major suggestions above, several minor suggestions can be made at this point. Instead of using the tachometer that is currently used, if a tachometer with a smaller diameter were used then the tachometer mount could be made smaller and again it would be easier to remove the clutch plate assembly. Instead of using 1 KOhm potentiometers, 10 KOhm potentiometers should have been used since the current drain is so large at present that the voltage regulators of the potentiometer power supply get too hot and are apt to fail. Instead of welding the cross-bars to the central bar that forms the spine of the body of the vehicle, and to the spacers for attaching to the hip joints, it would be better to use 1/4-20 bolts to fasten all three together. The hip azimuth joint housing would have to be drilled and tapped for the bolts, but the resulting joint would be stronger than a weld.

4.6 Summary

In this chapter the mechanical design of the hexapod vehicle has been detailed. The torque-capacity of each joint is about 200 foot-pounds. All parts in the joint have been designed around this value. Some suggestions for an improved mechanical design are also made herein. They include the design of a better clutch and an integrated housing for the motor, tachometer and worm gear trains. The integrated housing has the advantages of better protecting the motor and especially the tachometer. Also it is more efficient in terms of labor and space requirements.

The following chapter deals with the design and explanation of the real-time software for making the hexapod vehicle walk in a straight line on level terrain. It is hoped that covering the hexapod vehicle design in this chapter will lead to an easier understanding of the software employed for solving the straight-line locomotion problem.

CHAPTER 5

HEXAPOD SYSTEM REAL-TIME SOFTWARE DESIGN

5.1 Introduction

Speed of execution and program modularity are two important features of any real-time software system. Speed of execution is essential because if the program does not respond quickly enough to the real-time process, then this may affect its stability. The bandwidth of the process being controlled sets an upper limit on the control program execution time. A modular and well-structured program lends itself to easy debugging and modification.

The software for the hexapod has been written with these two concepts in mind. The walking speed of the hexapod is fairly low, about 0.5 feet/second, but even this low speed taxes the available control computer's execution speed. This is mainly due to the fact that the PDP-11/45 control computer used in this research lacks floating-point hardware so that all floating point calculations are done through software subroutines.

Execution speed is generally much higher in assembly language or machine language than in Fortran and therefore speed of execution requirements dictate that the programming should have been done in a lower-level language such as assembly language rather than Fortran. Assembly language programming is also more efficent in terms of program storage requirements. However, a Fortran program is much easier to write, debug, and modify than an assembly language program. Writing a Fortran program is made easy by the large number of mathematical functions that are very simply called in Fortran. The coordinate transformation equations presented later on in this chapter involve a larger number of trigonometric functions. Fortran is also a more "English-like" language and it is therefore easier to follow the flow of logic in Fortran than it is in assembly language. This is also due to the large number of equivalent assembly language statements for a single Fortran statement. The programs written for straight-line locomotion have been modified several times with relative ease because of their modularity in addition to their having been written in Fortran. Finally, due to the wide range of numbers used here, it is necessary to use floating-point arithmetic which is even harder to manipulate in assembly language than fixed point numbers. Thus, although speed of execution is such an important feature, it has been sacrificed in this research for the sake of ease of writing, debugging, and modifying the software.

Program modularity can be achieved by breaking up the main task of locomotion into separate tasks whereas good structure can be achieved by maintaining tables or vectors for the different locomotion parameters so that common task modules can be used to drive each of the six legs. Therefore, an attempt has been made to write a well-structured program. The program structures are suggested by the multiplicity of the legs and the similarity of the motion performed by each leg. In fact, the multiplicity of legs suggests the eventual possibility of using a multiprocessor structure where six identical microprocessors reside upon and control each leg and receive higher level commands from a coordination processor. From the modular structure of the present software, the breakdown of tasks is quite apparent between each leg's individual processor and the central processor. In fact, from the manner in which the present software is structured, it should become apparent that the present approach deliberately time-shares and thus serializes tasks that really should be performed in parallel.

Before delving into a detailed explanation of the flow chart for the program, a discussion of the major phases of the software is appropriate. A block diagram showing each major phase is presented in Figure 5.1 while a somewhat more detailed block diagram of the main program flow chart is shown in Figure 5.2.

As can be seen from Figure 5.1, the five major program phases are: data input, vehicle power-on and checkout, vehicle initialization, motion planning, and motion execution. Each of these phases is discussed in detail below.

5.2 Major Phases of Real Time Software

5.2.1 Data Input

The Data Input phase consists of reading parameters and receiving inputs from two sources - the operator and a data file stored on magnetic tape (Dectape). The operator is prompted to enter three inputs - the stride length, the forward speed of the vehicle, and a time parameter called ID with specifies the sampling period for the joint angles and joint rates in terms of the number of "clock ticks" (1/60 sec.) per sampling interval.

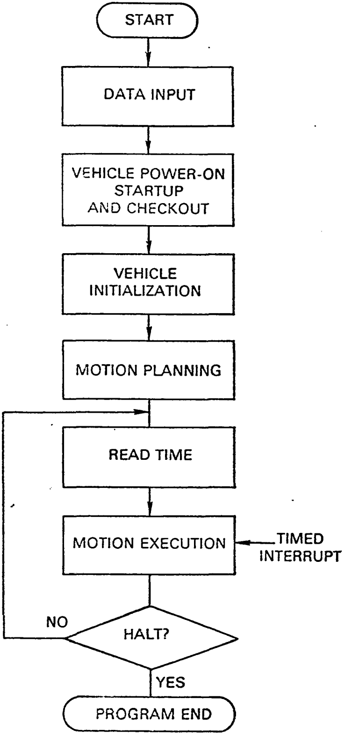

Figure 5.1. Overall Real-Time Software Organization.

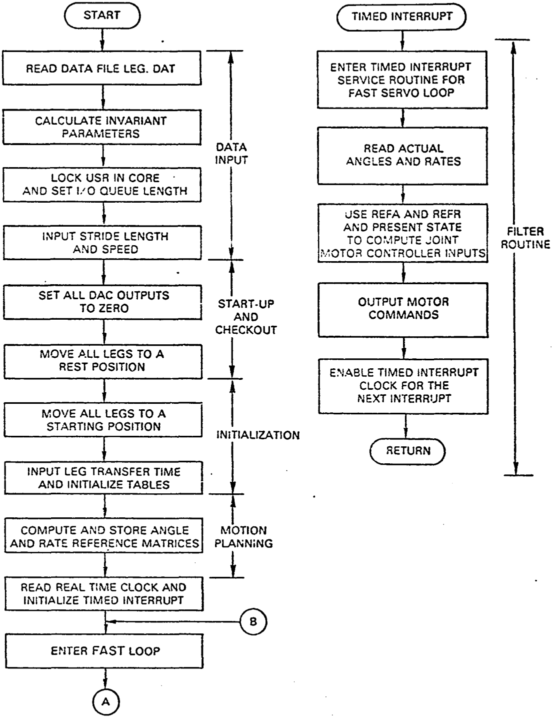

Figure 5.2. Flow Chart of the Main Program.

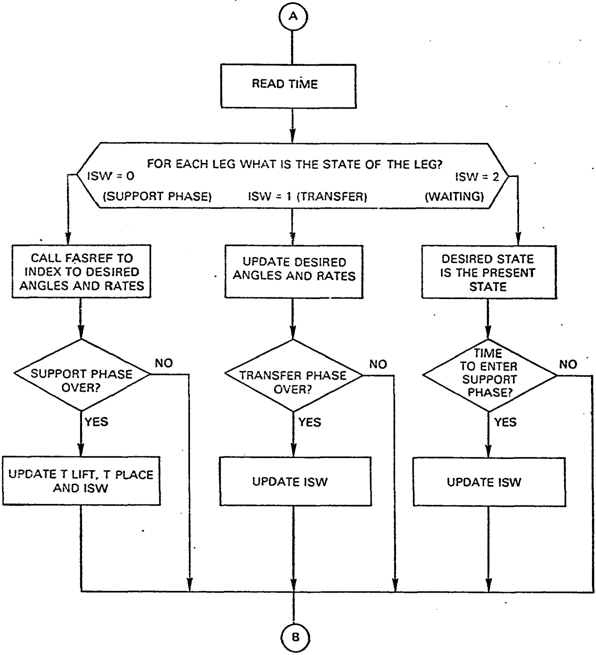

Figure 5.2. Flow Chart of the Main Program (Contd).

5.2.2 Vehicle Power-On, Start-Up, and Check Out

In this phase, first, all digital to analog converters (DACs) are cleared so that power to the hexapod can be turned on without the fear of random outputs on the DACs causing the joints to move in an uncontrolled fashion. Next, the machine goes through an "initial exercise" or checkout phase. All joints are moved to a rest configuration corresponding to zero reference angles and zero angular rates. It is necessary to come to a rest configuration before moving to the initial or starting position because movement to this configuration puts the machine into a stable condition from which initialization may proceded without fear of instability and also because visual inspection permits verification of correct functioning of the position transducers and the servo feedback loops. Thus, when the vehicle has gone through this phase successfully, one can conclude that all joints are operating correctly under computer control. After this phase, the program enters the vehicle initialization phase to place the limbs of the vehicle in their correct positions for initiation of locomotion for the selected gait.

5.2.3 Vehicle Initialization

The hexapod vehicle initialization phase performs two functions. First, as mentioned above, it physically positions the legs of the vehicle so that it is ready to take its first step and, secondly, it initializes certain program vectors that are used in the motion execution phase. A brief description of these vectors is presented here, but the manner in which they are utilized and a more detailed explanation of each vector is postponed until the section on the motion execution phase. The vector ISW contains six members, one member or element describing the current state of each leg. Each element can take one of the values 0, 1, or 2, where a value of 0 denotes that the associated leg is in the support phase, (on the ground), a leg state of 1 denotes that the leg is in the transfer phase (in the air), and leg state 2 denotes that the leg has completed the transfer phase too quickly and is waiting for the appropriate time to set the foot down and begin a support phase.

Two other vectors, TPLACE and TLIFT, are also maintained by the main program and are used by subroutine modules as well as by the main program itself. These two vectors keep track of when each leg is to be set down or lifted. Specifically, TPLACE(I) contains a value which tells when the ith leg will next be lifted to begin a transfer phase. The main program reads a real-time clock to keep track of the elapsed time. From a knowledge of the duty factor alone, it then updates TPLACE(I) and TLIFT(I) each time the ith leg begins a transfer phase, since, as explained in Chapter II,

$$\text{Transfer time} = (1-\beta)T \tag{5-1}$$

$$\text{Support time} = \beta T \tag{5-2}$$

where β is the duty cycle and T is the gait period.

Based upon a knowledge of the transfer time allowed by the operator, the stride length, and the speed, the program fills in the TPLACE and TLIFT vectors for the first time in the initialization phase. Three other variables that are computed in this phase are the duty factor, the support time (the time that each leg must spend on the ground), and the hip azimuth angle at the end of the transfer phase. It is assumed in every case that, for level locomotion, hip elevation and knee elevation angles of 0.1 radians should provide sufficient ground clearance in the transfer phase.

After the above computations have been made, all legs are then moved to an initial position which is that instant in the locomotion cycle when leg 1 (the left front leg) is just about to begin its support phase. Due to the choice of statically stable gaits only, the walking machine is able to stand in this initial position even with all power to the joints turned off. At this point the vehicle initialization phase is completed and the program enters the motion planning phase.

5.2.4 The Motion Planning Phase

If the hexapod vehicle were to truly operate in real-time, then motion planning and motion execution would be concurrent. However, as mentioned in the introduction to this chapter, the lack of floating point hardware in the computer available for this research slows it down so much that computation of the transformations that convert foot Cartesian coordinate positions and rates to joint angles and rates has to be done beforehand, thus separating motion planning from motion execution. The need for this separation has been verified by an attempt to accomplish motion planning in real time. As anticipated, the resulting cycle time was unacceptably long and gave rise to an undesirable jerkiness in the motion of the hexapod. Therefore, the *a priori* computations for the coordinate transformation from foot x, y, z, coordinates to joint angles and rates is done next by calling the subroutine TRAJ. Subroutine TRAJ divides the total time in the support phase into 500 points, and from a knowledge of the speed of the vehicle, fills two 3 x 500 reference matrices that store the desired joint angles and joint rates for the support-phase motion corresponding to the behavior determined in the Data Input phase of program execution. At each of these 500 points in time, a coordinate transformation is calculated and used to obtain the values stored in the reference matrices ANGLE and RATE. Thus, to know the desired angles and rates at any instant in time for a leg that is in the support phase, the time that has elapsed since the leg began the support phase is first calculated from the vector TPLACE. This elapsed time can then be used to index into the two reference matrices to retrieve the desired joint angles and rates.

Once the leg joint trajectory during the support phase has been computed entirely and stored, the motion execution phase can begin. This is the final phase and is described next.

5.2.5 The Motion Execution Phase

The motion execution phase implements the trajectory that was computed in the motion planning phase and essentially coordinates all six legs to operate the legged vehicle at the speed commanded by the operator in the program initialization phase. In order to attain the desired leg motions, some sort of a servo loop is required for each joint. Until recently, such a system would typically be analog in nature. However, in this research, it was decided that the flexibility of the digital computer should be taken advantage of by putting all joints under direct digital control. Closing the loops in this way provides many advantages, including the possibility of using different feedback control laws for the various phases of a leg cycle and dynamically changing feedback gains in accordance with the desired gait characteristics. The digital loop utilized in this research makes use of a timer that interrupts the main program every fixed number of clock ticks (1 tick = 1/60 sec), where the exact number is the value that the operator provides in the initialization phase. As a result of the interrupt, the program branches to a service routine called FILTER. Subroutine FILTER reads the desired joint angles and rates from two tables called REFA (REFerence Angle) and REFR (REFerence Rate), which are maintained and updated by the interrupted program. It also reads the actual joint angles and joint rates on the digital to analog converter channels and then uses motor controller joint input commands based upon the error between the desired angles and rates, and the actual joint angles and rates. The main program is itself executing the loop seen around the motion execution phase in Figure 5.1. This loop is called the slow loop because the digital servo loop might interrupt it several times before it is completed. Therefore, there are basically two loops operating together to achieve motion execution - a fast loop that interrupts the slow loop every fixed number of clock ticks and the slow loop that maintains time and updates all tables required to run the fast loop. The timed interrupt facility which the fast loop makes use of is available through a system subroutine called ITIMER. Toward the end of the routine FILTER, a call to ITIMER restarts a hardware timer in the computer which will subsequently issue the next timed interrupt to the computer after the desired number of clock ticks. FILTER specifies itself to be the interrupt service routine in the call to ITIMER so that at the end of the desired time interval it is reentered. Meanwhile, the slow loop may have updated some of the entries in the tables of desired angles and rates, REFA and REFR. The actual angles and rates may also have changed since the last time that they were read (on the previous interrupt), and so the routine FILTER calculates new motor input commands and outputs them. The fast loop therefore amounts to a servo loop that is closed in the control computer via software around each of the eighteen joints. The fast loop is started for the first time by calling FILTER just before entering the motion execution phase. After the first call, FILTER effectively calls itself.

The slow loop in the motion execution phase is already initialized when it is first entered. This occurs in the vehicle initialization phase. As mentioned in the section on vehicle initialization, the function of the main program in the execution phase is to constantly update tables so that the servo loop can take the appropriate action on the joint. For this purpose, it maintains three important tables that have been defined earlier - ISW on the leg-state vector, and TLIFT and TPLACE, which are the vectors that denote the leg placing and leg lifting events. The program therefore executes an endless loop (the slow loop) in which it looks at the position of each individual leg and takes a specific action depending upon the current state. Specifically, if ISW(I) is a 1, then leg I is assumed to be in the transfer phase. Hence, the desired joint angles are the ones that the leg would attain at the end of the transfer phase. The desired rates for all three joints are taken to be zero in this phase. The three angles and the three rates corresponding to Leg I in tables REFA and REFR are updated to reflect these new values. A check is also made to see if the leg has already reached the end of the transfer phase in which case ISW(I) is also updated to either a "0" or "2" so that the leg I next enters either the support phase or goes into a wait state depending upon whether the leg is ready to be set down or not. The leg is not ready to be set down if it completed the transfer phase in less time than that allotted by the operator at data entry time. Thus, if the leg return stroke is completed ahead of the scheduled time, then the leg goes through a waiting period. However, if the time allotted for the return stroke is too short, or if the leg is too slow in the transfer phase, then the leg is nevertheless set down when it is time to begin the support phase. The effect of this is obvious, namely, there is an automatic shortening of the stride length and thus an automatic decrease in the vehicle speed. This is extremely desirable because the vehicle can thus adjust its speed according to the capabilities of its legs. This is therfore a self-regulating feature of the software that never lets time synchronism be lost if for some reason one or more of the legs does not respond as quickly as planned. Such a regulatory feature is also essential because an operator might very well command an unrealistic speed that the machine is incapable of handling.

If ISW(I) is a "0" then the program calls the subroutine FASREF (FASt REFerence) which calculates the total time leg I has been on the ground in the support phase and uses this time to computer an address index into the reference matrices ANGLE and RATE which were computed during the motion planning phase. The three joint angles and joint rates at that address are then returned to the calling program which in turn enters these six values into the two vectors REFA and REFR. If leg I has completed the support phase then ISW(I) is changed to a "1" so that the leg can next enter the transfer phase. The ith entries in TLIFT and TPLACE are also updated so that the next time the leg will be lifted is after one full locomotion cycle period, and the next time that the leg will be set down is after the time period given by Eq. (5-1).

If ISW(I) is "2", implying that the leg ended the transfer phase too soon, then no action is taken on the leg until it it time to put down the leg as determined by the ith entry in TPLACE.

Time is kept by the executing program by reading the real time clock in the computer using a system routine called GTIM. Time-keeping is an important function of the executing program since changes in leg-state, position, and rate are all actions that depend on the current time.

The next section of this chapter describes individual program modules, some of which were only mentioned in the previous sections. This description is followed by a summary of this chapter.

5.3 Detailed Description of Program Modules

5.3.1 Coordinate Transformation Subroutines

Figure A.2 presents a schematic drawing of the leg of the hexapod showing the foot position X_1, Y_1, Z_1, as measured in the hip coordinate system, X, Y, Z. As shown in this figure, the X axis points in the direction of motion of the hexapod, the Z axis points downward towards the ground, and the Y axis forms a right-handed cartesian coordinate system together with the X and Z axes. Appropriate transformations can be used to express the three joint angles and three joint rates in terms of the foot X_1, Y_1, Z_1 coordinates and their derivatives. Specifically, the relationships between the foot X, Y, Z coordinates and the joint angles (as derived in Appendix A) are given by the following set of nonlinear equations:

$$\phi_1 = \sin^{-1}\left[\ell_3/\sqrt{Y_1^2+X_1^2}\right] + \tan^{-1}(X_1/Y_1) \tag{5-3}$$

$$\phi_2 = \sin^{-1}\left[Z_1 \Big/ \sqrt{(\ell_5+\ell_2\cos\phi_3)^2 + (\ell_1+\ell_2\sin\phi_3)^2}\right] + \tan^{-1}((\ell_5+\ell_2\cos\phi_3)/(\ell_1+\ell_2\sin\phi_3)) \tag{5-4}$$

$$\phi_3 = \sin^{-1}\left[((X_1-\ell_4\sin\phi_1+\ell_3\cos\phi_1)/\sin\phi_1)^2 + (Z_1^2-\ell_1^2-\ell_2^2-\ell_5^2)/\ 2\ell_2\ \sqrt{\ell_1^2+\ell_5^2}\right] - \tan^{-1}(\ell_5/\ell_1) \quad (5\text{-}5)$$

In contrast to the nonlinearity of the above angle equations, the relation between the joint angle rates and the rate of change of the foot XYZ coordinates is linear and can therefore be written in vector-matrix form:

$$\underline{\dot{\phi}} = \underline{J}^{-1}\ \underline{\dot{X}} \quad (5\text{-}6)$$

where

$$\underline{\dot{\phi}} = \begin{bmatrix} \dot{\phi}_1 \\ \dot{\phi}_2 \\ \dot{\phi}_3 \end{bmatrix}, \quad \underline{\dot{X}} = \begin{bmatrix} \dot{X} \\ \dot{Y} \\ \dot{Z} \end{bmatrix} \quad (5\text{-}7)$$

and J^{-1} is the inverse Jacobian matrix

$$J^{-1} = \begin{bmatrix} a_{11} & a_{12} & a_{13} \\ a_{21} & a_{22} & a_{23} \\ a_{31} & a_{32} & a_{33} \end{bmatrix} = \begin{bmatrix} \frac{\partial X_{11}}{\partial \phi_1} & \frac{\partial X_1}{\partial \phi_2} & \frac{\partial X_1}{\partial \phi_3} \\ \frac{\partial Y_1}{\partial \phi_1} & \frac{\partial Y_1}{\partial \phi_2} & \frac{\partial Y_1}{\partial \phi_3} \\ \frac{\partial Z_1}{\partial \phi_1} & \frac{\partial Z_1}{\partial \phi_2} & \frac{\partial Z_1}{\partial \phi_3} \end{bmatrix}^{-1} \quad (5\text{-}8)$$

The coefficients in this matrix are also derived in Appendix A with the following results:

$$a_{11} = +\cos\phi_1/(\ell_4+\ell_1\cos\phi_3+\ell_2\sin(\phi_2+\phi_3)+\ell_5\sin\phi_3) \qquad (5\text{-}9)$$

$$a_{12} = \sin\phi_1/(\ell_4+\ell_1\cos\phi_3+\ell_2\sin(\phi_2+\phi_3)+\ell_5\sin\phi_3) \qquad (5\text{-}10)$$

$$a_{13} = 0 \qquad (5\text{-}11)$$

$$\begin{aligned} a_{21} = {} & \cos\phi_1(\ell_1\cos\phi_3+\ell_2\sin(\phi_2+\phi_3)+\ell_5\sin\phi_3)/(\ell_2(\ell_1\cos\phi_2-\ell_5\sin\phi_2)) \\ & + \ell_3\sin\phi_1(\ell_1\cos\phi_3+\ell_2\sin(\phi_2+\phi_3)+\ell_5\sin\phi_3)/ \\ & (\ell_2(\ell_1\cos\phi_2-\ell_5\sin\phi_2)(\ell_4+\ell_1\cos\phi_3+\ell_2\sin(\phi_2+\phi_3) \\ & +\ell_5\sin\phi_3)) \qquad (5\text{-}12) \end{aligned}$$

$$\begin{aligned} a_{22} = {} & \sin\phi_1(\ell_1\cos\phi_3+\ell_2\sin(\phi_2+\phi_3)+\ell_5\sin\phi_3)/(\ell_2(\ell_1\cos\phi_2-\ell_5\sin\phi_2)) \\ & -\ell_3\cos\phi_1(\ell_1\cos\phi_3+\ell_2\sin(\phi_2+\phi_3)+\ell_5\sin\phi_3)/(\ell_2(\ell_1\cos\phi_2- \\ & \ell_5\sin\phi_2)(\ell_4+\ell_1\cos\phi_3+\ell_2\sin(\phi_2+\phi_3)+\ell_5\sin\phi_3)) \qquad (5\text{-}13) \end{aligned}$$

$$\begin{aligned} a_{23} = {} & (-\ell_1\sin\phi_3+\ell_2\cos(\phi_2+\phi_3)+\ell_5\cos\phi_3)/ \\ & \ell_2(\ell_1\cos\phi_2-\ell_5\sin\phi_2) \qquad (5\text{-}14) \end{aligned}$$

$$\begin{aligned} -a_{31} = {} & (\ell_2\sin(\phi_2+\phi_3)\cos\phi_1)/(\ell_2(\ell_1\cos\phi_2-\ell_5\sin\phi_2)) \\ & +\ell_2\ell_3\sin\phi_1\sin(\phi_2+\phi_3)/((\ell_4+\ell_1\cos\phi_3+\ell_2\sin(\phi_2+\phi_3)+\ell_5\sin\phi_3) \\ & (\ell_2(\ell_1\cos\phi_2-\ell_5\sin\phi_2))) \qquad (5\text{-}15) \end{aligned}$$

$$a_{32} = -(\ell_2\sin\phi_1\sin(\phi_2+\phi_3))/(\ell_2(\ell_1\cos\phi_2-\ell_5\sin\phi_2))$$

$$+\ell_2\ell_3\cos\phi_1\sin(\phi_2+\phi_3)/(\ell_2(\ell_1\cos\phi_2-\ell_5\sin\phi_2)$$

$$(\ell_4+\ell_1\cos\phi_3+\ell_2\sin(\phi_2+\phi_3)+\ell_5\sin\phi_3)) \tag{5-16}$$

$$a_{33} = -\ell_2\cos(\phi_2+\phi_3)/(\ell_2(\ell_1\cos\phi_2-\ell_5\sin\phi_2)) \tag{5-17}$$

These equations are incorporated in the transformation routines COORD and REF utilized at various points in the main program prior to motion execution. As can be seen from the equations, the computational burden on the computer for this part of the calculation is quite large. In fact, it is for just this reason that it was found necessary to divide the software system used in this research into successive rather than concurrent motion planning and execution phases. In order to speed execution of these routines, a large number of invariant calculations are done prior to the commencement of the locomotion cycle.

5.3.2 The Fast Loop Subroutine

The subroutine FILTER implements the fast loop mentioned earlier. It is entered as the service routine for a timed interrupt where the interrupt time interval is entered by the operator at the beginning of the program. FILTER reads all of the eighteen joint angles and joint rates and uses the two vectors REFA and REFR which reflect the desired joint angles and rates to computer the joint motor controller inputs. After outputting the motor controller inputs, the subroutine calls the system routine ITIMER to enable the real-time clock interrupt which will cause FILTER to be reeentered.

The eighteen dimensional vectors REFA and REFR, which specify the desired angle and rate for each joint, are updated by the phase of the main program which constitutes the slow loop mentioned earlier. The data for these vectors is obtained from reference matrices generated during motion planning. Subroutine TRAJ(ectory) is the subroutine called by the main program just before it enters the slow loop to fill up the two 3 x 500 matrices. If concurrent motion planning and motion execution should become possible in the future through hardware improvements, then this routine could perhaps be discarded. FASREF is the indexing subroutine that looks up the two reference matrices filled by TRAJ and, by knowing the amount of time that the leg has already spent on the ground, retrieves the correct desired angles and rates.

SERVO is a routine called by the main program during the checkout and initialization phases as well as during motion execution. Its function is to simulate a hardwired servo loop. It uses the known joint angles and rates and the desired angles and rates to calculate joint commands. It also returns a value to the main program to indicate whether the desired end-state has been achieved. SERVO implements the equation

$$U = K_\phi(\phi_d-\phi_a) + K_{\dot\phi}(\dot\phi_d-\dot\phi_a) \qquad (5\text{-}18)$$

where K_ϕ and $K_{\dot\phi}$ are the servo position and velocity gains and ϕ_d and ϕ_a are the desired joint angles and actual joint angle.

5.3.3 The Main Program

The slow loop portion of the main program is a supervisory program that performs tasks such as keeping track of the state of each leg, changing leg states, and updating the time vectors TLIFT and TPLACE. It also makes calls to various subroutines to help it make these decisions.

The main program requests the operator to give a speed command and a stride length command. From these two parameters it calculates and implements the optimum gait for the vehicle. McGhee and Sun [4] have shown that the optimal gait in terms of stability for a hexapod is one that maintains the following phase relationships between the individual legs. If T_i is the time at which leg i is placed on the ground in the locomotion cycle where the locomotion cycle begins with the placement of the front leg, then $T_1 = 0$, $T_3 = \beta$, $T_5 = 2\beta - 1$ where β is the duty factor defined as the fraction of time spent by a leg on the ground compared to the total locomotion cycle time. The times T_2, T_4, and T_6 which are the leg placement times for the legs on the other side of the machine are determined by making use of the fact that, in an optimal wave gait, the foot placement times of any right-left pair of legs differs by one-half of the gait period, T. Figure 5.3 shows the leg numbering sequence and Figure 5.4 shows a typical event sequence where each event consists of the placing or the lifting of a leg for a specific duty factor. This has also been discussed in Chapter 2. The main program maintains a running clock by reading the real-time clock once every time it enters the slow loop. This it updates an entry in TLIFT and

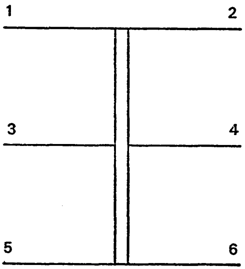

Figure 5.3. Leg Numbering Sequence.

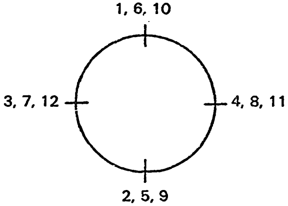

Figure 5.4. Event Sequence for the Optimum Wave Gait with $\beta = .75$.

TPLACE when the leg corresponding to that entry enters the transfer phase and is lifted off the ground. In order to calculate the entries in TLIFT and TPLACE for the first time, the program uses the following equations:

$$\text{Locomotion cycle period} = T = T_R + \lambda/\text{SPEED} \qquad (5\text{-}19)$$

where T_R is the transfer time and λ is the stride length. The program then calculates the duty factor from,

$$\beta = \frac{T-T_R}{T} \qquad (5\text{-}20)$$

where β is the duty factor. Based upon the value for β, the components of TPLACE for the left hand side of the vehicle are given by

$$\text{TPLACE}(1) = 0 \qquad (5\text{-}21)$$

$$\text{TPLACE}(3) = \beta \qquad (5\text{-}22)$$

$$\text{TPLACE}(5) = 2\beta-1 \qquad (5\text{-}23)$$

TPLACE for the even numbered or right legs is obtained by adding 1/2 to the entries for the corresponding left legs, and TLIFT is obtained by,

$$\text{TLIFT} = \text{TPLACE} + \beta \qquad (5\text{-}24)$$

Of course, all of the above calculations are done so that only the fractional part in excess of 1 is retained. Furthermore, all of the above times are normalized to cycle time and therefore must be multiplied by the gait period T in order to obtain actual time within a given cycle of gait.

A complete listing of all program modules is provided in Appendix C.

5.4 Summary

The preceding discussion has centered on the programming aspects of the straight-line locomotion problem. It must be pointed out that several major changes were made since a first working version was implemented. In the initial version there was no fast servo loop built into the software to take care of individual joints from one computation of the control input to the next. Secondly, the transfer phase was initially implemented by a bang-bang type of minimum time control system. This worked very well, but for the slow speeds attempted it was found that the support phase was the time restrictive factor. In other words, the leg always finished the transfer phase very quickly and wound up waiting in the air. Secondly, the sudden reversal of current in the motor field winding is hard on the brushes due to the reversal in the induced armature voltage. The manner in which the minimum time transfer was implemented is shown in Appendix B together with the theory behind the approach. In the future, when computations can be made more quickly, this approach can again be taken. In any case, the structural flexibility of the software was a great help since major changes were easily accomplished.

As discussed in the introduction to this chapter, it should be clear now that this problem is particularly amenable to a multiprocessor solution. The slow loop executed by the main program could be implemented on a central processor that would perform the same housekeeping and coordinating chores that the main program does here; namely, it would maintain tables that would reflect leg states, tell when each leg to be lifted or set down, etc. The individual leg processors could then run the fast loop, interrogate the central processor for information on what to do next with the leg, do the coordinate transformations, and implement the equivalent of a hardwired analog servo loop.

In the next chapter the performance of the system is evaluated in terms of limits imposed by both hardware and software Some suggestions are made for changes that should be made in the future.

CHAPTER 6

PERFORMANCE EVALUATION

6.1 Introduction

Some results of measurements taken on an actuator joint of the hexapod vehicle are first presented in this chapter. These results show how the joint may be modelled as a very simple system with a single pole transfer function where the input corresponds to the motor controller command in volts and the output corresponds to the joint velocity in degrees/second. The effect of using feedback gains on the joint is shown next. Based on the optimal control theory of minimum time response, some results are shown when the system is subjected to a bang-bang type of input. The performance of the vehicle when walking in a straight line and negotiating level terrain is described together with some angle and rate measurements. Finally, the limitations of the vehicle due to hardware and due to the software are pointed out.

6.2 Joint Modelling

Several tests were run on a single joint to determine the response of the joint. It was hoped that the results of these tests would allow the joint to be modelled quite simply so that desirable position and velocity gains could be computed and utilized to achieve locomotion in the hexapod vehicle.

The first of the tests concerns the velocity response of the joint to a step input to the motor controller. Figure 6.1 shows a plot of the observed velocity at the joint output in degrees/second when the joint is subjected to a 10 volt input under no-load conditions. As can be seen, the velocity reaches 63% of its final value in 0.33 seconds from which it may be concluded that, if the joint is to be modelled as a first-order system with a single pole, then the desired transfer function from joint motor controller input in volts to output velocity in degrees/second is

$$G_1(s) = \frac{4}{s+3} \text{ deg/sec/volt} \tag{6-1}$$

Thus, the transfer function from controller input in volts to output angle in degrees is

$$G(s) = \frac{4}{s(s+3)} \text{ deg/volt} \tag{6-2}$$

A block diagram of this transfer function is shown in Figure 6.2.

Figure 6.3 shows the joint transfer function with velocity and position feedback. In the presence of such feedback, the transfer function of the joint is given by,

$$G(s) = \frac{4}{s^2+s(3+ 4Kv)+ 4Kp} \tag{6-3}$$

By experimenting with the completed system, it was found that satisfactory performance resulted from choosing the system gains to be

$$K_v = .5 \text{ volts/deg/sec} \tag{6-4}$$

$$K_p = 1.5 \text{ volts/deg} \tag{6-5}$$

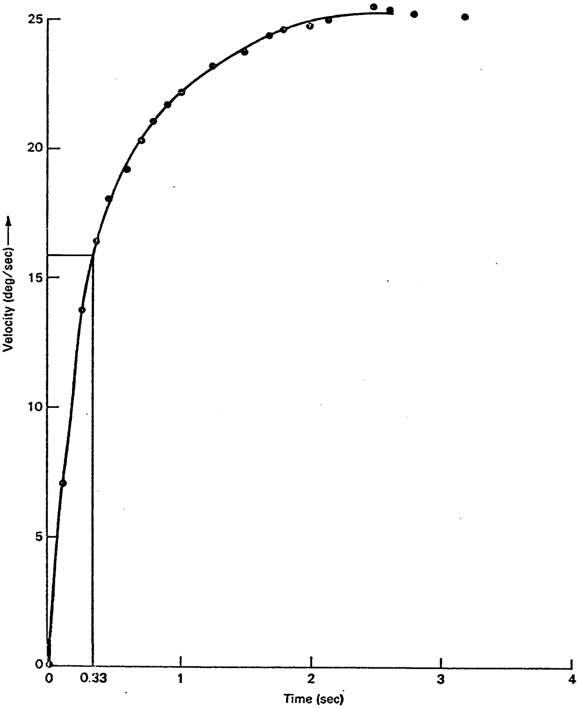

Figure 6.1. Joint Output Velocity for a Constant 10v Input.

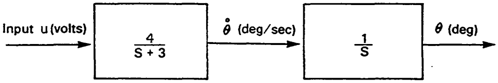

Figure 6.2. Joint Open Loop Transfer Function.

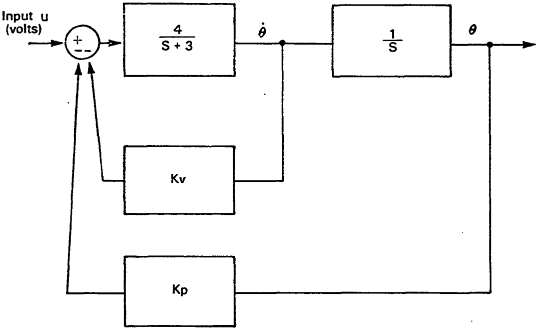

Figure 6.3. Joint Transfer Function With Feedback.

Substituting these values into Eq. 6-3, the characteristic polynomial for the closed loop system is

$$s^2 + 5s + 6 \tag{6-6}$$

with corresponding eigenvalues

$$s = -3 \ , \ s = -2 \tag{6-7}$$

From these values, it is to be expected that the joint response to a step command in angle should exhibit a total time constant somewhere between 1/2 and 5/6 seconds. Figure 6.4 verifies that this is indeed at least qualitatively correct for the measured response.

Due to the deadband in the motor controller, it is necessary to accept some error in the final state. The error that is tolerated in the present system is about 0.6 degrees. The next section of this chapter deals with the results of using a bang-bang type of control upon the joint modelled in this section. Some results obtained in this section are made use of to obtain the switching trajectory according to the theory in Appendix B.

6.3 Minimum Time Response

It has been shown from the results of Section 6.2 that an individual joint can be modelled as a simple transfer function with a single pole at 3 sec^{-1} where the output is considered to be the velocity of the joint output and the input is the motor controller input in volts. Based upon the theory in Appendix B, it follows that if the joint is to move from one position to

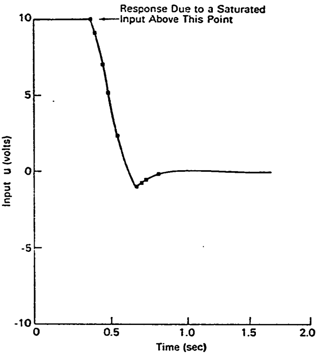

a) Joint Controller Command Voltage

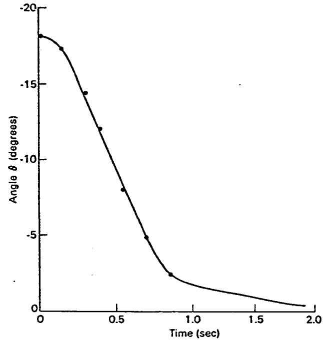

b) Joint Angle Response

Figure 6.4. Response of Closed Loop Joint Control System to a Step Input Command, K_v = .5 volts/deg/sec, K_p = 1.5 volts/deg.

another in the smallest amount of time with the input amplitude being constrained to a limit, then a bang-bang type of control is required where the switching occurs when the term D defined in Eq. (B-23) of Appendix B changes sign. This corresponds to the switching trajectory or curve shown in Figure B-1. Figures 6.5 and 6.6 show the results of using this type of a control system on the joint. As can be seen from the input voltage waveform in Figure 6.5, the control is not strictly optimal. That is, the input first changes sign when the switching condition is satisfied, but once the joint state is close to the desired position, the control switches from an open-loop bang-bang type to a linear feedback type of control. As Orin [25] has shown, the leg transfer time must be short as possible to maximize the speed or the duty factor (and thus the stability) for a given speed, hence it is hoped that these results will be of value when computational speed is no longer the limiting factor so far as the speed of the vehicle is concerned.

6.4 Straight Line Locomotion

Straight line locomotion has been successfully obtained by the hexapod vehicle employing a variety of wave gaits with duty factors as low as 0.5, corresponding to the tripod gain in which at any time only three legs are on the ground. Angle, rate, and power measurements were made at vehicle speeds of 1.5 inches/second, 4.0 inches/second,and 6.5 inches/second. The stride length employed by the vehicle at these three speeds is such as to yield a leg duty factor of 5/6 at 1.5 inches/second, 2/3 at 4.0

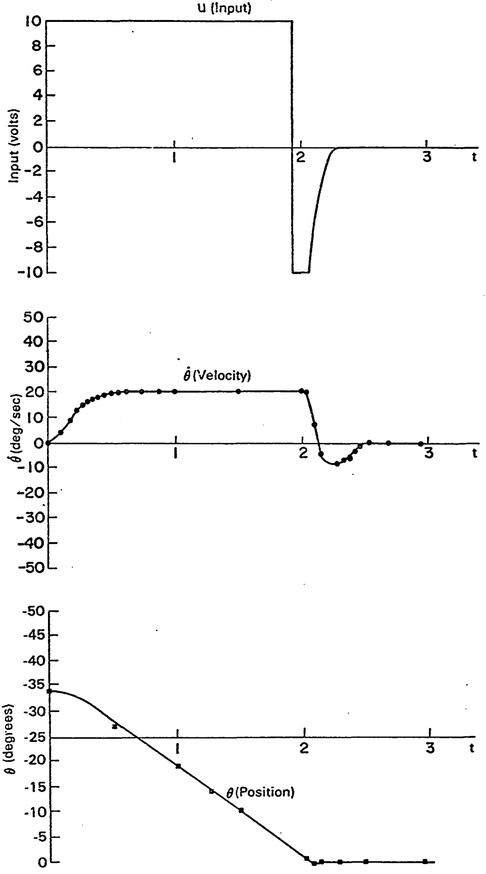

Figure 6.5. Minimum Time Response.

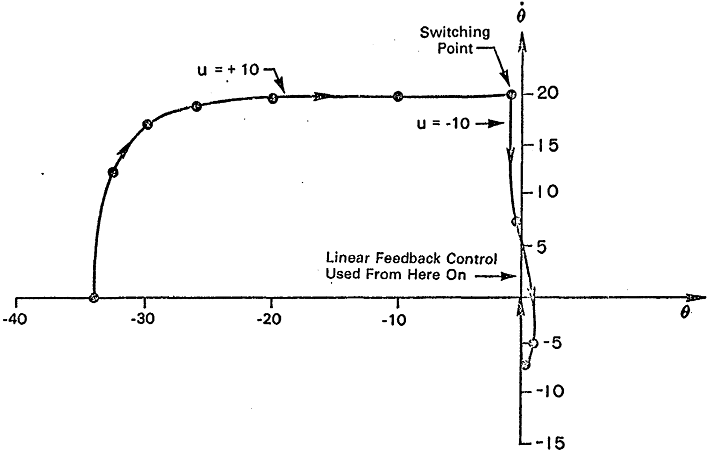

Figure 6.6. Phase-Plane Trajectory for Minimum Time Response.

inches/second and 1/2 at 6.5 inches/second. Thus, at any given instant in the locomotion cycle, there are always five legs on the ground at 1.5 inches/second, at 4.0 inches/second there are always four legs on the ground, and at 6.5 inches/second there are always three legs on the ground. The leg transfer times are nearly identical at the three speeds. Figure 6.7 shows the completed vehicle photographed while moving at a speed of 4.0 inches/second.

Figure 6.8 shows a plotof actual angles and rates as a function of time as the vehicle moves at a speed of 6.5 inches/second. Figure 6.9 shows the corresponding commanded angles. The azimuth angle is seen to swing approximately 50 degrees on both sets of curves. The overall waveform of the measured azimuth angle is nearly triangular since the leg transfer and leg support phases are of equal time duration, for a duty cycle of one-half. The azimuth rate plot is observed to saturate during both phases at about 24 degrees/second thus yielding the linear azimuth angle slopes. By examining the segment of the azimuth rate where it changes from a negative saturation value to a positive saturation value, it can be seen that the azimuth rate response is not exponential. This again is due to the fact that the azimuth joint controller input is saturated due to the large position error so that the expected exponential rise is absent.

The observed knee angle and its rate are seen to be nearly constant during the leg transfer phase. This is due to the fact that the change in knee angle from the end of the support phase to the end of the transfer phase is extremely small

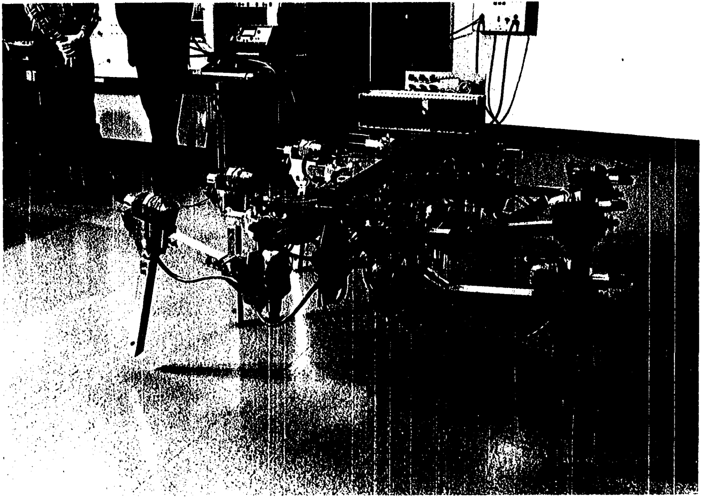

Figure 6.7. Completed Hexapod Vehicle Exhibiting Optimal Wave Gait With Duty Factor, $\beta = 2/3$.

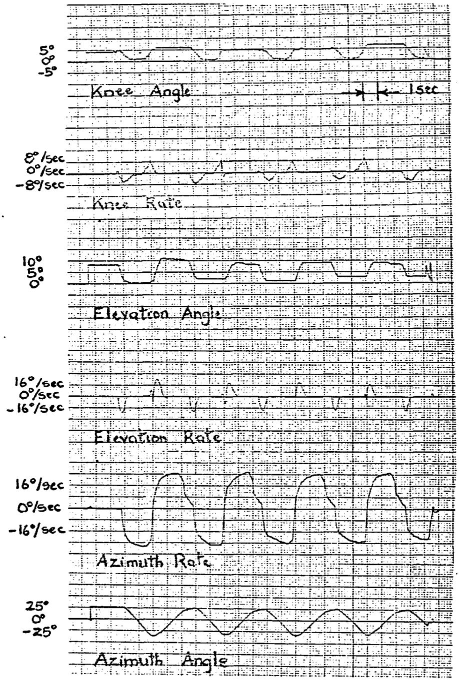

Figure 6.8. Measured Joint Angles and Rates at a Vehicle Speed of 6.5 inches/second.

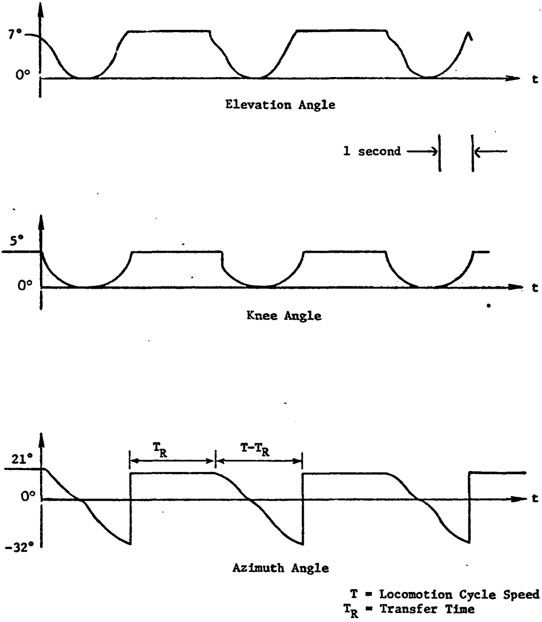

Figure 6.9. Commanded Joint Angles at a Vehicle Speed of 6.5 inches/second.

so that the knee rate is nearly zero during the transfer phase. During the support phase the knee joint moves together with the elevation joint so as to try to maintain constant body altitude. The maximum knee angle variation is only 5 degrees during the entire locomotion cycle. The elevation angle and elevation rate plots reveal that the elevation joint is fairly constant not only during the transfer phase, but also during the support phase.

The elevation angle is constant during the transfer phase for the same reason that the knee angle is constant during the transfer phase. The change in elevation angle from one end of support to end of transfer is small. However, the lack of variation in elevation angle during the support phase is not quite so easily explained. In fact, Figure 6.9 shows that the commanded elevation angle during the support phase exhibits a continuous variation unlike the actual elevation angle which quickly achieves a constant value during the support phase, remains at that value for a considerable portion of the support phase, and then quickly increases once again to a new value. The elevation rate is correspondingly zero during a major portion of the support phase. Thus the elevation joint is unable to follow the commanded joint angle during the support phase. The following paragraph provides an explanation for the deterioration of the elevation joint performance under load.

The error in the elevation angle and rate during support is small enough so that only a small torque is commanded at the joint. This input torque is however less than the load torque so that the elevation joint cannot be moved by the input torque. However, due to the irreversible property of the worm gear in the drive train, the load torque cannot move the elevation joint against the input torque either. Thus the elevation joint locks up during that portion of the support phase when the maximum torque input available to the joint due to the elevation joint angle and elevation rate error is less than the load torque due to the weight of the machine. Since the elevation joint is locked during this time, there is no back electromotive force (emf) voltage generated in the armature of the motor and the applied voltage appears directly across the armature and field winding resistances. Thus all of the applied power is dissipated as resistive losses. So long as the rate and angle error is constant, the applied voltage is constant, and a constant amount of power is dissipated in the field winding resistance and the armature winding resistance [46].

Figures 6.10 and 6.11 show joint angle and joint rate variation at 4.0 inches/second and 1.5 inches/second respectively. The azimuth rate no longer saturates at these lower speeds so that the azimuth angle variation during the support phase is no longer as linear as it is at a vehicle speed of 6.5 inches/second. The elevation angle is again observed to lock up during the support phase. In Figure 6.11 the azimuth rate during the support phase is only about 5 degrees/second and is fairly constant. The knee angle in Figure 6.11 is observed to exhibit a peak at the start of the support phase as well as the end of the support phase which

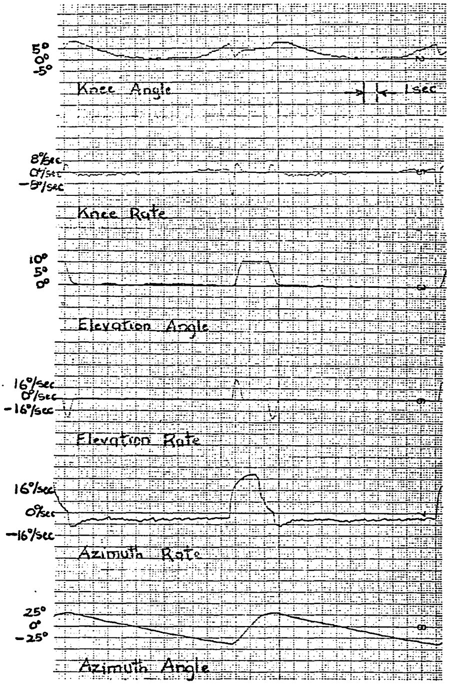

Figure 6.10. Measured Joint Angles and Rates at a Vehicle Speed of 1.5 inches/second.

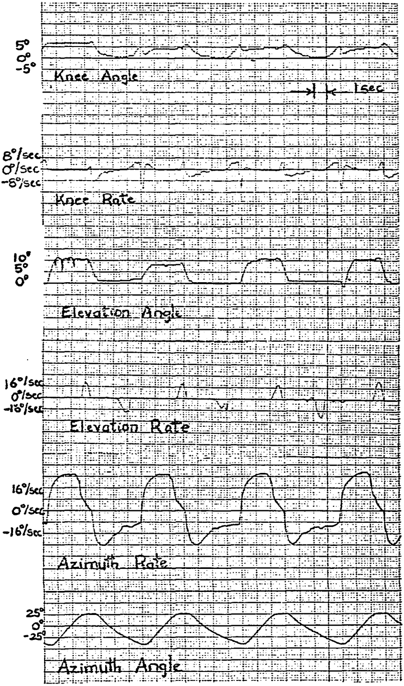

Figure 6.11. Measured Joint Angles and Rates at a Vehicle Speed of 4.0 inches/second.

is greater than the value achieved during the transfer phase. This is due to the longer stride length that was used at 1.5 inches/second which causes a larger knee and elevation angle excursion at the beginning and end of the support phase corresponding to the two end points of the net azimuth swing.

The average power levels measured at the three different speeds and at standby are listed below. The values shown were obtained using an electromechanical wattmeter with a rated accuracy of 1/2% at frequencies up to 133 Hz. Observation of current waveforms on a storage type of oscilloscope showed that the vehicle current exhibited no spikes and could be rather accurately represented by the first three harmonics of the 60 Hz line frequency. It is felt therefore, that these power measurements are accurate to within five percent or better of the true values.

Average Power Requirements Versus Vehicle Speed

Speed (inches/second)	Power (kilowatts)
0	.080
1.5	1.5
4.0	2.1
6.5	2.6

As can be seen from Table 10, standby power of nearly 80 watts is required for the electronics, out of which 20 watts are required for the position sensing potentiometers at each joint. At the lowest vehicle speed of 1.5 inches/second, when the machine is crawling with five legs on the ground at all times, the average power required is 1.5 kilowatts. Thereafter, there is an increase in average power requirements as vehicle speed increases, although less than would be expected due to the increased motor speed and braking losses.

If the energy required to move the vehicle a fixed distance at different speeds is considered, then the vehicle appears to be more efficient at higher speeds than it is at lower speeds. Energy required to move the vehicle a distance of 1 foot is computed by multiplying the average power requirement by the time taken by the vehicle to move 12 inches at the given vehicle speed. The relevant information about these bearings is given below [51].

Energy Required to Move the Hexapod Vehicle a Distance of One Foot Over Level Ground

Speed (inches/second)	Energy (Joules)
1.5	12.0
4.0	6.3
6.5	4.8

The results presented in Table 11 are counter-intuitive. That is, since the vehicle is only carrying its own weight at all speeds, and all losses are due solely to mechanical friction or electrical resistance, the energy required to move a fixed distance at different vehicle speeds would be expected to be constant. If anything, the energy losses due to braking should be larger at higher speeds, and hence one would expect that the vehicle would be most efficient at the lowest speed. To understand why this is not so, it is necessary to separately consider the support and transfer phase for each leg since the overall vehicle power requirement is the sum of the individual leg power requirements. These are expected to be nearly identical since all legs have the same duty factor. Leg transfer is implemented by commanding the leg to reach the final point just before touchdown. Due to the high gains utilized, the leg proceeds to move to this point with the azimuth motor controller input saturated due to the large position error. Leg transfer is thus independent of vehicle speed and the same amount of energy is consumed for all gaits and for all speeds, although the number of leg transfer sequences implemented by a leg varies linearly with vehicle speed. Hence, this aspect of vehicle behavior implies that average power requirements should vary linearly with speed. Thus, it appears that the explanation for increased energy requirements at low speed must be found by a careful examination of leg behavior during the support phase.

Two factors make the average power required during the leg support phase vary nonlinearly with speed. Both of these factors make locomotion more efficient at higher speeds. The first of these factors is the locking effect of the elevation joint mentioned earlier. The elevation joint is the most heavily loaded joint during the support phase since it must do work against the load torque due to the weight of the machine. Hence, it tends to lock up during the support phase since the error torque is insufficient to work against the load torque. During the support phase, therefore, all input power to this joint is dissipated as resistive losses in the motor windings. Hence, with respect to this joint, the support phase is largely a constant power phase rather than a constant energy phase so that the energy lost varies linearly with the amount of time that the leg spends on the ground and inversely with the vehicle speed. There is another factor which causes greater power losses at lower speeds. At lower speeds the coefficient of friction at the gear teeth is much higher than it is at higher speeds. The coefficient of static friction is 0.15 compared to the value of 0.02 which exists at the worm gear velocity that corresponds to the maximum motor speed of 1000 rpm [50].

The above results and discussion show that energy optimization is a nonlinear problem which deserves further work since it has not been a concern of this dissertation. The elevation joint locking effect observed during the support phase can be alleviated by using higher gains during the support phase than during the leg transfer phase. In fact, this observation clearly points to the need for at least two different sets of position and velocity gains corresponding to the leg support and leg transfer phases. In conclusion, it must also be mentioned that the actual power requirements are very much higher than the 750 watts predicted by simulation studies. This again is due at least in part to the locking effect and the high friction and resistive losses mentioned earlier.

The maximum vehicle speed included in these experiments is about 6.5 inches/second. As seen in Figure 6.8, the azimuth joint rate saturates at this vehicle speed so that the speed limitation with the present system is due to the motor and its associated drive train which is incapable of producing a higher speed for the given load, rather than due to the computational burden on the computer which is a software limitation. However, if concurrent motion planning and motion execution were to be attempted with the present control computer, then no more than four or five leg position computations could be made per second so that the motor controller inputs would only be updated four or five times per second. This sampling rate is inadequate and not only limits the speed of the machine, but it has been observed to produce a jerky motion in the joints. If the motion of the joint is to appear smooth, then the sampling rate must be roughly ten times as much or about thirty to sixty times per second. This can be justified as follows. It has been shown that the joint can be modelled as a simple first order transfer function with a pole at 3 sec^{-1} and another at 2 sec^{-1}. Thus the joint acts as a low-pass filter. If the input is updated too infrequently, then the joint cannot filter out the effects of sampling which are manifested in a jerky motion. However, if the input is updated thirty or more times per second then the joint filters out the 30 Hz components as well as the higher harmonics to yield essentially smooth motion. There is another reason why it is desirable to use a high sampling rate. With a higher sampling rate it is possible to use higher feedback gains which yields a faster responding joint; i.e. the effect of the higher gains is to move the natural frequency of the joint further into the left half plane.

The Black and Decker drill motor has a no-load speed of 1000 rpm. This should yield a joint output rate of about 40 degrees/second under no-load when subject to a constant 110 V AC input. However, according to [46], the no-load speed of the joint is only 28 degrees/second at full scale imput. This discrepancy arises due to the fact that the motor controller designed in [46] is a half-wave controller so that the motor is only subjected to a half-wave rectified AC at full scale (10 V) motor controller input. Obviously the use of a full-wave controller could yield a much faster joint, but since speed of the vehicle was not a major factor in its design, this approach was discarded [46].

For a stride length of 18 inches and present leg length parameters, the azimuth rotation is about 90° so that for a duty factor of $\beta = 0.5$, the speed of the vehicle should be a maximum of 1.0 feet/sec. However, this calculation does not take into account the time taken to lift and place the legs and to change direction of joint rotation. If this is also taken into account, the maximum possible speed of the vehicle is only about 0.7 feet/second.

The current vehicle mechanical hardware also imposes a limitation on the performance of the vehicle. In Chapter 4 it was mentioned that the hollow bolt which is part of the joint lower clutch plate assembly (Figure 4.4), has a tendency to shear off under impact loading. In Section 4.5.1 a simple means for correcting this problem has been shown. Until it is implemented, however, care must be taken in subjecting the vehicle to excessive loads such as might be experienced at high speeds or during climbing of obstacles.

A final limitation in the performance of the vehicle is presented by the lack of force sensing or even contact sensing. The motion of the vehicle is fairly uneven due to the fact the different legs share the load differently, i.e., proper load distribution between the legs is not possible. By properly tuning the instrumentation system (adjusting zero offsets in the potentiometer amplification circuits and adjusting gains of all the joint position and joint velocity feedback circuits) it is possible to obtain quite reasonable performance of the hexapod vehicle. However, the gain adjust and zero adjust potentiometers tend to vibrate and shift position and the LM 741 operational amplifiers tend to drift with time and temperature with the result that over time each of the leg position and velocity feedback systems tends to become mismatched with respect to the other systems. This mismatch is reflected in improper leg load distribution and uneven locomotion even over level terrain. It is possible to eliminate this with the use of force feedback and this should probably be the next major thrust in the study of locomotion of the hexapod vehicle [53]. In the absence of force feedback, a partial solution to this problem is presented in the next section wherein the software system compensates for drifts in gain and zero offset. The problem of improper load distribution resulting in uneven locomotion is especially evident in any gait where there are more than three legs on the ground at a given time. In such a case, the legs in contact with the ground form a statically indeterminate system so that loads could easily be mismatched to the point where one leg may carry no load at all.

Thus, although the hexapod vehicle has successfully demonstrated its ability to walk, there is considerable scope for improvement in the vehicle's capabilities.

6.5 Improvements and Suggestions

One recurrent problem has been mentioned in the previous section. This problem concerns the drift in the scale calibration and the zero positions of the joint angles. The reason for this drift is firstly that the sliders of the trimpots that set the gains and null positions tend to move because of the shock and vibration resulting from the mounting of the electronics on the vehicle itself, and secondly, due to zero shifts in the operational amplifiers in the signal conditioning electronics. Thus unless the machine is "re-tuned" every time locomotion begins, there is bound to be a steady deterioration in its performance. However, this can be an extremely laborious process which can be avoided by using a set of limit switches on each joint. Then, as part of the initialization and check-out procedure, the machine can exercise each joint separately, and from reading the limit switch outputs,the actual scale factors can be computed so that calibration and nulling takes place only in the computer. The actual hardware recalibration then needs to be done only very infrequently. This seems to be an extremely important feature and it is only through ignorance that it was omitted.

Another area where modification might be necessary is the use of redundant sensors and control computers, for extra reliability.

Failure of a potentiometer or a tachometer is quite likely in normal operation since the vehicle might inadvertently run into an object. Some added degree of reliability can be obtained by using redundant sensors. The limit switches described above might be an adequte emergency replacement for the joint angle potentiometers, for example. Redundant computing could also be a desireable alternative. Moreover, it might even be worthwhile to devote one processor solely to vehicle operation monitoring so that it could ensure fail-safe operation. This could also tie in with the multiprocessor architecture suggested earlier in Chapter 5, with each leg's processor performing its own control task and one central processor sending out commands and monitoring the hexapod vehicle. The central processor's output to the local leg processor would typically be commands with end-point specifications and it would be the task of the individual leg's processor to determine the joint inputs to take the foot from end-point to end-point. The individual processor could even taken over the task of the motor control and directly output SCR firing pulses at proper intervals to achieve the desired joint motion [54]. This would also eliminate the nonlinearity of the present motor controller.

6.6 Summary

In has been shown that to obtain a first approximation to the feedback gains to be used for the tachometer and potentiometer outputs, the vehicle joint can be adequately modelled as a simple first-order transfer function followed by an integrator. The model serves to predict the response of the joint to a bang-bang type of control system. The performance of the hexapod vehicle in exhibiting straight-line locomotion is discussed and some suggestions for improved straight-line locomotion are made. The suggestions pertain mostly to hardware modifications.

In the next and concluding chapter, the achievements of this dissertation are briefly noted and further extensions of the work to be done on the hexapod vehicle are outlined.

CHAPTER 7

CONTRIBUTIONS AND EXTENSIONS

7.1 Research Contributions

A walking machine under complete computer control has been built and this machine has successfully demonstrated an ability to walk in a straight line over level terrain employing a variety of wave gaits. To the author's knowledge, no such experiment succeeded before the work of this dissertation. Human interaction has been minimized and has been restricted solely to giving higher level commands such as speed and stride length. It has been shown that a mini-computer with moderate computing capability and sufficient analog input-output capability can successfully solve the linkage control problem to implement a variety of wave gaits in a hexapod vehicle. Another basic contribution of this research was to organize the software into table-driven structural modules. Such an organization is necessary if the software is eventually to be realized by a multiple processor computing system. Such a computing system is also suggested by the two loops - the slow loop and the fast loop - executed by the software and described in Chapter 5.

A major accomplishment has been the mechanical design of the hexapod vehicle. The designed vehicle has the mechanical capabilities for walking up slopes, climbing staircases, and negotiating obstacles. Each joint is structurally designed to carry the maximum load that it is likely to encounter and protected in case of overload. Every component selected for the joint was chosen with great care to insure reliability and maximum performance. The resulting vehicle leg is more powerful by a very large margin than any other electrically powered manipulator or artificial limb known to the author [55].

7.2 Extensions

What remains to be done furtheris to first incorporate other modes of locomotion described above. Some of the modes require force sensing in each leg, while others, such as turning control and slope-climbing, require the use of horizontal and vertical gyros. Thus, with respect to the hardware, the hexapod vehicle capabilities need to be enhanced to incorporate force sensors and gyros. The electronics for the vehicle could be improved to incorporate a full-wave controller to meet the increased demands for power sometime in the future.

With regard to the software, a multiple-processor solution needs to be implemented as pointed out in Chapter 5. This would leave the central computer free to perform other tasks such as energy optimization and load distribution [19,53]. The software also needs to incorporate some type of automatic scaling of position and velocity gains and zero offsets, as described in Chapter 6. This together with force sensing would ensure a smoother limb motion.

In the more distant future, it is hoped that the vehicle can be equipped with an on-board television system and a remote control feature to demonstrate the true independent capabilities inherent in it. Then it could operate more or less as an intelligent "animal" obeying commands sent by its master over a telemetry link, and adapting itself to the environment it sees itself in to carry out these commands. Such a machine might be able to replace human beings in certain dangerous tasks such as fire-fighting, explosive ordnance disposal, nuclear reactor servicing, etc.

APPENDIX A

Figure A.1 shows the true leg geometry of the hexapod vehicle, taking into account offsets between leg joint axes. The joint angles ϕ_1, ϕ_2, and ϕ_3 and a set of xyz coordinate axes fixed to the body at the hip rotation joint are also shown. The foot xyz coordinates are first derived below in terms of joint angles ϕ_1, ϕ_2 and ϕ_3.

Figure A.2 shows a three-dimensional perspective view of the leg of the hexapod vehicle. By taking the projections of all leg segments along the y-axis, one may write down the following relationship, where x, y, and z are the foot coordinates:

$$y = \ell_4\cos\phi_1 + \ell_3\sin\phi_1 + \ell_1\cos\phi_2\cos\phi_1 + \ell_5\sin\phi_2\cos\phi_1$$
$$+ \ell_2\sin(\phi_3+\phi_2)\cos\phi_1 \qquad \text{(A-1)}$$

Here $\ell_1\cos\phi_2$ and $\ell_5\sin\phi_2$ are the projections of the segments ℓ_1 and ℓ_5 on the xy plane and $\ell_2\cos[90-(\phi_2+\phi_3)]$ is the projection of the segment ℓ_2 on the xy plane. Similarly, taking projections of all leg segments on the xy plane and then taking the components of all projections along the x-axis, one obtains

$$x = \ell_4\sin\phi_1 - \ell_3\cos\phi_1 + \ell_1\cos\phi_2\sin\phi_1 + \ell_5\sin\phi_2\sin\phi_1$$
$$+ \ell_2\sin(\phi_3+\phi_2)\ \sin\phi_1 \qquad \text{(A-2)}$$

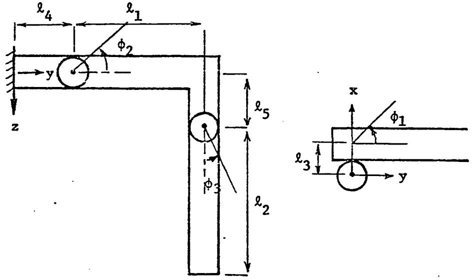

a) Front View

b) Top View

Figure A.1. Hexapod Vehicle Leg Geometry.

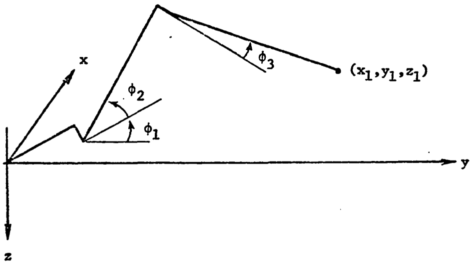

Figure A.2. Schematic Three-Dimensional Representation of the Hexapod Vehicle Leg.

Finally, taking projections along the z-axis,

$$z = -\ell_1 \sin\phi_2 + \ell_2 \cos(\phi_3+\phi_2) + \ell_5 \cos\phi_2 \tag{A-3}$$

Multiplying Equation (A-1) by $\sin\phi_1$ and (A-2) by $\cos\phi_1$ and then subtracting produces the results

$$y\sin\phi_1 - x\cos\phi_1 = \ell_3 \tag{A-4}$$

and

$$\frac{y}{\ell_3} \sin\phi_1 - \frac{x}{\ell_3} \cos\phi_1 = 1 \tag{A-5}$$

Equation (A-5) can be written as,

$$\frac{y}{\ell_3} \sin\phi_1 - \frac{x}{\ell_3} \cos\phi_1 = E\sin(\phi_1+\phi) = E\sin\phi_1\cos\phi$$

$$+ E\cos\phi_1\sin\phi \tag{A-6}$$

Or,

$$E\cos\phi = \frac{y}{\ell_3} \tag{A-7}$$

$$E\sin\phi = -\frac{x}{\ell_3} \tag{A-8}$$

Taking the ratio of (A-8) and (A-7), one obtains

$$\tan\phi = -\frac{x}{y} \tag{A-9}$$

Squaring (A-7) and (A-8) and adding,

$$E^2 = \frac{y^2+x^2}{\ell_3{}^2} \tag{A-10}$$

so

$$E = \frac{1}{\ell_3} \sqrt{y^2+x^2} \tag{A-11}$$

From (A-5) and (A-6),

$$E\sin(\phi_1+\phi) = 1 \tag{A-12}$$

and thus

$$\phi_1 = \sin^{-1} \frac{1}{E} - \phi \tag{A-13}$$

Substituting for E and ϕ from (A-9) and (A-11),

$$\phi_1 = \sin^{-1}\left[\frac{\ell_3}{\sqrt{y^2+x^2}}\right] + \tan^{-1} \frac{x}{y} \tag{A-14}$$

The angles ϕ_2 and ϕ_3 are next derived as a function of the foot coordinates as follows. Rewriting Eqs. (A-2) and (A-3),

$$\frac{x - \ell_4\sin\phi_1 + \ell_3\cos\phi_1}{\sin\phi_1} = \cos\phi_2(\ell_1+\ell_2\sin\phi_3) + \sin\phi_2(\ell_5+\ell_2\cos\phi_3) \tag{A-15}$$

and

$$z = \cos\phi_2(\ell_5+\ell_2\cos\phi_3) - \sin\phi_2(\ell_1+\ell_2 \sin\phi_3) \tag{A-16}$$

Squaring (A-15) and (A-16) and adding, it follows that:

$$\left[\frac{x - \ell_4\sin\phi_1 + \ell_3\cos\phi_1}{\sin\phi_1}\right]^2 + z^2 = (\ell_1+\ell_2\sin\phi_3)^2 + (\ell_5+\ell_2\cos\phi_3)^2 \tag{A-17}$$

Expanding the right hand side of Eq. (A-17) yields the result

$$\left[\frac{x-\ell_4\sin\phi_1+\ell_3\cos\phi_1}{\sin\phi_1}\right]^2 + z^2 = \ell_1^{\,2}+2\ell_1\ell_2\sin\phi_3+\ell_2^{\,2}\sin^2\phi_3+\ell_5^{\,2}+\ell_2^{\,2}\cos^2\phi_3$$
$$+ 2\ell_2\ell_5\cos\phi_3 \qquad \text{(A-18)}$$

$$=\ell_1^{\,2}+\ell_2^{\,2}+\ell_5^{\,2}+2\ell_2[\ell_1\sin\phi_3+\ell_5\cos\phi_3] \qquad \text{(A-19)}$$

Following a method identical to the one used for solving (A-4) by writing $\ell_1\sin\phi_3+\ell_5\cos\phi_3$ as the constant E times the sine of the sum of ϕ_3 and a dummy angle ϕ and solving for the constant and the angle ϕ, one obtains,

$$\left[\frac{x-\ell_4\sin\phi_1+\ell_3\cos\phi_1}{\sin\phi_1}\right]^2 + z^2 = \ell_1^{\,2}+\ell_2^{\,2}+\ell_5^{\,2}+2\ell_2\sqrt{\ell_1^{\,2}+\ell_5^{\,2}}$$
$$\sin(\phi_3+\tan^{-1}\frac{\ell_5}{\ell_1}) \qquad \text{(A-20)}$$

Finally, substituting (A-20) in (A-18) and solving for ϕ_3,

$$\phi_3 = \sin^{-1}\left[\frac{\left[\dfrac{x-\ell_4\sin\phi_1+\ell_3\cos\phi_1}{\sin\phi_1}\right]^2+z^2-\ell_1^{\,2}-\ell_2^{\,2}-\ell_5^{\,2}}{2\ell_2\sqrt{\ell_1^{\,2}+\ell_5^{\,2}}}\right]$$
$$-\tan^{-1}\frac{\ell_5}{\ell_1} \qquad \text{(A-21)}$$

Similarly, one may obtain an expression for ϕ_2 from Eq. (A-16) as follows:

$$z = -\sin\phi_2(\ell_1+\ell_2\sin\phi_3) + \cos\phi_2(\ell_5+\ell_2\cos\phi_3) = A\sin(\phi_2+\phi) \tag{A-22}$$

where A and ϕ are again dummy variables. Expanding the right-hand side of this equation,

$$A\sin\phi_2\cos\phi+A\cos\phi_2\sin\phi = -\sin\phi_2(\ell_1+\ell_2\sin\phi_3) + \cos\phi_2(\ell_5+\ell_2\cos\phi_3) \tag{A-23}$$

Thus, collecting terms,

$$A\cos\phi = -(\ell_1+\ell_2\sin\phi_3) \tag{A-24}$$

$$A\sin\phi = (\ell_5+\ell_2\cos\phi_3) \tag{A-25}$$

and consequently

$$\tan\phi = -\frac{\ell_5+\ell_2\cos\phi_3}{\ell_1+\ell_2\sin\phi_3} \tag{A-26}$$

and

$$A = \sqrt{(\ell_1+\ell_2\sin\phi_3)^2 + (\ell_5+\ell_2\cos\phi_3)^2} \tag{A-27}$$

From Eq. (A-22),

$$\phi_2 = \sin^{-1}\frac{z}{A} - \phi \tag{A-28}$$

Finally, substituting from (A-26) and (A-27) for A and ϕ,

$$\phi_2 = \sin^{-1}\left[\frac{z}{\sqrt{(\ell_5+\ell_2\cos\phi_3)^2 + (\ell_1+\ell_2\sin\phi_3)^2}}\right] + \tan^{-1}\left[\frac{\ell_5+\ell_2\cos\phi_3}{\ell_1+\ell_2\sin\phi_3}\right] \tag{A-29}$$

Thus, from a knowledge of the foot xyz coordinates it is possible to compute ϕ_1 from Eq.(A-14). Knowing ϕ_1, it is then possible to compute ϕ_3 from Eq. (A-21). Finally from the x,y,z coordinates and the computed values of ϕ_1 and ϕ_3, ϕ_2 may be computed from (A-29).

Having determined the joint angles from the foot x,y,z coordinates, it is now desired to find a relationship between the foot velocity coordinates, $\dot{x}$, $\dot{y}$ and $\dot{z}$ and the three joint angles $\dot{\phi}_1$, $\dot{\phi}_3$ and $\dot{\phi}_2$. Knowing the relationship

$$\dot{\underline{X}} = J\dot{\underline{\phi}} \tag{A-30}$$

where

$$\underline{X} = \begin{bmatrix} x \\ y \\ z \end{bmatrix} \tag{A-31}$$

and

$$\phi = \begin{bmatrix} \phi_1 \\ \phi_2 \\ \phi_3 \end{bmatrix} \tag{A-32}$$

the easiest way to find the inverse Jacobian matrix defined by,

$$\dot{\underline{\phi}} = J^{-1}\,\dot{\underline{X}} \tag{A-33}$$

is from the definition of the inverse ofa matrix, as the transpose of the matrix of cofactors divided by the determinant of the matrix.

The Jacobian matrix J is obtained by differentiating (A-1), (A-2), and (A-3) to obtain the following:

$$\begin{bmatrix} \dot{X} \\ \dot{Y} \\ \dot{Z} \end{bmatrix} = \begin{bmatrix} j_{11} & j_{12} & j_{13} \\ j_{21} & j_{22} & j_{23} \\ j_{31} & j_{32} & j_{33} \end{bmatrix} \begin{bmatrix} \dot{\phi}_1 \\ \dot{\phi}_2 \\ \dot{\phi}_3 \end{bmatrix} \tag{A-34}$$

$$j_{11} = \ell_4\cos\phi_1 + \ell_3\sin\phi_1 + \ell_1\cos\phi_1\cos\phi_3 + \ell_2\sin(\phi_2+\phi_3)\cos\phi_1 + \ell_5\sin\phi_3\cos\phi_1 \tag{A-35}$$

$$j_{12} = -\ell_1\sin\phi_1\sin\phi_3 + \ell_2\cos(\phi_2+\phi_3)\sin\phi_1 + \ell_5\cos\phi_3\sin\phi_1 \tag{A-36}$$

$$j_{13} = \ell_2\cos(\phi_2+\phi_3)\sin\phi_1 \tag{A-37}$$

$$j_{21} = -\ell_4\sin\phi_1 - \ell_1\cos\phi_3\sin\phi_1 - \ell_2\sin(\phi_2+\phi_3)\sin\phi_1 - \ell_5\sin\phi_3\sin\phi_1 + \ell_3\cos\phi_1 \tag{A-38}$$

$$j_{22} = -\ell_1\sin\phi_3\cos\phi_1 + \ell_2\cos(\phi_2+\phi_3)\cos\phi_1 + \ell_5\cos\phi_3\cos\phi_1 \tag{A-39}$$

$$j_{23} = \ell_2\cos(\phi_2+\phi_3)\sin\phi_1 \tag{A-40}$$

$$j_{31} = 0 \tag{A-41}$$

$$j_{32} = -\ell_1\cos\phi_3 - \ell_2\sin(\phi_2+\phi_3) - \ell_5\sin\phi_3 \tag{A-42}$$

$$j_{33} = -\ell_2\sin(\phi_2+\phi_3) \tag{A-43}$$

The determinant of the matrix J is given by

$$|J| = -\ [\ell_4+\ell_1\cos\phi_3+\ell_2\sin(\phi_2+\phi_3) + \ell_5\sin\phi_3]$$
$$[\ell_1\ell_2\cos\phi_3-\ell_2\ell_5\sin\phi_2] \qquad \text{(A-44)}$$

Thus, taking the inverse of the Jacobian matrix,

$$\underline{\dot{\phi}} = J^{-1}\ \underline{\dot{X}} = A\dot{X} \qquad \text{(A-45)}$$

$$A = \begin{bmatrix} a_{11} & a_{12} & a_{13} \\ a_{12} & a_{22} & a_{23} \\ a_{13} & a_{23} & a_{33} \end{bmatrix} \qquad \text{(A-46)}$$

$$a_{11} = \cos\phi_1/(\ell_4+\ell_1\cos\phi_3+\ell_2\sin(\phi_2+\phi_3)+\ell_5\sin\phi_3) \qquad \text{(A-47)}$$

$$a_{12} = \sin\phi_1/(\ell_4+\ell_1\cos\phi_3+\ell_2\sin(\phi_2+\phi_3)+\ell_5\sin\phi_3) \qquad \text{(A-48)}$$

$$a_{13} = 0 \qquad \text{(A-49)}$$

$$a_{21} = \cos\phi_1(\ell_1\cos\phi_3+\ell_2\sin(\phi_2+\phi_3)+\ell_5\sin\phi_3)/(\ell_2(\ell_1\cos\phi_2-\ell_5\sin\phi_2))$$
$$+\ell_3\sin\phi_1(\ell_1\cos\phi_3+\ell_2\sin(\phi_2+\phi_3)+\ell_5\sin\phi_3)/(\ell_2(\ell_1\cos\phi_2-\ell_5\sin\phi_2)$$
$$(\ell_4+\ell_1\cos\phi_3+\ell_2\sin(\phi_2+\phi_3)+\ell_5\sin\phi_3)) \qquad \text{(A-50)}$$

$$a_{22} = \sin\phi_1(\ell_1\cos\phi_3+\ell_2\sin(\phi_2+\phi_3)+\ell_5\sin\phi_3)/(\ell_2(\ell_1\cos\phi_2-\ell_5\sin\phi_2)).$$

$$-\ell_3\cos\phi_1(\ell_1\cos\phi_3+\ell_2\sin(\phi_2+\phi_3)+\ell_5\sin\phi_3)/(\ell_2(\ell_1\cos\phi_2-\ell_5\sin\phi_2)$$

$$(\ell_4+\ell_1\cos\phi_3+\ell_2\sin(\phi_2+\phi_3)+\ell_5\sin\phi_3)) \qquad \text{(A-51)}$$

$$a_{23} = (-\ell_1\sin\phi_3+\ell_2\cos(\phi_2+\phi_3)+\ell_5\cos\phi_3)/\ell_2(\ell_1\cos\phi_2-\ell_5\sin\phi_2) \qquad \text{(A-52)}$$

$$-a_{31} = (\ell_2\sin(\phi_2+\phi_3)\cos\phi_1)/(\ell_2(\ell_1\cos\phi_2-\ell_5\sin\phi_2))$$

$$+\ell_2\ell_3\sin\phi_1\sin(\phi_2+\phi_3)/((\ell_4+\ell_1\cos\phi_3+\ell_2\sin(\phi_2+\phi_3)+\ell_5\sin\phi_3)$$

$$(\ell_2(\ell_1\cos\phi_2-\ell_5\sin\phi_2))) \qquad \text{(A-53)}$$

$$a_{32} = -(\ell_2\sin\phi_1\sin(\phi_2+\phi_3))/(\ell_2(\ell_1\cos\phi_2-\ell_5\sin\phi_2))$$

$$+\ell_2\ell_3\cos\phi_1\sin(\phi_2+\phi_3)/(\ell_2(\ell_1\cos\phi_2-\ell_5\sin\phi_2)$$

$$(\ell_4+\ell_1\cos\phi_3+\ell_2\sin(\phi_2+\phi_3)+\ell_5\sin\phi_3)) \qquad \text{(A-54)}$$

$$a_{33} = -\ell_2\cos(\phi_2+\phi_3)/(\ell_2(\ell_1\cos\phi_2-\ell_5\sin\phi_2)) \qquad \text{(A-55)}$$

Thus equations (A-14), (A-21), (A-31) and equations (A-47) through (A-54) are the required equations for obtaining joint angles and joint rates from foot position and foot velocity coordinates.

APPENDIX B

The equations derived below form the basis for using a minimum time approach for transfer of the joint from one position to another. The development of the equations is based upon the derivation in [56], for constant linear systems with a scalar input. It has been assumed, of course, that a joint can be modelled by a simple type 1 transfer function where the scalar input u is the joint motor controller input and the position and velocity are the two states, X_1 and X_2. The results of using this approach for transferring the azimuth joint from any one joint angle position to another have been presented in the chapter on performance evaluation.

For a linear system, the following equations hold true [56]:

$$\dot{\underline{X}} = A\underline{X} + \underline{b}u \qquad \text{(B-1)}$$

where $\underline{X}$ is the state vector and u is a scalar input which is constrained between limits,

$$-1 \leq u \leq 1 \qquad \text{(B-2)}$$

If J is the criterion function to be minimized and

$$J = \int_{t_o}^{t_f} dt = t_f - t_o \qquad \text{(B-3)}$$

then the Hamiltonian for the problem is given by,

$$H = 1 + \underline{\lambda}^T(t)\ \underline{A}\ \underline{X}\ (t) + \underline{\lambda}^T(t)\ \underline{b}\ u(t) \tag{B-4}$$

In order to minimize H with respect to a choice of u(t), it is required that

$$u(t) = -\text{sign}(\underline{\lambda}^T(t)\ \underline{b}) \tag{B-5}$$

so that the Hamiltonian with the control optimum is

$$H = 1 + \lambda^T(t)\ \underline{A}\ \underline{X}\ (t) - |\underline{\lambda}^T\ (t)\ \underline{b}| \tag{B-6}$$

Since the terminal time is free, and since H does not explicitly depend on time, it can be shown [56], that H is equal to 0 for all t such that $t_o \leq t \leq t_f$ on the optimal trajectory. The canonic equations are

$$\dot{\underline{X}} = \frac{\partial H}{\partial \underline{Y}} = \underline{A}\ \underline{X} + \underline{b}\ u = \underline{A}\ \underline{X} - b\ \text{sign}[\underline{\lambda}^T\ (t)\ \underline{b}] \tag{B-7}$$

$$\dot{\underline{\lambda}} = \frac{\partial H}{\partial \underline{X}} = \underline{A}^T\ \underline{\lambda} \tag{B-8}$$

The solution to (B-8) is,

$$\underline{\lambda}(t) = e^{-\underline{A}(t-t_f)}\ \underline{\lambda}\ (t_f) \tag{B-9}$$

Equation (B-7) can be rewritten in terms of the time to go as follows. By letting t_o be 0,

$$\tau = t_f - t \tag{B-10}$$

$$\underline{Z}(\tau) = \underline{X}(t) = \underline{X}(t_f - \tau) \tag{B-11}$$

$$= -\underline{A}\ \underline{\dot{Z}}\ (\tau) + \underline{b}\ \text{sign}(\underline{\lambda}^T(t_f)\ e^{\underline{A}\tau}\ \underline{b}) \tag{B-12}$$

where (B-9), (B-10) and (B-11) have been used in (B-7) to obtain (B- 12)

Since

$$\underline{Z}(0) = X(t_f) = 0 \tag{B-12}$$

it follows that Eq. (B-12) has as its solution

$$\underline{Z}(\tau) = \int_0^\tau e^{-\underline{A}(\tau-p)}\underline{b}\ \text{sign}\ [\underline{\lambda}^T(t_f)\ e^{\underline{A}p}\ \underline{b}]\ dp \tag{B-13}$$

For the present simple system,

$$\dot{X}_1 = X_2 \tag{B-15}$$

$$\dot{X}_2 = -\alpha\ X_2 + u \tag{B-16}$$

$$X_1(0) = X_{10},\ X_2(0) = X_{20} \tag{B-17}$$

or,

$$\begin{bmatrix} \dot{X}_1 \\ \dot{X}_2 \end{bmatrix} = \begin{bmatrix} 0 & 1 \\ 0 & -\alpha \end{bmatrix} \begin{bmatrix} X_1 \\ X_2 \end{bmatrix} + \begin{bmatrix} 0 \\ 1 \end{bmatrix} U \tag{B-18}$$

The state transition matrix $e^{\underline{A}t}$ is therefore,

$$e^{\underline{A}t} = \begin{bmatrix} 1 & 1/\alpha(1-e^{-\alpha t}) \\ 0 & e^{-\alpha t} \end{bmatrix} \tag{B-19}$$

and the equation which determines when switching occurs is,

$$Z(\tau_s) = \begin{bmatrix} 1 & 1/\alpha(1-e^{\tau_s}) \\ 0 & e^{\alpha\tau_s} \end{bmatrix} \int_0^{\tau_s} \begin{bmatrix} 1/\alpha(1-e^{-\alpha p}) \\ e^{-\alpha p} \end{bmatrix} x$$

$$\text{sign } \{\lambda_1(t_f)[1-e^{-\alpha p})] + \lambda_2(t_f)\ e^{-\alpha p}\}\ dp \tag{B-20}$$

where (B-17) and (B-18) have been substituted in (B-13) and where τ_s is the time to go when the control switches.

A switch may occur at the instant when

$$\lambda_1(t_f)[1/\alpha(1-e^{-\alpha\tau_s}) = -\ \lambda_2(t_f)\ e^{-\alpha\tau_s} \tag{B-21}$$

Substituting Eq. (B-21) in (B-20) and using the relation,

$$\underline{X}(t_s) = \underline{Z}(\tau_s) \tag{B-22}$$

it follows that switching occurs when

$$X_1(t_s) + 1/\alpha\ X_2(t_s) - \{\frac{\text{sign } X_2(t_s))}{\alpha^2}\}\ \{\ell_n\ [1 + \alpha|X_2(t)|]\} = 0 \tag{B-23}$$

If the approximation is made that when switching occurs, $\frac{X_2}{\alpha}$ is much larger than $1/\alpha^2[\ell_n[1 + \alpha|X_2|]$, since the second term is a logarithmic term and since it is known that the pole α is of the order of 1 or 2, then switching must occur when,

$$D = X_1 + \frac{X_2}{\alpha} = 0 \qquad \text{(B-24)}$$

This corresponds to the switching curve shown in Figure B.1 below.

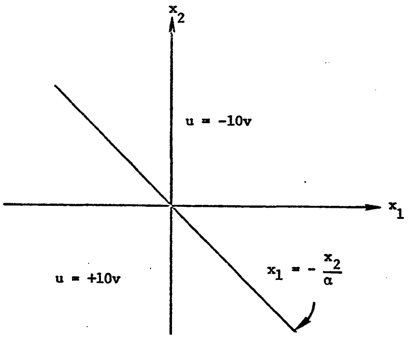

Figure B.1. Switching Curve for Minimum Time Response.

When the initial state lies to the left of the switching curve, the value u = +10V is used until term D in Eq. (B-24) changes sign after which u = -10V, and the opposite occurs when the initial state lies to the right of the switching curve.

APPENDIX C

REAL-TIME CONTROL PROGRAM FOR HEXAPOD VEHICLE

This appendix lists the program used for real-time control of the hexapod vehicle. The program incorporates the five different phases discussed in Chapter 5 - the data input phase, the vehicle power-on, start-up and check-out phase, the vehicle initialization phase, the motion planning phase, and the motion execution phase. The notation used for the angles and rates is as follows: the aximuth, elevation and knee angles denoted by ϕ_1, ϕ_2 and ϕ_3 in Appendix A, are referred to as PSI, TH1, and TH2 respectively in the program while the corresponding derivatives are DPSI, DTH1, and DTH2.

```
      DIMENSION IBUF1(256),BUF(48),
     6US(3),ISW(6),IWAITS(6),TLIFT(6),TPLACE(6)
     6,XD(3)
      REAL L1,L2,L3,L4,L5
      INTEGER*4 ITIM,IT8
      COMMON /BLANK/BETA,ALAM,SPEED,SGNU,VELG(3),POSG(3),AMP,RANGE,
     6POLE,REFDTH(3),REFTH(3),T,SCAV(6),SCAIN(3),TH1UP,TH2UP
      COMMON /DATA/X(36),U(18),TR,PSILIM,IMINT(6),
     6TH1LIM,TH2LIM,L1,L2,L3,L4,L5,LEGNO,XS(6),TOLER
      COMMON /SINCOS/CP,SP,CT1,CT2,ST1,ST2,ATL5L1,
     6SQL1,SQL2,SQL5,RTL1L5
      COMMON /FAST/ID,U1(18),U2(18),SLOPE(18),DT(6),
     6TOLD(6),DELT,SCALU(18),SCALE(36),REFA(6,3),REFR(6,3)
      EQUIVALENCE (BUF(1),BETA),(BUF(2),ALAM),(BUF(3),SPEED),
     6(BUF(4),SGNU),(BUF(11),AMP),(BUF(12),RANGE),
     6(BUF(13),POLE),(BUF(20),T),(BUF(30),TH1UP),
     6(BUF(31),TH2UP)
      ASIN(X)=ATAN2(X,SQRT(1.-X**2))
      CALL ASSIGN (2,'LEG.DAT',0,'RDO')
      DEFINE FILE 2(1,256,U,I11)
      READ (2'1,ERR=120)IBUF1
      GO TO 125
120   PAUSE 'READ ERROR'
125   DECODE (512,50,IBUF1)BUF
50    FORMAT(8(6F10.4,4X))
      WRITE (5,60)BUF
      L1=BUF(32)
      L2=BUF(33)
      L3=BUF(34)
      L4=BUF(35)
      L5=BUF(36)
      TOLER=BUF(37)
      SQL1=L1**2
      SQL2=L2**2
      SQL5=L5**2
      RTL1L5=2.*L2*SQRT(SQL1+SQL5)
      ATL5L1=ATAN2(L5,L1)
      CALL LOCK
      CALL IPOKE("177546,"100)
      IF (IQSET(9).NE.0)STOP 'QUEUE ELEMENT ERROR'
      PAUSE 'CLOCK PERIOD IN TICKS-I2 FORMAT'
      READ (5,57)ID
      WRITE (5,57)ID
57    FORMAT(I2)
      PAUSE 'SPEED CORRECTION FACTOR FOR FAST LOOP'
      READ (5,50)SPGAIN
      WRITE (5,60)SPGAIN
      DELT=ID
      DELT=DELT/60.*SPGAIN
C ***********CLEAR ALL DAC CHANNELS***********
      DO 7 J=1,18
      U(J)=0.
7     CONTINUE
60    FORMAT (1X,6F10.5)
61    WRITE (5,10)
10    FORMAT(1X,7HLAMBDA=)
      READ (5,50)ALAM
      WRITE (5,60)ALAM
      WRITE (5,20)
20    FORMAT (1X,6HSPEED=)
      READ (5,50)SPEED
      WRITE(5,60)SPEED
      DO  30 J=1,3
      VELG(J)=BUF(4+J)
```

```
      POSS(J)=BUF(7+J)
      SCAIN(J)=BUF(26+J)
      SCAV(J)=BUF(20+J)
      SCAV(J+3)=BUF(23+J)
30    CONTINUE
      DO 32 J=1,3
      REFTH(J)=0.
      REFDTH(J)=0.
32    CONTINUE
      DO 33 K=1,6
      SCALE(K)=SCAV(K)
33    CONTINUE
      DO 34 K=7,36
      SCALE(K)=SCALE(K-6)
34    CONTINUE
      DO 35 K=1,3
      SCALU(K)=SCAIN(K)
35    CONTINUE
      DO 36 K=4,18
      SCALU(K)=SCALU(K-3)
36    CONTINUE
      CALL SSDAC(U,18,0,17,SCALU)
C*******************************************
C     RESET ALL LEGS TO THE STARTING POSITION
C*************************************************
D     PAUSE 'BEGIN INITIALISE EXERCISE'
      DO 46 LEGNO=1,6
45    CALL SSADC (XS,6,(LEGNO-1)*6.LEGNO*6-1,SCAV)
      CALL SERVO (US,IERR)
      CALL SSDAC (US,3,(LEGNO-1)*3,LEGNO*3-1,SCAIN)
      IF (IERR.NE.1) GO TO 45
46    CONTINUE
      IF (SPEED)70,70,80
70    SGNU=-1.
      GO TO 90
80    SGNU=1.
C*************************************************
C     CALCULATE THE LIMIT OF THE FORWARD STROKE AND MOVE LEG
C     1 TO THAT POSITION TO GET AN IDEA OF THE TRANSFER TIME
C*************************************
D     PAUSE 'CALCULATE LIMIT OF FORWARD STROKE'
90    XD(1)=ALAM/2.
      XD(2)=L1+L4
      XD(3)=L2+L5
      CALL COORD(XD)
      PSILIM=REFTH(3)
      TH1LIM=REFTH(1)
      TH2LIM=REFTH(2)
D     WRITE (5,60)TH1LIM,TH2LIM,PSILIM
      CTH1L=COS(TH1LIM)
      STH1L=SIN(TH1LIM)
      CTH2L=COS(TH2LIM)
      STH2L=SIN(TH2LIM)
      STHSL=SIN(TH1LIM+TH2LIM)
C*************************************************
C
D     PAUSE 'TRANSFER TIME'
D     READ (5,50)TR
56    FORMAT (I1)
C
C**************************************************
C*************************************************
C     MOVE ALL LEGS TO POINTS JUST BEFORE TOUCHDOWN OF
C     LEG 1 IN THE LOCOMOTION CYCLE-LEGS TO BE LIFTED IN THE AIR
C     ARE ALL  MOVED TO END OF TRANSFER PHASE POSITION
C****************************************************
```

```
3867    TOT=TR+ALAM/SPEED
        BETA=(TOT-TR)/TOT
        TPLACE(1)=0.
        TPLACE(3)=BETA
        TPLACE(5)=2.*BETA-1.
        TPLACE(2)=TPLACE(1)+0.5
        TPLACE(4)=TPLACE(3)+0.5
        TPLACE(6)=TPLACE(5)+0.5
        DO 222 J=1,6
        TLIFT(J)=TPLACE(J)+BETA
222     CONTINUE
        DO 223 J=1,6
        IF (TPLACE(J).LT.1.)GO TO 224
        TPLACE(J)=TPLACE(J)-1.
224     TPLACE(J)=TPLACE(J)*TOT
        IF (TLIFT(J).LT.1.)GO TO 2225
        TLIFT(J)=TLIFT(J)-1.
2225    TLIFT(J)=TLIFT(J)*TOT
223     CONTINUE
D       PAUSE 'TRANSFER TIME'
D       WRITE (5,60)TR
D       PAUSE 'LEG PLACEMENT TIMES'
D       WRITE (5,60)TPLACE
D       PAUSE 'LEG LIFTOFF TIMES'
D       WRITE (5,60)TLIFT
D       PAUSE 'BETA'
D       WRITE (5,60)BETA
D       PAUSE 'CONTINUE'
456     T=0.
        DO 243 J=1,3
        REFDTH(J)=0.
243     CONTINUE
        DO 328 LEGNO=2,6
        IWAITS(LEGNO)=0
        IF (TPLACE(LEGNO).GT.TLIFT(LEGNO))GO TO 340
        ISW(LEGNO)=2
        IWAITS(LEGNO)=1
        GO TO 328
340     ISW(LEGNO)=1
        TPLACE(LEGNO)=TPLACE(LEGNO)-TOT
328     CONTINUE
        REFTH(1)=TH1UP
        REFTH(2)=TH2UP
        REFTH(3)=PSILIM
        LEGNO=1
106     CALL SSADC(XS,6,0,5,SCAV)
        CALL SERVO(US,IERR)
        CALL SSDAC(US,3,0,2,SCAIN)
        IF (IERR.NE.1)GO TO 106
        ISW(1)=1
358     DO 368 LEGNO=2,6
        IF (ISW(LEGNO).EQ.1)GO TO 355
        REFTH(1)=TH1UP
        REFTH(2)=TH2UP
        REFTH(3)=PSILIM
375     DO 12555 J=1,3
        REFA(LEGNO,J)=REFTH(J)
        REFR(LEGNO,J)=0.
12555   CONTINUE
3755    CALL SSADC(XS,6,(LEGNO-1)*6,LEGNO*6-1,SCAV)
        CALL SERVO (US,IERR)
        CALL SSDAC(US,3,(LEGNO-1)*3,LEGNO*3-1,SCAIN)
        IF (IERR.NE.1)GO TO 3755
368     CONTINUE
        GO TO 385
355     XD(1)=ALAM/2.-SPEED*(T-TPLACE(LEGNO))
```

```
      XD(2)=L1+L4
      XD(3)=L2+L5
      CALL COORD(XD)
      GO TO 375
385   T=0.
      ISW(1)=1
C****************************************************
C     INITIALISE ALL SWITCHES BEFORE COMMENCING LOCOMOTION CYCLE
C****************************************************
      DO 102 LEGNO=1,6
      IMINT(LEGNO)=0
102   CONTINUE
      CALL TRAJ(TOT)
D     PAUSE ' BEGIN LOCOMOTION CYCLE '
      CALL GTIM(IT0)
      CALL CVTTIM(IT0,IHR0,IMIN0,ISEC0,ITIC0)
C****************************************************
C     START OF LOCOMOTION CYCLE AND CONTROL LOOP
C****************************************************
      CALL FILTER(ID)
225   CALL SSADC(X,36,0,35,SCALE)
      CALL GTIM(ITIM)
      CALL CVTTIM(ITIM,IHRS,IMIN,ISEC,ITIC)
      DEL=ITIC-ITIC0
      T=60*(IMIN-IMIN0)+ISEC-ISEC0
      T=T+DEL/60.
      DO 210 LEGNO=1,6
      IF (ISW(LEGNO).EQ.1)GO TO 1000
      IF (ISW(LEGNO).EQ.2)GO TO 2000
      IF (ISW(LEGNO).EQ.0)GO TO 3000
210   CONTINUE
      GO TO 225
C************************************************************
C     THE LEG IS ON THE GROUND-CALCULATE THE REFERENCE
C     TRAJECTORY ANDTHE DESIRED INPUTS AND RETURN
C************************************************************
1000  DO 1240 J=1,6
      XS(J)=X((LEGNO-1)*6+J)
1240  CONTINUE
      CALL FASREF(TPLACE,TOT)
      DO 12556 J=1,3
      REFA(LEGNO,J)=REFTH(J)
      REFR(LEGNO,J)=REFDTH(J)
12556 CONTINUE
      CALL SERVO(US,IERR)
      IF (T.LT.TLIFT(LEGNO)) GO TO 2110
      ISW(LEGNO)=2
      IMINT(LEGNO)=0
      TLIFT(LEGNO)=T+TOT
      TPLACE(LEGNO)=T+TR
2110  DO 2120 J=1,3
      U((LEGNO-1)*3+J)=US(J)
2120  CONTINUE
      GO TO 210
C************************************************************
C     THE LEG IS IN THE TRANSFER PHASE-CALCULATE THE
C     DESIRED INPUTS AND RETURN-SET A SWITCH IF TRANSFER PHASE
C     IS OVER TOO SOON AND LEG MUST WAIT IN THE AIR
C************************************************************
2000  IF (IWAITS(LEGNO).EQ.1)GO TO 1001
      DO 2240 J=1,6
      XS(J)=X((LEGNO-1)*6+J)
2240  CONTINUE
      REFDTH(1)=0.
      REFDTH(2)=0.
      REFDTH(3)=0.
```

```
      REFTH(1)=TH1UP
      REFTH(2)=TH2UP
      REFTH(3)=PSILIM
      DO 12557 J=1,3
      REFA(LEGNO,J)=REFTH(J)
      REFR(LEGNO,J)=0.
12557 CONTINUE
      CALL SERVO (US,IERR)
      IMINT(LEGNO)=IMINT(LEGNO)+1
      IF (IERR.EQ.1)GO TO 1001
3100  DO 3120 J=1,3
      U((LEGNO-1)*3+J)=US(J)
3120  CONTINUE
      GO TO 210
1001  IF (T.GT.TPLACE(LEGNO))GO TO 1011
      IWAITS(LEGNO)=1
      GO TO 210
1011  ISW(LEGNO)=0
      IWAITS(LEGNO)=0
      GO TO 3100
C**************************************************************
C     BEGIN TO SET THE LEG DOWN AND PREPARE TO
C     COMMENCE THE DUTY CYCLE
C**************************************************************
3000  DO 4240 J=1,6
      XS(J)=X((LEGNO-1)*6+J)
4240  CONTINUE
      REFTH(1)=TH1LIM
      REFTH(2)=TH2LIM
      REFTH(3)=PSILIM
      DO 12558 J=1,3
      REFR(LEGNO,J)=0.
      REFA(LEGNO,J)=REFTH(J)
12558 CONTINUE
      CALL SERVO(US,IERR)
      DO 5240 J=1,3
      U((LEGNO-1)*3+J)=US(J)
5240  CONTINUE
      ISW(LEGNO)=1
      IF (LEGNO.NE.1)GO TO 210
D     WRITE (5,60)T
      GO TO 225
      STOP
      END
      SUBROUTINE SERVO(US,IERR)
      REAL L1,L2,L3,L4,L5
      DIMENSION BUF(48),US(3)
      COMMON /BLANK/BETA,ALAM,SPEED,SGNU,VELG(3),POSG(3),AMP,RANGE,
     6POLE,REFDTH(3),REFTH(3),T,SCAV(6),SCAIN(3),TH1UP,TH2UP
      COMMON /DATA/X(36),U(18),TR,PSILIM,IMINT(6),
     6TH1LIM,TH2LIM,L1,L2,L3,L4,L5,LEGNO,XS(6),TOLER
      COMMON /SINCOS/CP,SP,CT1,CT2,ST1,ST2,ATL5L1,
     6SQL1,SQL2,SQL5,RTL1L5
      COMMON /FAST/ID,U1(18),U2(18),SLOPE(18),DT(6),
     6TOLD(6),DELT,SCALU(18),SCALE(36),REFA(6,3),REFR(6,3)
      EQUIVALENCE (BUF(1),BETA),(BUF(2),ALAM),(BUF(3),SPEED),
     6(BUF(4),SGNU),(BUF(11),AMP),(BUF(12),RANGE),
     6(BUF(13),POLE),(BUF(20),T),(BUF(30),TH1UP),
     6(BUF(31),TH2UP)
      ERR=0.
      IERR=0
      DO 10 I=1,3
      US(I)=VELG(I)*(REFDTH(I)-XS(I+3))+POSG(I)*
     6(REFTH(I)-XS(I))
      ERR=ERR+ABS(REFDTH(I)-XS(I+3))+
     6ABS(REFTH(I)-XS(I))
```

```
10      CONTINUE
        DO 20 I=1,3
        IF (US(I).GT.9.5)US(I)=9.5
        IF (US(I).LT.-9.5)US(I)=-9.5
20      CONTINUE
        IF (ERR.GT.TOLER)RETURN
        IERR=1
        US(1)=0.
        US(2)=0.
        US(3)=0.
        DO 40 J=1,3
40      CONTINUE
        RETURN
        END
        SUBROUTINE REF(TPLACE)
        REAL L1,L2,L3,L4,L5
        DIMENSION BUF(48),US(3),TPLACE(6)
        COMMON /BLANK/BETA,ALAM,SPEED,SGNU,VELG(3),POSG(3),AMP,RANGE,
     6POLE,REFDTH(3),REFTH(3),T,SCAV(6),SCAIN(3),TH1UP,TH2UP
        COMMON /DATA/X(36),U(18),TR,PSILIM,IMINT(6),
     6TH1LIM,TH2LIM,L1,L2,L3,L4,L5,LEGNO,XS(6),TOLER
        COMMON /SINCOS/CP,SP,CT1,CT2,ST1,ST2,ATLSL1,
     6SQL1,SQL2,SQL5,RTL1L5
        COMMON /FAST/ID,U1(18),U2(18),SLOPE(18),DT(6),
     6TOLD(6),DELT,SCALU(18),SCALE(36),REFA(6,3),REFR(6,3)
        EQUIVALENCE (BUF(1),BETA),(BUF(2),ALAM),(BUF(3),SPEED),
     6(BUF(4),SGNU),(BUF(11),AMP),(BUF(12),RANGE),
     6(BUF(13),POLE),(BUF(20),T),(BUF(30),TH1UP),
     6(BUF(31),TH2UP)
        DX=-SPEED
        DY=0.
        DZ=0.
        Y=L1+L4
        Z=L2+L5
        X1=ALAM/2.-SPEED*(T-TPLACE(LEGNO))
        US(1)=X1
        US(2)=Y
        US(3)=Z
        CALL COORD(US)
        TH=REFTH(1)+REFTH(2)
        STH=SIN(TH)
        CTH=COS(TH)
        CT1=COS(REFTH(1))
        ST1=SIN(REFTH(1))
        TN1=L1*CT1+L2*STH+L5*ST1
        D1=L4+TN1
        D2=L2*(L1*CT2-L5*ST2)
        A11=-SP/D1
        A21=-(L2*STH*CP/D2+L3*SP*STH/D1/D2)
        A31=CP*TN1/D2+L3*SP*TN1/D1/D2
        A12=CP/D1
        A22=-L2*SP*STH/D2+L2*L3*CP*STH/D1/D2
        A32=SP*TN1/D2-L3*CP*TN1/D1/D2
        A13=0.
        A23=-L2*CTH/D2
        A33=(-L1*ST1+L2*CTH+L5*CT1)/D2
        REFDTH(1)=A21*DX+A22*DY+A23*DZ
        REFDTH(2)=A31*DX+A32*DY+A33*DZ
        REFDTH(3)=-(A11*DX+A12*DY+A13*DZ)
        RETURN
        END
        SUBROUTINE COORD(XD)
        REAL L1,L2,L3,L4,L5
        DIMENSION BUF(48),US(3),XD(3)
        COMMON /BLANK/BETA,ALAM,SPEED,SGNU,VELG(3),POSG(3),AMP,RANGE,
     6POLE,REFDTH(3),REFTH(3),T,SCAV(6),SCAIN(3),TH1UP,TH2UP
```

```
      COMMON /DATA/X(36),U(18),TR,PSILIM,IMINT(6),
     6TH1LIM,TH2LIM,L1,L2,L3,L4,L5,LEGNO,XS(6),TOLER
      COMMON /SINCOS/CP,SP,CT1,CT2,ST1,ST2,ATL5L1,
     6SQL1,SQL2,SQL5,RTL1L5
      COMMON /FAST/ID,U1(18),U2(18),SLOPE(18),DT(6),
     6TOLD(6),DELT,SCALU(18),SCALE(36),REFA(6,3),REFR(6,3)
      EQUIVALENCE (BUF(1),BETA),(BUF(2),ALAM),(BUF(3),SPEED),
     6(BUF(4),SGNU),(BUF(11),AMP),(BUF(12),RANGE),
     6(BUF(13),POLE),(BUF(20),T),(BUF(30),TH1UP)
     6,(BUF(31),TH2UP)
      ASIN(X)=ATAN2(X,SQRT(1.-X**2))
      X1=XD(1)
      Y=XD(2)
      Z=XD(3)
      PSI=-ASIN(L3/SQRT(Y**2+X1**2))+ATAN2(X1,Y)
      CP=SIN(PSI)
      SP=COS(PSI)
      T1=((Y-L4*SP+L3*CP)/SP)**2+Z**2-SQL1-SQL2-SQL5
      TH2=ASIN(T1/RTL1L5)-ATL5L1
      CT2=COS(TH2)
      ST2=SIN(TH2)
      T1=L5+L2*CT2
      T2=L1+L2*ST2
      TH1=-ASIN(Z/(SQRT(T1**2+T2**2)))+ATAN2(T1,T2)
      REFTH(1)=TH2
      REFTH(2)=TH1
      REFTH(3)=PSI
      RETURN
      END
      SUBROUTINE FILTER (ID)
      INTEGER*2 AREA(4)
      REAL L1,L2,L3,L4,L5
      EXTERNAL FILTER
      DIMENSION BUF(48)
      COMMON /BLANK/BETA,ALAM,SPEED,SGNU,VELG(3),POSG(3),AMP,RANGE,
     6POLE,REFDTH(3),REFTH(3),T,SCAV(6),SCAIN(3),TH1UP,TH2UP
      COMMON /DATA/X(36),U(18),TR,PSILIM,IMINT(6),
     6TH1LIM,TH2LIM,L1,L2,L3,L4,L5,LEGNO,XS(6),TOLER
      COMMON /SINCOS/CP,SP,CT1,CT2,ST1,ST2,ATL5L1,
     6SQL1,SQL2,SQL5,RTL1L5
      COMMON /FAST/I1,U1(18),U2(18),SLOPE(18),DT(6),
     6TOLD(6),DELT,SCALU(18),SCALE(36),REFA(6,3),REFR(6,3)
      EQUIVALENCE (BUF(1),BETA),(BUF(2),ALAM),(BUF(3),SPEED),
     6(BUF(4),SGNU),(BUF(11),AMP),(BUF(12),RANGE),
     6(BUF(13),POLE),(BUF(20),T),(BUF(30),TH1UP),
     6(BUF(31),TH2UP)
      DO 10 J=1,6
      DO 20 K=1,3
      REFA(J,K)=REFA(J,K)+DELT*REFR(J,K)
20    CONTINUE
10    CONTINUE
      CALL SSADC(X,36,0,35,SCALE)
      DO 30 J=1,6
      DO 40 I=1,3
      M=(J-1)*3+I
      N=(J-1)*6+I
      U(M)=POSG(I)*(REFA(J,I)-X(N))
     6+VELG(I)*(REFR(J,I)-X(N+3))
40    CONTINUE
30    CONTINUE
      CALL SSDAC(U,18,0,17,SCALU)
      CALL ITIMER(0,0,0,ID,AREA,ID,FILTER)
      RETURN
      END
      SUBROUTINE TRAJ(TOT)
      REAL L1,L2,L3,L4,L5
```

```
      DIMENSION BUF(48),US(3),TPLACE(6)
      COMMON /BLANK/BETA,ALAM,SPEED,SGNU,VELG(3),POSG(3),AMP,RANGE,
     6POLE,REFDTH(3),REFTH(3),T,SCAV(6),SCAIN(3),TH1UP,TH2UP
      COMMON /DATA/X(36),U(18),TR,PSILIM,IMINT(6),
     6TH1LIM,TH2LIM,L1,L2,L3,L4,L5,LEGNO,XS(6),TOLER
      COMMON /SINCOS/CP,SP,CT1,CT2,ST1,ST2,ATL5L1,
     6SQL1,SQL2,SQL5,RTL1L5
      COMMON /FAST/ID,U1(18),U2(18),SLOPE(18),DT(6),
     6TOLD(6),DELT,SCALU(18),SCALE(36),REFA(6,3),REFR(6,3)
      COMMON /XTERP/ANGLE(3,500),RATE(3,500)
      EQUIVALENCE (BUF(1),BETA),(BUF(2),ALAM),(BUF(3),SPEED),
     6(BUF(4),SGNU),(BUF(11),AMP),(BUF(12),RANGE),
     6(BUF(13),POLE),(BUF(20),T),(BUF(30),TH1UP),
     6(BUF(31),TH2UP)
      LEGNO=1
      T=0.
      TPLACE(1)=0.
      TON=TOT-TR
      TINC=TON/500.
      DO 100 I=1,500
      CALL REF(TPLACE)
      DO 200 J=1,3
      RATE(J,I)=REFDTH(J)
      ANGLE(J,I)=REFTH(J)
200   CONTINUE
      T=T+TINC
100   CONTINUE
60    FORMAT (1X,F12.4,3X,F12.4)
300   CONTINUE
      T=0.
      RETURN
      END
      SUBROUTINE FASREF(TPLACE,TOT)
      REAL L1,L2,L3,L4,L5
      DIMENSION BUF(48),US(3),TPLACE(6)
      COMMON /BLANK/BETA,ALAM,SPEED,SGNU,VELG(3),POSG(3),AMP,RANGE,
     6POLE,REFDTH(3),REFTH(3),T,SCAV(6),SCAIN(3),TH1UP,TH2UP
      COMMON /DATA/X(36),U(18),TR,PSILIM,IMINT(6),
     6TH1LIM,TH2LIM,L1,L2,L3,L4,L5,LEGNO,XS(6),TOLER
      COMMON /SINCOS/CP,SP,CT1,CT2,ST1,ST2,ATL5L1,
     6SQL1,SQL2,SQL5,RTL1L5
      COMMON /FAST/ID,U1(18),U2(18),SLOPE(18),DT(6),
     6TOLD(6),DELT,SCALU(18),SCALE(36),REFA(6,3),REFR(6,3)
      COMMON /XTERP/ANGLE(3,500),RATE(3,500)
      EQUIVALENCE (BUF(1),BETA),(BUF(2),ALAM),(BUF(3),SPEED),
     6(BUF(4),SGNU),(BUF(11),AMP),(BUF(12),RANGE),
     6(BUF(13),POLE),(BUF(20),T),(BUF(30),TH1UP),
     6(BUF(31),TH2UP)
      TON=T-TPLACE(LEGNO)
      TINC=(TOT-TR)/500.
      IAD=TON/TINC
      IF (IAD.GT.500)IAD=500
      DELTA=TON-TINC*IAD
      DO 100 J=1,3
      REFTH(J)=ANGLE(J,IAD)+DELTA*(ANGLE(J,IAD+1)-
     6ANGLE(J,IAD))/TINC
      REFDTH(J)=RATE(J,IAD)+DELTA*(RATE(J,IAD+1)
     6-RATE(J,IAD))/TINC
100   CONTINUE
      RETURN
      END
*
```

REFERENCES

1. McGhee, R. B., "Some Finite State Aspects of Legged Locomotion," Mathematical Biosciences, Vol. 2, Number 1/2, pp. 67-68, February 1968.

2. McGhee, R. B., "Robot Locomotion," Neural Control of Locomotion Plenum Publishing Corporation, New York, pp. 237-264, 1976.

3. McGhee, R. B., and Jain, A. K., "Some Properties of Regularly Realizable Gait Matrices," Mathematical Biosciences, Vol. 13, Number 1/2, pp. 179-193, February 1972.

4. McGhee, R. B., and Sun, Shu-Shen, "On the Problem of Selecting a Gait for a Legged Vehicle," Proceedings of IV IFAC Symposium on Automatic Control in Space, USSR, August 1974.

5. Koozekanani, S. H., and McGhee, R. B., "Occupancy Problems with Pairwise Exclusion Constraints - An Aspect of Gait Enumeration," Journal of Cybernetics, Vol. 2, No. 4, pp. 14-26, December 1972.

6. Hildebrand, M., "Symmetrical Gaits of Horses," Science, Vol. 150, pp. 701-708, November 1965.

7. Hildebrand, M., "Analysis of the Symmetrical Gaits of Tetrapods," Fol. Biotheoret., Vol. VI, pp. 9-22, 1966.

8. Muybridge, E., Animals in Motion, Dover Publications, Inc., New York, 1957 (first published in 1899).

9. Muybridge, E., The Human Figure in Motion, Dover Publications, Inc., New York, 1955 (first published in 1901).

10. Tomovic, R., and Karplus, W. J., "Land Locomotion - Simulation and Control," Proc. Third International Analogue Computation Meeting, Opatija, Yugoslavia, pp. 385-390, September 1961.

11. Sun, Shu-Shen, A Theoretical Study of Gaits for Legged Locomotion Systems, Ph.D. dissertation, Department of Electrical Engineering, The Ohio State University, Columbus, Ohio 43210, March 1974.

12. McGhee, R. B., A Study of Legged Locomotion Concepts Relative to the Mobility Needs of a Master-Slave Manipulator System, Final Report, Contract No. 3-35874, National Bureau of Standards, Washington, D. C., April 1973.

13. Morawski, J. M., and Wojcieszak, I., "Miniwalker, A Resonant Model of Human Locomotion," VIth International Congress of Biomechanics, Copenhagen, Denmark, July 1977.

14. Okhotsimsky, D. E., Platonov, A., Borovin, A., and Karpov, I., Computer Simulation of the Movement of a Walking Machine, Inst. of Applied Mathematics, Academy of Sciences, Moscow, USSR, 1971.

15. Bessonov, A. P., and Umnov, N. V., "The Analysis of Gaits Six-Legged Vehicles According to Their Static Stability," Proc. of the Symposium on Theory and Practice of Robots and Manipulators, International Centre for Mechanical Sciences, Udine, Italy, September 1973.

16. Bessonov, A. P., and Umnov, N. W., "Choice of Geometric Parameters of Walking Machines," On Theory and Practice of Robots and Manipulators, Polish Scientific Publishers, Warsaw, pp. 63-76, 1976.

17. Frank, A., On the Stability of Algorithmic Biped Locomotion Machine," Journal of Terramechanics, Vol. 8, No. 1, pp. 41-50, 1971.

18. Vukobratovic, M., Legged Locomotion Robots and Anthropomorphic Mechanisms, Research Monograph, Mihailo Pupin Institute, Beograd, 1975.

19. McGhee, R. B., and Orin, D. E., "A Mathematical Programming Approach to Control of Joint Positions and Torques in Legged Locomotion Systems," On Theory and Practice of Robots and Manipulators, Polish Scientific Publishers, Warsaw, pp. 231-240, 1976.

20. Kugushev, E., and Jaroshevskij, V., "Problems of Selecting a Gait for an Integrated Locomotion Robot," Proc. of Fourth International Conference on Artificial Intelligence, Tbilisi, Georgian SSR, USSR, pp. 789-793, September 1975.

21. Iswandhi, J., and McGhee, R. B., Optimization of Support State Sequences for Legged Locomotion Systems, Communication and Control Systems Laboratory Technical Note No. 22, Ohio State University, March, 1978.

22. Okhotsimsky, D., and Platonov, A., "Perceptive Robot Moving in 3D World," Proc. of the Fourth International Conference on Artificial Intelligence, Tbilisi, Georgian SSR, USSR, pp. 798-802, September 1975.

23. Okhotsimsky, D., and Platonov, A., "Walker's Motion Control," On Theory and Practice of Robots and Manipulators, Polish Scientific Publishers, Warsaw, pp. 221-230, 1976.

24. McGhee, R. B., and Orin, D. E., "An Interactive Computer Control System for a Quadruped Robot," Proceedings of ROMANSY-73 Symposium, Udine, Italy, September 1973.

25. Orin, D. E., Interactive Control of a Six-Legged Vehicle With Optimization of Both Stability and Energy, Ph.D. dissertation, Department of Electrical Engineering, The Ohio State University, Columbus, Ohio 43210, March 1976.

26. Chao, Ching-Shu, A Software System for On-Line Control of a Hexapod Vehicle Utilizing a Multiprocessor Computing Structure, M.S. thesis, Department of Electrical Engineering, The Ohio State University, Columbus, Ohio 43210, August 1977.

27. Petternella, M., and Salinari, S., Six Legged Walking Vehicles, Report No. 74-31, Instituto di Automatica, University of Rome, Rome, Italy, 1974.

28. Jaswa, V. C., Dynamic Stability and Control of a Three Link Model of a Human Being, M.S. thesis, Department of Electrical Engineering, The Ohio State University, Columbus, Ohio 43210, 1975.

29. Park, W. T., and Fegley, K. A., "Control of a Multi-Legged Vehicle," Proc. of V IFAC Symposium on Automatic Control in Space, Genoa, Italy, June 1973.

30. Shigley, J., The Mechanics of Walking Vehicles, Land Locomotion Laboratory Report No. LL-71, U.S. Army Tank Automotive Command, Warren, Michigan, September 1960.

31. Baldwin, W. C., and Miller, J. V., Multi-Legged Walker, Final Report, Space General Corporation, El Monte, California, January 30, 1966.

32. Cox, W., "Big Muskie," News in Engineering, Ohio State University, pp. 25-27, January 1970.

33. Mosher, R. S., "Test and Evaluation of a Versatile Walking Truck," Proc. of Off-Road Mobility Research Symposium, International Soc. for Terrain Vehicles, Washington, D. C., pp. 359-379, June 1968.

34. Frank. A. A., Automatic Control Systems for Legged Locomotion, Ph.D. dissertation, University of Southern California, Los Angeles, California, 1968.

35. Kato, I., et al., "Information Power Machine With Senses and Limbs," Proc. of ROMANSY-73 Symposium, Udine, Italy, 1973.

36. Tomovic, R., and McGhee, R. B., "A Finite State Approach to the Synthesis of Bioengineering Control Systems," IEEE Trans. on Human Factors in Electronics, Vol. HFE-2, pp. 65-69, June 1966.

37. Wilson, D. M., "Stepping Patterns in Tarantula Spiders," J. Exp. Biology, Vol. 47, pp. 133-151, 1967.

38. Wilson, D. M., "Insect Walking," Annual Review of Entomology, Vol. II, pp. 103-121, 1966.

39. Okhotsimsky, D., Gurfinkel, V., Devyanin, E., and Platonov, A., "Integrated Walking Robot Development," Institute of Mechanics, Moscow State University. Presented at the 1977 Engineering Foundation Conference on Cybernetic Modeling of the Human Neuromuscular System, Henniker, New Hampshire, August, 1977.

40. McGhee, R. B., and Pai, A. L., "An Approach to Computer-Control of Legged Vehicles," Journal of Terramechanics, Vol. 11, No. 2, pp. 9-27, 1974.

41. Nichols, T., and Houk, J., "Improvement in Linearity and Regulation of Stiffness That Results from Actions of Stretch Reflex," Journal of Neurophysiology, Vol. 39, No. 1, pp. 119-142, 1976.

42. Pieper, D. L., The Kinematics of Manipulators Under Computer Control, Ph.D. dissertation, Department of Computer Science, Stanford University, October 1968.

43. Paul, R., Modelling, Trajectory Calculation and Servoing of a Computer Controlled Arm, Ph.D. dissertation, Department of Computer Science, Stanford,University, November 1972.

44. Vukobratovic, M., Ciric, V., Hristic, D., and Stepanenko, J., "Contribution to the Study of Anthropomorphic Robots," Paper 18.1, Proc. of IFAC V World Congress, Paris, June 1972.

45. Frank, A. A., and McGhee R. B., "Some Considerations Relating to the Design of Autopilots for Legged Vehicles," Journal of Terramechanics, Vol. 6, No. 1, pp. 23-35, 1969.

46. Buckett, J. R., Design of an On-Board Electronic Joint Control System for a Hexapod Vehicle, M.S. thesis, Department of Electrical Engineering, The Ohio State University, Columbus, Ohio 43210, March 1977.

47. Anon., Boston Gear Catalog 60, Boston Gear Works, North American Rockwell, 1969.

48. Houghton, P. S., Gears: Spur, Helical, Bevel, Internal, Epicyclic and Worm, London Technical Press, 1970.

49. Spotts, M. F., Design of Machine Elements, Englewood Cliffs, N. J., Prentice-Hall, 1971.

50. Buckingham, E., Analytical Mechanics of Gears, McGraw-Hill Book Co., Inc., 1950.

51. Anon., Catalog 70, Bearings Inc., 3634 Euclid Ave., Cleveland, Ohio 44115, 1970.

52. Anon., 1975 Catalog, AST/Servo Systems, Inc., 930 Broadway, Newark, N. J. 07104, 1975.

53. Briggs, R. L., Real-Time Digital Control of an Electrically Powered Vehicle Leg Using Vector Force Feedback, M.S. thesis, Department of Electrical Engineering, The Ohio State University, Columbus, Ohio 43210, December 1977.

54. Broughton, M. B., "Pulse Frequency Modulation Applied to the Digital Control of a Thyristor," IEEE Transactions on Industrial Electronics and Control Instrumentation, Vol. IECI-24, No. 2, pp. 173-177, May 1977.

55. Orin, D. E., Frank, A. A., Buckett, J. R., Jaswa, V. C., "Design of a Manipulator Arm for an Interactive Computer-Controlled Legged Locomotion System," Proceedings of the 1976 Milwaukee Symposium on Automatic Computation and Control, Milwaukee, 1976.

56. Sage, A. P., Optimum Systems Control, Prentice-Hall, Englewood Cliffs, N. J., 1968.